UNIVERSITAT ROVIRA I VIRGILI
MEMBRANE FOULING CHARACTERIZATION BY CONFOCAL SCANNING LASER MICROSCOPY
Maria Malgorzata Zator
ISBN:978-84-693-0712-0/DL:T-422-2010

UNIVERSITAT ROVIRA I VIRGILI
MEMBRANE FOULING CHARACTERIZATION BY CONFOCAL SCANNING LASER MICROSCOPY
Maria Malgorzata Zator
ISBN:978-84-693-0712-0/DL:T-422-2010

UNIVERSITAT ROVIRA I VIRGILI
MEMBRANE FOULING CHARACTERIZATION BY CONFOCAL SCANNING LASER MICROSCOPY
Maria Malgorzata Zator
ISBN:978-84-693-0712-0/DL:T-422-2010

MARIA MAŁGORZATA ZATOR

MEMBRANE FOULING CHARACTERIZATION BY CONFOCAL SCANNING LASER MICROSCOPY

Philosophy Doctor Thesis

Supervised by Dr. Carme Güell

Department of Chemical Engineering

UNIVERSITAT ROVIRA I VIRGILI

Tarragona

2009

UNIVERSITAT ROVIRA I VIRGILI
MEMBRANE FOULING CHARACTERIZATION BY CONFOCAL SCANNING LASER MICROSCOPY
Maria Malgorzata Zator
ISBN:978-84-693-0712-0/DL:T-422-2010

UNIVERSITAT ROVIRA I VIRGILI
MEMBRANE FOULING CHARACTERIZATION BY CONFOCAL SCANNING LASER MICROSCOPY
Maria Malgorzata Zator
ISBN:978-84-693-0712-0/DL:T-422-2010

UNIVERSITAT ROVIRA I VIRGILI
Chemical Engineering Department

Avinguda dels Països Catalans,26
Campus Sescelades
43007 Tarragona
Tel. 977 55 97 00
Fax. 977 55 96 99

Dr. Carme Güell Saperas, associate professor of the Chemical Engineering Department at the Universitat Rovira i Virgili,

CERTIFY:

That the doctoral thesis entitled “Membrane fouling characterization by confocal scanning laser microscopy”, submitted by Maria Zator to obtain the degree of Philosophy Doctor from Universitat Rovira i Virgili, has been carried out under my supervision at the Department of Chemical Engineering of the Universitat Rovira i Virgili .

Tarragona, 29th of December 2008.

UNIVERSITAT ROVIRA I VIRGILI
MEMBRANE FOULING CHARACTERIZATION BY CONFOCAL SCANNING LASER MICROSCOPY
Maria Malgorzata Zator
ISBN:978-84-693-0712-0/DL:T-422-2010

UNIVERSITAT ROVIRA I VIRGILI
MEMBRANE FOULING CHARACTERIZATION BY CONFOCAL SCANNING LASER MICROSCOPY
Maria Malgorzata Zator
ISBN:978-84-693-0712-0/DL:T-422-2010

EXAMINATION BOARD MEMBERS

Prof. Antonio Hernández

Departamento de Física Aplicada, Facultad de Ciencias, Universidad de Valladolid, Spain

Dr. Joseph Font Capafonts

Departament d'Enginyeria Química, ETSEQ, Universitat Rovira i Virgili, Spain

Prof. Wojciech Kujawski

Department of Physical Chemistry, Faculty of Chemistry, Nicolaus Copernicus University, Poland

Dr. Carlos Télez

Departamento de Ingeniería Química y Tecnologías del Medio Ambiente, Centro Politécnico Superior, Universidad Zaragoza, Spain

Prof. Susana Luque

Departamento de Ingeniería Química y del Medio Ambiente, Universidad de Oviedo, Spain

UNIVERSITAT ROVIRA I VIRGILI
MEMBRANE FOULING CHARACTERIZATION BY CONFOCAL SCANNING LASER MICROSCOPY
Maria Malgorzata Zator
ISBN:978-84-693-0712-0/DL:T-422-2010

UNIVERSITAT ROVIRA I VIRGILI
MEMBRANE FOULING CHARACTERIZATION BY CONFOCAL SCANNING LASER MICROSCOPY
Maria Malgorzata Zator
ISBN:978-84-693-0712-0/DL:T-422-2010

Durante estos años son muchas las personas e instituciones que han participado en este trabajo y a quienes quiero expresar mi gratitud por el apoyo y la confianza que me han prestado de forma desinteresada.

En primer lloc, de forma molt especial, vull deixar constància del meu agraïment a la Dra. Carme Güell, qui em va obrir un camp molt desconegut per a mi i que em va portar de la mà durant tot el camí i que va suposar transmetre'm la seva il·lusió per despertar en mi el "cuquet" de la investigació, la persona que ha sigut per a mi un autèntic privilegi tindre-la com a directora de la tesi. Voldria francament agrair-li tot el que m'ha ensenyat en aquests anys, i sobretot, el temps, la paciència i l'esforç que m'ha dedicat. Moltes Gràcies.

A la Universitat Rovira i Virgili pel seu suport econòmic.

A la Dra. Montserrat Ferrando i el Dr. Francisco López per donar-me el seu suport.

A mis compañeros y amigos con los cuales he compartido despacho y laboratorio e incontables horas de trabajo. Gracias por los buenos y malos momentos, por aguantarme y por escucharme.

En general quisiera agradecer a todas y cada una de las personas que han vivido conmigo la realización de esta tesis doctoral, con sus altos y bajos y que no necesito nombrar porque tanto ellas como yo sabemos que desde los más profundo de mi corazón les agradezco el haberme brindado todo el apoyo, colaboración, ánimo y sobre todo cariño y amistad.

Por último, en el apartado personal, mi gratitud y todo mi amor a Javi, por ser mi compañero y amigo. Por su inestimable apoyo y comprensión para sobrellevar el abandono al que ha estado sometido durante todas las horas que he dedicado a éste trabajo, y a pesar de ello me ha prestado siempre el cariño necesario que sólo una gran persona puede dar. Porque en su compañía las cosas malas se convierten en buenas, la tristeza se transforma en alegría y la soledad no existe.

UNIVERSITAT ROVIRA I VIRGILI
MEMBRANE FOULING CHARACTERIZATION BY CONFOCAL SCANNING LASER MICROSCOPY
Maria Malgorzata Zator
ISBN:978-84-693-0712-0/DL:T-422-2010

UNIVERSITAT ROVIRA I VIRGILI
MEMBRANE FOULING CHARACTERIZATION BY CONFOCAL SCANNING LASER MICROSCOPY
Maria Malgorzata Zator
ISBN:978-84-693-0712-0/DL:T-422-2010

To my family

UNIVERSITAT ROVIRA I VIRGILI
MEMBRANE FOULING CHARACTERIZATION BY CONFOCAL SCANNING LASER MICROSCOPY
Maria Malgorzata Zator
ISBN:978-84-693-0712-0/DL:T-422-2010

UNIVERSITAT ROVIRA I VIRGILI
MEMBRANE FOULING CHARACTERIZATION BY CONFOCAL SCANNING LASER MICROSCOPY
Maria Malgorzata Zator
ISBN:978-84-693-0712-0/DL:T-422-2010

ABSTRACT

In fields such as the food and dairy industries, biotechnology, and the treatment of industrial effluents, pressure-driven membrane processes such as microfiltration are increasingly being used for the separation, purification and clarification of protein-containing solutions. A major limitation to the widespread use of membrane filtration, however, is fouling. Fouling is usually attributed to pore constriction, pore blocking or the deposition of cells and cell debris on the membrane surface and can lead to a reduction in the filtrate flux of more than an order of magnitude. Progress in developing a means for characterizing, controlling and preventing membrane fouling has been impeded by lack of suitable non-invasive fouling-measurement techniques. The main aim of this study is to develop suitable strategies for applying Confocal Scanning Laser Microscopy (CSLM) to characterise membrane fouling caused by biological macromolecules. Microfiltration experiments of single, binary and ternary model solutions of proteins, polysaccharides and polyphenols were carried out and CSLM images of the membranes at the end of the different filtration runs were obtained, in order to obtain quantitative and qualitative information about fouling patterns. Some trials of on-line monitoring of cross-flow microfiltration processes were also carried out.

This thesis is divided into five chapters. In Chapter 1 we describe the state of the art of monitoring techniques for characterising fouling phenomena in pressure-driven membrane processes, present the most important results obtained so far, list the main aims of the project and report the most relevant conclusions.

In Chapter 2 we present the protocols developed for the off-line and on-line characterization of protein fouling by CSLM. First we discuss the main characteristics of CSLM, such as its ability to provide high-resolution images from different depths of a three-dimensional object. Second we develop suitable strategies for using CSLM for characterising membrane fouling during the microfiltration of protein solutions (single and binary solutions of BSA–fluorescein and ovalbumin–Texas red) through polycarbonate membranes. The protocols describe in detail the preparation and analysis of the membrane samples by CSLM (image acquisition) and the use of image analysis software and 3D reconstruction software to obtain qualitative and quantitative information from the image stacks gathered by CSLM. Our most significant results show that CSLM can be used to locate and visualize, on top of and inside the membranes, each protein individually. Quantitative data on the presence of the proteins inside the pores can also be obtained using a parameter specially defined for this purpose (P_s, i.e. the fraction of the pore surface where the protein is detected). Finally, we present a critical assessment of CSLM limitations in the characterization of membrane fouling. We conclude that the visualization of the pores under CSLM is possible only for microfiltration membranes. Also, the main limitation for on-line visualization is the lack of suitable, commercially available objectives.

UNIVERSITAT ROVIRA I VIRGILI
MEMBRANE FOULING CHARACTERIZATION BY CONFOCAL SCANNING LASER MICROSCOPY
Maria Malgorzata Zator
ISBN:978-84-693-0712-0/DL:T-422-2010

In Chapter 3 we apply the protocols for characterising membrane fouling caused by solutions containing a protein and a polysaccharide, which are model solutions for the major foulants in membrane bioreactors (MBRs). The characterization is conducted using macroscopic data (permeate flux evolution and resistance) and microscopic analysis by CSLM. We also study how the presence of fluorescent probe conjugates affects membrane fouling. Our results show that for all operating conditions (different solutions of BSA and dextrans 70 kDa and 150 kDa with total concentration of 0.5 g/L, polycarbonate and mixed esters membranes), internal fouling is the prevailing mechanism. However, when the binary solution of protein/dextran contains the dextran with the lowest molecular weight, fouling is more severe and the time needed to reach the steady state is lower. From the images obtained by CSLM we calculated the fraction of the pore surface where protein and/or dextran are detected (P_s), thus obtaining information about the degree of pore blockage. In that specific study, we obtained values of P_s up to a depth of 3 μm inside the membrane. Our results show that fluorescent probe conjugates may have a significant impact on the fouling of high surface porosity membranes (i.e. mixed esters) but a negligible effect on membranes with a low surface porosity (i. e. polycarbonate).

In Chapter 4 we focus on the application of CSLM for the characterization of membrane chemical cleaning processes. We studied the efficiency of permeate flux recovery after water rinsing cycles and chemical cleaning by a commercial cleaning agent (P3 Ultrasil 53) for polycarbonate membranes fouled by protein/polysaccharide solutions. Water rinsing cycles lasted for 30 minutes. For chemical cleaning with P3 Ultrasil 53, several cleaning times (5, 15 and 30 minutes) and cleaning agent concentrations (0.1 and 0.5 %) were tested. We used CSLM to calculate the fraction of pore surface where protein and/or dextran were detected (P_s) and obtain qualitative information from 3D image reconstructions. P_s profiles and data on water flux permeate recovery suggested that water rinsing did not improve membrane permeability. On the other hand, when a protein was involved in membrane fouling, the values of P_s obtained after a rinsing cycle were higher inside the membrane than for the fouled membrane after filtration. For chemical cleaning, the cleaning operating conditions (the concentration of the cleaning agent and the cleaning time) were determinant for water flux recovery. From analyses of P_s profiles and CSLM images, we found that most of the protein and dextran were removed from the membrane during chemical cleaning.

Since most of the biological streams are complex mixtures of proteins, polysaccharides and polyphenols, in Chapter 5 we characterise membrane fouling caused by ternary model solutions containing a protein (BSA-FITC, 0.25 g/L), a polysaccharide (dextran-RITC, 0.25 g/L) and a polyphenol (tannic acid, 0.25, 0.5 and 1 g/L) filtered using polycarbonate membranes with a mean pore size of 0.8 μm. Our results clearly show that the presence of tannic acid reduced permeate flux, regardless of its concentration. Though tannic acid could not be visualized under the imaging conditions used during CSLM analysis, its effect on membrane fouling was clear since in all analyzed membranes we detected a 8.5–17.5 μm thick deposited cake layer that was absent when a protein/dextran solution of the same concentration was studied. The formation of protein/polyphenol and/or protein/dextran/polyphenol complexes is believed to be

UNIVERSITAT ROVIRA I VIRGILI
MEMBRANE FOULING CHARACTERIZATION BY CONFOCAL SCANNING LASER MICROSCOPY
Maria Malgorzata Zator
ISBN:978-84-693-0712-0/DL:T-422-2010

the main cause of external fouling and the decrease in permeate flux. A higher tannic acid concentration in the solution increased the presence of the protein inside the pores. For the highest polyphenol concentration, P_s reached 100% and was maintained from the membrane surface up to 1 μm inside the membrane. The effect of the presence of the polyphenol in the solution on dextran deposition/adsorption on the pores was less obvious than for the protein. However, for all tannic acid concentrations, there was a slight increase in P_s for dextran when tannic acid was present. In the final part of Chapter 5 we study the chemical cleaning of membranes fouled with ternary solutions of BSA/dextran/tannic acid. The chemical cleaning protocol was similar to those for binary solutions and the results, with water permeate flux recoveries of between 35-55%, were similar to those in Chapter 4.

UNIVERSITAT ROVIRA I VIRGILI
MEMBRANE FOULING CHARACTERIZATION BY CONFOCAL SCANNING LASER MICROSCOPY
Maria Malgorzata Zator
ISBN:978-84-693-0712-0/DL:T-422-2010

UNIVERSITAT ROVIRA I VIRGILI
MEMBRANE FOULING CHARACTERIZATION BY CONFOCAL SCANNING LASER MICROSCOPY
Maria Malgorzata Zator
ISBN:978-84-693-0712-0/DL:T-422-2010

RESUMEN

En sectores tan diversos como la industria alimentaria, la biotecnología y el tratamiento de aguas residuales, la filtración tangencial con membranas se viene utilizando de forma creciente en la separación, purificación y clarificación de distintas corrientes de proceso que contienen gran variedad de compuestos orgánicos. La limitación principal para el empleo industrial de las técnicas de separación por membranas es el ensuciamiento de éstas. El ensuciamiento se atribuye, de forma general, a la reducción en el diámetro de los poros, a su bloqueo y/o a la formación de un depósito en la superficie de la membrana. El avance en el desarrollo de técnicas para la caracterización, el control y la prevención del ensuciamiento de las membranas ha estado limitado por la falta de técnicas adecuadas y no invasivas para la medición del ensuciamiento. El objetivo principal del presente proyecto es desarrollar estrategias apropiadas para aplicar microscopía láser confocal de barrido (CSLM) al estudio del ensuciamiento de membranas de filtración, centrándose en el ensuciamiento causado por macromoléculas biológicas. En la tesis se han llevado a cabo experimentos de microfiltración (MF) de soluciones modelo puras y de mezclas de proteínas, polisacáridos y polifenoles. Las imágenes captadas mediante CSLM de las membranas al final de diferentes experimentos de filtración, han servido para obtener información cualitativa, sobre localización de las distintas moléculas, y cuantitativa, sobre la presencia individual de cada compuesto en el interior y la superficie de la membrana. Se han realizado también intentos de aplicación de visualización en línea mediante CSLM del proceso de microfiltración.

La tesis se ha dividido en cinco capítulos. El Capítulo 1 se ha dedicado a presentar una breve introducción sobre las técnicas principales utilizadas en la caracterización del ensuciamiento de las membranas de MF, y los principales resultados obtenidos hasta el momento. También ha servido para presentar los objetivos generales de la tesis y las conclusiones más destacables.

El Capítulo 2 presenta los protocolos desarrollados para la caracterización del ensuciamiento de membranas de MF durante (on-line) y después (off-line) de la filtración de soluciones de proteínas mediante CSLM. En primer lugar se presentan las características principales de CSLM, técnica que permite obtener imágenes de alta resolución a diferentes profundidades de un objeto tridimensional, sin necesidad de una preparación previa de la muestra. A continuación se desarrollan las estrategias apropiadas para que CSLM pueda ser utilizado en la caracterización del ensuciamiento de membranas durante la filtración de soluciones de proteína (soluciones puras y mezclas de BSA-fluoresceína y ovoalbúmina–Texas red) mediante membranas de policarbonato. Estas estrategias incluyen desde los protocolos de análisis de las membranas en el microscopio, hasta la aplicación de programas de análisis de imagen y de reconstrucción tridimensional que permitan obtener información cualitativa y cuantitativa sobre el ensuciamiento. Los resultados más importantes muestran que CSLM puede ser

UNIVERSITAT ROVIRA I VIRGILI
MEMBRANE FOULING CHARACTERIZATION BY CONFOCAL SCANNING LASER MICROSCOPY
Maria Malgorzata Zator
ISBN:978-84-693-0712-0/DL:T-422-2010

utilizado para la localización y visualización de las dos proteínas fluorescentes de forma individual, tanto sobre la superficie de la membrana como en el interior de los poros. También es posible realizar la cuantificación de la presencia de las proteínas en el interior de los poros, mediante un parámetro definido para este propósito. Se han evaluado de forma crítica las limitaciones de CSLM para la caracterización del ensuciamiento de membranas. Se ha concluido que si se desea visualizar los poros de la membrana, CSLM restringe su aplicación únicamente a membranas de MF. En el caso de la visualización en línea, la principal limitación está relacionada con la escasez de objetivos comerciales adecuados.

En el Capítulo 3 se han aplicado los protocolos desarrollados a la caracterización del ensuciamiento de membranas causado por soluciones modelo de una proteína y un polisacárido, como intento de aproximación a los principales causantes del ensuciamiento en bioreactores de membranas. La caracterización se ha realizado combinando datos macroscópicos (evolución de flujo de permeado y resistencias) y el análisis microscópico de las membranas mediante CSLM. Además, se ha estudiado el efecto de la presencia de los fluoróforos en el ensuciamiento, comparando experimentos realizados con mezclas fluorescentes y no fluorescentes. Los resultados muestran que, para todas las condiciones de operación utilizadas (diferentes soluciones de BSA y dextranos 70 kDa y 150 kDa con una concentración total de 0.5 g/L, membranas de policarbonato y de acetato de celulosa), el mecanismo predominante es el ensuciamiento interno, sin embargo, cuando la solución binaria proteína/dextrano contiene el dextrano de menor peso molecular, el ensuciamiento es más severo y en un tiempo menor se alcanzan valores de flujo muy reducidos en menor tiempo. Las imágenes obtenidas con CSLM han permitido calcular la fracción de superficie de poro donde la proteína y/o dextrano se han detectado (P_s), proporcionando información sobre el grado de obstrucción de los poros. En el presente proyecto ha sido posible obtener valores de P_s hasta una profundidad de 3 μm en el interior de la membrana. Respecto al efecto del marcaje fluorescente sobre el ensuciamiento, los resultados indican que puede ser apreciable en membranas de porosidad superficial grande, como las de acetato de celulosa, mientras que con membranas de porosidad superficial muy baja (membranas de policarbonato) el efecto es prácticamente inapreciable.

El Capítulo 4 se ha centrado en la aplicación de CSLM para caracterizar procesos de limpieza de membranas. Se ha estudiado la eficacia en la recuperación del flujo de permeado de la aplicación de ciclos de lavado con agua y de ciclos de limpieza con un agente químico comercial. Este estudio ha utilizado membranas de policarbonato después de la filtración de soluciones proteína/polisacárido. La duración del ciclo de lavado con agua se ha mantenido constante a 30 min, mientras que para el agente químico (P3 Ultrasil 53) se han variado tanto el tiempo de aplicación (5, 15 y 30 min) como la concentración (0.1 y 0.5 %). CSLM se ha utilizado para calcular la fracción de superficie de poro donde la proteína y/o dextrano están

UNIVERSITAT ROVIRA I VIRGILI
MEMBRANE FOULING CHARACTERIZATION BY CONFOCAL SCANNING LASER MICROSCOPY
Maria Malgorzata Zator
ISBN:978-84-693-0712-0/DL:T-422-2010

presentes (P_s) y obtener información cualitativa con reconstrucciones 3D. Estos resultados combinados con los datos sobre recuperación del flujo de agua, han permitido concluir que el lavado con agua no mejora la permeabilidad de la membrana, y en el caso concreto de la proteína se obtienen valores de P_s mayores en el interior de la membrana, comparados con los obtenidos después de la filtración. Para la limpieza química, se observa que las condiciones de operación (concentración del agente y el tiempo de limpieza) son determinantes en la recuperación del flujo del agua. El análisis de los perfiles de P_s y las imágenes de CSLM, indican que la mayor parte de la proteína y del dextrano se han eliminado de la membrana durante la limpieza química.

Como la mayor parte de las soluciones biológicas están compuestas por mezclas complejas de proteínas, polisacáridos y polifenoles, en el Capítulo 5 se ha caracterizado el ensuciamiento de una solución modelo ternaria constituida por una proteína (BSA-FITC, 0.25 g/L), un polisacárido (dextrano-RITC, 0.25 g/L) y un polifenol (ácido tánico, 0.25, 0.5 y 1 g/L) filtrada a través de membranas de policarbonato de 0.8 μm. Los resultados obtenidos muestran claramente que la presencia de ácido tánico reduce el flujo de permeado, independientemente de su concentración. Aunque el ácido tánico no puede ser visualizado en las condiciones de captación del microscopio confocal, el efecto de su presencia se hace evidente, ya que en todas las membranas analizadas se ha observado la presencia de un depósito en la superficie de la membrana de espesor entre 8.5 y 17.5 μm. La formación de complejos proteína/polifenol y/o proteína/dextran/polifenol se cree que es la causa principal de este aumento del ensuciamiento. El aumento de la concentración de ácido tánico en la solución aumenta la presencia BSA-FITC dentro de los poros, llegando a obtenerse, para la concentración más alta de ácido tánico, unos valores de P_s del 100 % que se mantienen hasta una profundidad de 1μm dentro de la membrana. La presencia del ácido tánico sobre la deposición/adsorción de dextrano en los poros de la membrana tiene un efecto menos marcado que para la proteína, sin embargo, para todas las concentraciones estudiadas, se observa un leve aumento de los valores de P_s para el dextrano. Se han aplicado también protocolos de limpieza química sobre las membranas utilizadas durante la filtración de soluciones ternarias, obteniéndose resultados similares a los comentados en el Capítulo 4.

UNIVERSITAT ROVIRA I VIRGILI
MEMBRANE FOULING CHARACTERIZATION BY CONFOCAL SCANNING LASER MICROSCOPY
Maria Malgorzata Zator
ISBN:978-84-693-0712-0/DL:T-422-2010

UNIVERSITAT ROVIRA I VIRGILI
MEMBRANE FOULING CHARACTERIZATION BY CONFOCAL SCANNING LASER MICROSCOPY
Maria Malgorzata Zator
ISBN:978-84-693-0712-0/DL:T-422-2010

NOMENCLATURE

A_f	surface of the pore in which a fluorescent foulant is detected [%]
A_P	surface occupied by pores [%]
C_b	polyphenol concentration [g/L]
C_p	protein concentration [g/L]
FREC	flux recovery [%]
FRED	flux reduction [%]
J	permeate flux [kg/(m^{2}h)]
$J_{cleaning}$	pure water flux after cleaning [kg/(m^{2}h)]
$J_{filtration}$	pure water flux or buffer flux after filtration [kg/(m^{2}h)]
$J_{original}$	pure water flux of the clean membrane [kg/(m^{2}h)]
J_{rising}	pure water flux or buffer flux after rinsing [kg/(m^{2}h)]
μ	viscosity [Pa·s]
ΔP	transmembrane pressure [Pa]
P_s	fraction of pore surface in which protein is detected [%]
P_{s0}	P_s value at the membrane surface [%]
R	rejection [%]
$R_{fouling}$	polarization and fouling resistance [m^{-1}]
R_m	clean membrane hydraulic resistance [m^{-1}]
R_{total}	total resistance [m^{-1}]
z	depth from the surface [μm]
$z_{1/2}$	z value where $P_s = P_{s0}/2$ [μm]

UNIVERSITAT ROVIRA I VIRGILI
MEMBRANE FOULING CHARACTERIZATION BY CONFOCAL SCANNING LASER MICROSCOPY
Maria Malgorzata Zator
ISBN:978-84-693-0712-0/DL:T-422-2010

UNIVERSITAT ROVIRA I VIRGILI
MEMBRANE FOULING CHARACTERIZATION BY CONFOCAL SCANNING LASER MICROSCOPY
Maria Malgorzata Zator
ISBN:978-84-693-0712-0/DL:T-422-2010

LIST OF FIGURES

UNIVERSITAT ROVIRA I VIRGILI
MEMBRANE FOULING CHARACTERIZATION BY CONFOCAL SCANNING LASER MICROSCOPY
Maria Malgorzata Zator
ISBN:978-84-693-0712-0/DL:T-422-2010

UNIVERSITAT ROVIRA I VIRGILI
MEMBRANE FOULING CHARACTERIZATION BY CONFOCAL SCANNING LASER MICROSCOPY
Maria Malgorzata Zator
ISBN:978-84-693-0712-0/DL:T-422-2010

UNIVERSITAT ROVIRA I VIRGILI
MEMBRANE FOULING CHARACTERIZATION BY CONFOCAL SCANNING LASER MICROSCOPY
Maria Malgorzata Zator
ISBN:978-84-693-0712-0/DL:T-422-2010

UNIVERSITAT ROVIRA I VIRGILI
MEMBRANE FOULING CHARACTERIZATION BY CONFOCAL SCANNING LASER MICROSCOPY
Maria Malgorzata Zator
ISBN:978-84-693-0712-0/DL:T-422-2010

UNIVERSITAT ROVIRA I VIRGILI
MEMBRANE FOULING CHARACTERIZATION BY CONFOCAL SCANNING LASER MICROSCOPY
Maria Malgorzata Zator
ISBN:978-84-693-0712-0/DL:T-422-2010

LIST OF TABLES

UNIVERSITAT ROVIRA I VIRGILI
MEMBRANE FOULING CHARACTERIZATION BY CONFOCAL SCANNING LASER MICROSCOPY
Maria Malgorzata Zator
ISBN:978-84-693-0712-0/DL:T-422-2010

LIST OF PUBLICATIONS

I **M. Zator**, M. Ferrando, F. López, C. Güell, (2009), Microfiltration of protein/dextran/polyphenol solutions: characterization of fouling and chemical cleaning efficiency using confocal microscopy, Journal of Membrane Science, submitted.

II M. Ferrando, **M. Zator**, F. López, C. Güell, (2008), Confocal Scanning Laser Microscopy: Fundamentals and uses on membrane fouling characterization and opportunities for on-line monitoring in "Monitoring and Visualizing Membrane – based Processes", Whiley-VCH Verlag GmbH & Co.KGcA Wanheim, Germany, pp. 57-77.

III **M. Zator,** J. Warczok, M. Ferrando, F. López, C. Güell, (2009), Chemical cleaning of polycarbonate membranes fouled by BSA/dextran mixtures, Journal of Membrane Science 327, pp 59-68.

IV **M. Zator**, M. Ferrando, F. López, C. Güell, (2007), Membrane Fouling Characterization by confocal microscopy during filtration of BSA/dextran mixtures, Journal of Membrane Science 30, pp. 57-66.

V **M. Zator**, M. Ferrando, F. López, C. Güell, (2006), Characterization of foulant removal by confocal scanning laser microscopy, Desalination 200, pp. 203-204.

VI M. Ferrando, A. Różek, **M. Zator**, F. López, C. Güell, (2005), An approach to membrane fouling characterization by confocal scanning laser microscopy, Journal of Membrane Science 250, pp. 283-293.

UNIVERSITAT ROVIRA I VIRGILI
MEMBRANE FOULING CHARACTERIZATION BY CONFOCAL SCANNING LASER MICROSCOPY
Maria Malgorzata Zator
ISBN:978-84-693-0712-0/DL:T-422-2010

UNIVERSITAT ROVIRA I VIRGILI
MEMBRANE FOULING CHARACTERIZATION BY CONFOCAL SCANNING LASER MICROSCOPY
Maria Malgorzata Zator
ISBN:978-84-693-0712-0/DL:T-422-2010

CONTENTS

UNIVERSITAT ROVIRA I VIRGILI
MEMBRANE FOULING CHARACTERIZATION BY CONFOCAL SCANNING LASER MICROSCOPY
Maria Malgorzata Zator
ISBN:978-84-693-0712-0/DL:T-422-2010

UNIVERSITAT ROVIRA I VIRGILI
MEMBRANE FOULING CHARACTERIZATION BY CONFOCAL SCANNING LASER MICROSCOPY
Maria Malgorzata Zator
ISBN:978-84-693-0712-0/DL:T-422-2010

UNIVERSITAT ROVIRA I VIRGILI
MEMBRANE FOULING CHARACTERIZATION BY CONFOCAL SCANNING LASER MICROSCOPY
Maria Malgorzata Zator
ISBN:978-84-693-0712-0/DL:T-422-2010

UNIVERSITAT ROVIRA I VIRGILI
MEMBRANE FOULING CHARACTERIZATION BY CONFOCAL SCANNING LASER MICROSCOPY
Maria Malgorzata Zator
ISBN:978-84-693-0712-0/DL:T-422-2010

1

PROJECT THESIS OVERVIEW

UNIVERSITAT ROVIRA I VIRGILI
MEMBRANE FOULING CHARACTERIZATION BY CONFOCAL SCANNING LASER MICROSCOPY
Maria Malgorzata Zator
ISBN:978-84-693-0712-0/DL:T-422-2010

UNIVERSITAT ROVIRA I VIRGILI
MEMBRANE FOULING CHARACTERIZATION BY CONFOCAL SCANNING LASER MICROSCOPY
Maria Malgorzata Zator
ISBN:978-84-693-0712-0/DL:T-422-2010

1.1. State of the art

In recent years, considerable progress has been made in the development of membrane separation technologies. Pressure-driven membrane separation processes are important and attractive because of their high removal efficiencies, and can be applied in a variety of industrial fields such as food, dairy, biotechnology and the treatment of industrial effluents. However, several problems still have to be solved, before pressure-driven membrane techniques are widely accepted in industry. One of the most important challenges is to understand membrane fouling and subsequent permeate flux decline, which are inevitably associated with membrane processes. Recently, non–invasive microscopic techniques have become the key to breakthroughs in our comprehension of fouling phenomena [1-4] and considerable effort is being made in this area.

1.1.1. Membrane microfiltration

Membrane microfiltration is increasingly used for the separation, purification and clarification of protein-containing solutions. Microfiltration is a pressure-driven membrane process well-suited to the separation of particles ranging in size from approximately 0.02 to 10.00 μm. In microfiltration, when a new membrane is used, its clean water flux is directly proportional to the applied transmembrane pressure. The main advantages of this technique are simplicity, continuity and rapidity. However, its major drawbacks are flux decline and changes in rejection characteristics due to membrane fouling [5-11].

1.1.2. Membrane fouling

Membrane fouling is one of the critical factors that determines the effectiveness of membrane processes. External fouling occurs on the top surface of the membrane due to the accumulation of cells or large particles that do not enter the pores, whereas internal fouling occurs within the internal pore structure of the membrane due to deposition and adsorption of small particles and proteins or other macromolecules which are able to pass into the pores. The internal and external fouling models used to interpret the data are based on Darcy´s law, which provides a relationship between flow rate and pressure drop across a cake layer

$$J = \frac{\Delta P}{\mu R_{total}} \tag{1.1}$$

where J is the permeate flux, ΔP is the transmembrane pressure, μ is the viscosity and R_{total} is the total resistance.

Although proteins and polysaccharide molecules are generally one order of magnitude smaller than the pore size of typical microfiltration membranes, they cause significant fouling. Internal fouling takes place when particles enter the membrane pores, deposit and/or adsorb to the pore walls or entrance. External fouling occurs when particles are deposited as a layer on the surface of the membrane.

To describe internal fouling, two simple models have been developed: the standard blocking model (SBM) and the pore blocking model (PBM) which can be described by complete pore blockage (CBM) and intermediate pore blockage (IBM). SBM assumes that the flux decline is caused by foulants being deposited evenly along the pore walls, decreasing the pore diameter; however, the number of active pores per unit area is assumed to remain constant. It is also assumed that the change in pore volume due to fouling is proportional to the filtrate volume. The other internal fouling model, PBM, assumes that the number of pores that become plugged increases proportionally to the filtrate volume, while pore diameter remains constant [6-7]. Jiraratananon *et al.* [8] and Duclos-Orsello *et al*. [9] use two other blocking models to describe the PBM model: the complete blocking model (CBM) and intermediate blocking model (IBM). In CMB, particles cannot superimpose on one another. IBM, however, is less restrictive: not every particle necessarily blocks the pores and some particles may settle on top of the other particles. External fouling is described by the cake formation model (CFM), which assumes that cake resistance increases with time due to the deposition of rejected material (cells, cell debris, protein aggregates and others) on the membrane surface [6-9].

1.1.3. Membrane fouling characterization

Many theories and techniques have been investigated and developed in order to better understand and help prevent membrane fouling. Most of the research on protein fouling has focused on indirect observation of the process by measuring macroscopic parameters such as permeate flux, pressure drop and solute rejection, and although they provide some information about microscopic phenomena, they are not suitable for validating mechanistic models.

In the last 10 years several novel non-invasive techniques have been developed and many of the existing ones have been improved. Chan and Chen [12] reviewed current advancements in membrane characterization techniques, and Chen *et al*. [13] presented a critical survey of in situ monitoring techniques for fouling phenomena in pressure driven membrane filtration processes.

UNIVERSITAT ROVIRA I VIRGILI
MEMBRANE FOULING CHARACTERIZATION BY CONFOCAL SCANNING LASER MICROSCOPY
Maria Malgorzata Zator
ISBN:978-84-693-0712-0/DL:T-422-2010

1.1.4. Applications of confocal scanning laser microscopy to membranes and membrane processes

Microscopic techniques have been successfully applied to visualize and monitor fouling progress on membrane surfaces and to monitor the dynamics of cake layer buildup. Conventional optical microscopy enables particle deposition to be directly visualized during filtration, but its resolution is low, and is ultimately limited by the wavelength of light. It is for this reason that the resolution of the electron microscope, which relies instead on beams of electrons, is greater. Electronic microscopy, such as Scanning Electron Microscopy (SEM), Transmission Electron Microscopy (TEM) and currently Environmental Scanning Electron Microscopy (ESEM) have been extensively applied to provide qualitative information on foulant structure and morphology. These techniques offer high resolution images (up to 1 nm for SEM) of the membrane surface and of the cross section of membrane pores, while internal deposition within the pores and differentiation among several foulants when a multicomponent suspension is filtrated are still difficult to detect. Additionally, SEM and TEM require special specimen preparation, which can result in membrane alteration and artifacts.

Confocal Scanning Laser Microscopy (CSLM) is an optical microscopic technique that has been commercially available since the late 1980s and which has several advantages over conventional optical and electronic microscopy. Confocal microscopy, as a result of optical sectioning, simplifies specimen preparation in a non-invasive and non-destructive manner, without any environment modification. It provides extraordinary three dimensional, high resolution imaging of specimens not just on the surface but also at different depths of the membrane. Series of optical coplanar cross-sections, collected at different depths so that a given volume can be scanned, provide extensive three-dimensional structural data. CSLM imaging uses multiple color channels to record the information about individual elements such as the membrane or the species involved in membrane fouling [14-16].

A confocal microscope can operate in transmission, reflection or fluorescence modes, although the fluorescent mode seems to be the most powerful. The laser light of a chosen wavelength excites the fluorescent labeled specimen. The emitted fluorescence, which scatters in all directions, is then channeled through a pinhole or confocal aperture. Emitted in-focus light passes through the aperture and is detected by a photomultiplier connected to a computer that builds up an image. Out-of-focus light does not pass through the aperture and is not detected, resulting in a considerably sharper image than the one provided by convectional fluorescence microscopy. Different focus levels make optical sectioning possible, and combining the information of several focal levels, recorded as a stack of through-focus images, gives the possibility to built up a three dimensional reconstruction of the specimen.

Although some macromolecules that can be used in microfiltration processes present autofluorescence or have an inherent fluorescence capacity, most of them do not, so the most common way of operating is to induce fluorescence in the specimens by chemical treatment, which is known as secondary fluorescence. Nowadays, up to 28 commercial fluorophores are in practical use and they cover the overall range of commercial laser sources available in CSLM microscopes [17].

Applying commercially available software to digitized CSLM images makes it possible to obtain both qualitative and quantitative information about feature-specific parameters related to object/structure dimensions (area, length, width, perimeter, surface area, volume, grey level) and shapes (form factor, convexity, number of holes and so forth) [18].

Scientists quickly realized that confocal microscopy makes it possible to investigate the microscopic world in three dimensions. However, its application to the characterization of membranes and membrane fouling has been rather limited. Early research used CSLM to characterize the morphologies of microporous membranes and to obtain values of surface porosity and pore size. Some perspectives and limitations of this relatively new technique in the area of membrane technology were also discussed. CSLM was also applied to study the interactions between proteins and ion-exchange membranes and for the first time the adsorption of protein on ion exchange membrane was observed in situ. Subsequently these investigations were extended to other types of membranes and foulants. Recent developments and improvements have pushed this technique to the limit and obtained not only qualitative information about the three-dimensional distribution of each foulant on the top of the membrane and/or inside the pores but also quantitative data. However, CSLM is currently creating considerable expectation in the ambit of membrane and membrane-process characterization because of the possibility of quantitative analysis during real-time, on-line monitoring of pore constriction and cake-formation process. This kind of information will be a huge step forward in the understanding of fouling mechanisms, and help to develop much more effective cleaning procedures that can be useful for designing large-scale membrane processes.

Recently, Ferrando *et al*. [18] have extensively reviewed current developments in the application of CSLM to characterize pressure-driven membrane processes. They have also provided a detailed explanation of CLSM fundamentals, the conditions in which specimens can be visualized correctly and also some examples of image analysis that lead to quantitative information of membrane structure and the extent of fouling.

As mentioned above early research used CSLM to characterize the morphologies of microporous membranes and to obtain values of surface porosity and pore size. In 1995, Berg *et al*. [19] used CSLM together with AFM to characterize the differences in the morphology of polypropylene membranes. Furthermore, Charcosset and Bernengo [20], and Charcosset *et al*.

UNIVERSITAT ROVIRA I VIRGILI
MEMBRANE FOULING CHARACTERIZATION BY CONFOCAL SCANNING LASER MICROSCOPY
Maria Malgorzata Zator
ISBN:978-84-693-0712-0/DL:T-422-2010

[21-22] investigated CSLM for the characterization of the morphology of five microfiltration membranes. They showed how accurate CSLM images were, and also discussed the advantages and disadvantages of CSLM compared to SEM. They concluded that CSLM characterizes the morphology of the investigated microporous membranes much more accurately than SEM, which only provides surface views. Its low resolution (≈0.4 μm), however, is undoubtedly its main drawback.

Thomas *et al*. [23] studied the in situ visualization of polyamide membrane formation to acquire greater understanding of the mechanism and kinetics of the process. Two slope-casting chambers were designed so that the precipitation process could be observed from both the substrate side and the bath side. This new application of confocal microscopy has measured the dynamics of nylon membrane precipitation with sufficient time and depth resolution to permit quantitative testing of models of the precipitation process. Turner and Cheng [24] used CSLM together with hydrophilic fluorescent probes of varying molecular weights to directly visualize changes in the interpenetrating polymer network (IPN) morphology formed during the polymerization-induced phase separation (PIPS) of polydimethyl siloxane-polymethacrylic acid (PDMS-PMAA) IPNs. The images obtained showed the complexity and spacial distribution of differently-sized superimposed hydrophilic domain structures. They found that this morphology was assigned to the phase-separated structures formed and partially arrested at continuously varying quench depths during the PIPS process. This observation provides information about morphology development in PIPS and contributes to a better understanding of the process.

The application of CSLM in conjunction with AFM, SEM and X-ray photoelectron spectroscopy made it possible to characterize the morphology, surface composition, in situ surface and internal structure of the membranes in aqueous media of various pHs [25]. Green *et al*. recently presented the first attempt to establish CSLM with 3D image reconstruction as a state-of-the-art method for quantifying the micromechanical deformations caused by stretching and to characterize pore structure in microporous composite membranes [26]. By applying this technique they quantified the membrane deformation and the increase in membrane porosity caused by stretching. They determined the factors that affect the mechanical behavior of the membrane and obtained information about the mechanism governing the formation of membrane morphology. Other studies that successfully applied CSLM as an effective tool for investigating microporous membrane characteristics underline its unique advantage over other advanced microscopic techniques: that is, the three-dimensional information that can be used to accurately depict structure and, therefore, give some insight into real membrane models. The application of CSLM in fluorescent and reflection modes provided information to determine pore dimensions, surface roughness, morphology and structure, and the distribution of alumina particles in poly(vinylidene fluoride) (PVDF) organic-inorganic membranes [27]. It was found that the addition of alumina particles not only increased pore size and the number of pores in PDVF

membranes, but also increased the roughness of membrane surface morphology. The final result was an increase in the effective filtration area and in the permeation flux of the membrane. CSLM was also shown to be an effective and practical technique for porous membrane analysis. Protocols based on the rational segmentation of sets of CSLM images were used to obtain quantitative information about NaX zeolite membrane thickness and surface roughness [28]. Image calibration based on the fluorescent intensity of the fluorophores was used to estimate the size of sub-resolution features. This technique, coupled with the evaluation of statistical metrics such as porosity, feature autocorrelation and feature size distribution, enabled more quantitative and conclusive rationalization of even subtle differences in permeation performance based upon membrane polycrystallinity. This study, for the first time, provided a very good understanding of the film growth process, underscoring the viability of CSLM as a powerful tool for quantitative membrane characterization.

CSLM has also found a great number of applications in the characterization of membrane processes such as monitoring the adsorption and deposition of particles within the membrane pores and surface, and protein/membrane interactions. Ljunglöf and Thömmes [29] and Linden *et al*. [30] studied the uptake of different proteins (lyzosome, human IgG, BSA) to cation-exchange porous adsorbents during batch experiments in a finite bath, and obtained intensity profiles of the fluorescently labeled protein distribution. They concluded that confocal scanning images have unforeseen potential for comparing experimental results with theoretical predictions. According to these authors, CSLM offers a unique opportunity for directly observing protein concentration within porous particles and for measuring the distribution of proteins during various stages of the uptake process. They also believe that CSLM could be a valuable method for validating experimentally simpler and cheaper techniques, which could then be tested for their reliability and their potential for obtaining information on protein sorption. Ahmed and Pyle [31] used CSLM to study the distribution of fluorescently labeled ovalbumin and BSA on two anion exchangers. CSLM images and intensity profiles showed that both proteins bind preferentially to the surface rather than the core of the spherical anion exchangers. According to these authors, CSLM is an excellent tool for selecting among different ion exchangers for the optimization of protein purification processes.

Reichert *et al*. [32] used confocal microscopy to visualize in situ adsorption of a single model protein (BSA or lysozyme) onto an ion-exchange asymmetric membrane for the first time. They labeled both the membrane and the protein with fluorescent dyes and created dual-color images of areas with localized fouling. Their investigation showed that fluorescent intensity profiles obtained after the translation of confocal images can be used to quantitatively estimate adsorbent uptake into the ligand layer. Because of the optical limitation of the confocal microscope the analysis could only be performed to a depth of approximately 50 μm in a 200-μm-thick membrane. Hayama *et al*. [33-34] visualized the distribution of an endotoxin (Et)

UNIVERSITAT ROVIRA I VIRGILI
MEMBRANE FOULING CHARACTERIZATION BY CONFOCAL SCANNING LASER MICROSCOPY
Maria Malgorzata Zator
ISBN:978-84-693-0712-0/DL:T-422-2010

trapped inside various kinds of Et-blocking filtration dialysis membranes. Using CSLM together with other techniques such as AFM, they studied the influence of the physicochemical properties of membrane material and structure in order to clarify the mechanisms governing Et-blocking. They saw Et adsorption on the membranes, followed by pore narrowing and, finally, complete pore plugging, thus clarifying the mechanisms responsible of Et rejection by Et-blocking membranes. Ferrando *et al*. [10] investigated microfiltration membranes fouled by a biological stream consisting of single or binary protein solutions (BSA-fluorescein and ovalbumin-Texas red). They developed appropriate strategies and standardized protocols for sample analysis so that CSLM could be applied to characterize fouling patterns. They managed to visualize and identify both proteins, and then, by applying image analysis algorithms, they obtained quantitative information on fouling location, defined as the fraction of pore surface in which protein has been detected (P_s, equation 1.2), which is related to the presence of proteins inside the pores.

$$P_S = \frac{A_f}{A_p} \tag{1.2}$$

where A_f is the surface of the pore in which a fluorescent foulant was detected and A_p the surface occupied by pores.

On the three-dimensional reconstructions, they also showed qualitative data related to the morphology of the adsorption/deposition of proteins (BSA and ovalbumin) on the membrane surface and/or inside the pores. Doumèche *et al*. [35] used CSLM together with Attenuated Total Reflection Fourier Transform Infrared (ATR-FTIR) spectroscopy, lectin-binding analysis and epifluorescence microscopy to characterize the composition and organization of membrane foulants in a French drinking water production plant. They applied multiple stains and recorded them simultaneously. The results gathered in this study confirmed that most of the polysaccharides analyzed were located extracellularly throughout the biofilm matrix. A high degree of heterogeneity and special organization were observed within the fouling material, and the stained parts of the fouling matter varied in depth from 6 to 27 μm. The organization of microbial cells in microcolonies in the superficial layer of fouling deposits suggested that the cake layer was organized as an interpenetrated network mainly composed of exopolysaccharides supporting microbial cell adhesion.

Very recently, some studies on fouling characterization in membrane bioreactors (MBRs) have been published. Chen *et al*. [36] used a quadruple staining protocol combined with CSLM to generate three-dimensional distributions of nucleic acids, proteins and polysaccharides in the fouling layer formed on a mixed cellulose ester membrane. For the first time, this study constructed a three-dimensional volumetric grid model representing the fouling layer structure on the basis of a series of CLSM images. It also presented quantitative structural information about the fouling layer and the distribution of the four foulants. They also assumed that

structural information obtained on the fouling layer could be applied for further study: for example, the exploration of the fouling mechanisms of membranes or the construction of a comprehensive fouling layer model. More recently, Tian and coworkers [37-38] used CSLM to observe the distribution of stained polysaccharides (ConA-FITC with d-glucose or d-mannose) and different bacteria (all dyed with Rhodamine) in a fouling layer attached to the membrane surface in membrane coagulation bioreactors (MCBRs) and MBRs. They observed that polysaccharides were extensively distributed on the membrane surface of both MCBRs and MBRs, together with some bacteria. In some regions, bacteria and polysaccharides were found to coexist and/or overlap within the membrane surface. The information obtained from CSLM images and supported by data taken from SEM images indicated that the polysaccharides could be adsorbed onto the membrane surface and form the gel layer. It also proved the existence of a dense and nonporous fouling cake.

Yang *et al*. [39] combined CSLM analysis with a six-fold staining protocol to determine the distribution of nucleic acids, proteins, polysaccharides and lipids in the biofouling layer formed on a mixed cellulose ester membrane. By image processing they produced the volumetric grid model of the fouling layer structure, which was used to simulate the intra-layer flow field during filtration. Consequently, they were able to estimate the effective permeability of the fouling layer and the effects of pore blockage inside the layer. Hawang *et al*. [40] applied CSLM-Image analysis to study the effects of a membrane fouling reducer (a cationic polymeric material) on flux enhancement in a submerged MBR.

CSLM has also been successfully used together with particle size analysis, SEM, X-ray fluorescence, energy-diffusive X-ray analysis and FTIR spectroscopy to study the mechanism behind the formation of the cake layer in MBR [41]. Meng and Yang [42] investigated the fouling behavior of bulking sludge, deflocculated sludge and normal sludge in hollow-fiber membrane bioreactors. They used CSLM to distinguish between different species and visualize the on-line adsorption/deposition process that occurs at different depths of the fouling layer. On the basis of the three dimensional CSLM image reconstruction, it was clear that the cake layer formed with normal sludge had significant voids and channels and was more porous than those formed with bulking and deflocculated sludge, which tend to form dense cake layers. They also observed that cake layers formed with bulking sludge were thicker (97.81 μm) than those formed with normal (58.31μm) and deflocculated sludge (46.53 μm). The main contribution of this study was to show that CSLM could be used to illustrate the deposition of bacterial cells and biopolymers onto the membrane surface as a determinant cause of membrane fouling.

Recently, a study of wastewater treatment membrane bioreactors (MBR) used CSLM in conjunction with a triple staining method to identify the major foulants in the MBR suspension and the sludge fouling layer on the membrane surface. By using image analysis software they identified the size and number of biopolymer clusters (BPCs) in the liquid phase of the MBR

UNIVERSITAT ROVIRA I VIRGILI
MEMBRANE FOULING CHARACTERIZATION BY CONFOCAL SCANNING LASER MICROSCOPY
Maria Malgorzata Zator
ISBN:978-84-693-0712-0/DL:T-422-2010

sludge. Some fluorescently stained bacteria were also embedded within the clusters, although typical microbial aggregates were not observed. The CSLM images indicate that BPC are clusters of organic molecules such as polysaccharides and proteins between 2.5 and about 40 μm in bulk active sludge and between 2.5 and 60 μm in cake sludge. They are expected to play a crucial role in the formation of the fouling layer on the membrane surface. A filtration test with CLSM observation indicated that BPCs are formed by the adsorption and affinity clustering of soluble microbial products (SMP) and colloidal organic matter within the sludge layer deposited on the membrane. Therefore, BPC acts as a glue which facilitates the formation and growth of an impermeable sludge cake on the membrane surface, resulting in serious MBR fouling [43].

Clech *et al*. [44] used CSLM and three other visualization techniques—SEM, ESEM and direct observation (DO)—to observe the fouling of alginate, used as a model compound for polysaccharides, which are considered one of the main foulants in MBRs. They showed the advantages and disadvantages of each technique, and pointed out the high cost of the fluorescent markers used in CSLM. They also suggested that both ESEM and CSLM are novel techniques and require further research to assess their full potential in this field of applications.

An essential requirement to control fouling is periodical membrane cleaning, so suitable methods need to be developed not just to monitor fouling but also to evaluate cleaning efficiency. Spettnann *et al*. [45] filtered a mixture of fluorescently labeled foulants (bacterial cells stained with DAPI or SYTO 62, crimson-fluorescent FluoSpheres, FITC-dextran) through a polyethersulfone ultrafiltration membrane and then cleaned it by ultrasounds in such a way that the deposit was only partly removed. CSLM was able to localize uncleaned, poorly cleaned and completely cleaned areas on the membrane surface and the extend of ultrasound-induced membrane cleaning could be localized. It was found that the CSLM technique could be used with image analysis not only for the three-dimensional reconstruction of the fouling layer and the location of each foulant separately in muli-layer deposits, but also for evaluating cleaning efficiency by comparing fouled membranes before and after ultrasonic treatment.

Kanani *et al*. [46] discussed reversible and irreversible fouling of concentrated protein solutions through cellulose acetate microfiltration membranes. Using CSLM they localized and identified the fluorescently labeled proteins deposited within the membrane. They found that protein fouling was reversible upon front washing with phosphate buffer and there was no need for any kind of physical or chemical cleaning. Further comparison of the thickness of fluorescent zones confirms this observation. According to these authors, membrane fouling had three phases, and the thickness of the protein deposition zone increased with the extent of filtration. At the end of phase I it was 2 μm, at the end of phase II it was around 5 μm, and at the end of phase III it was more than 10 μm. Reversible fouling increased most in phase II while the fouling during phase I was almost irreversible. They observed that protein aggregates provided the initiation points for further deposition of protein monomers, so when the aggregates were removed from the feed

solution, fouling was negligible. CSLM observation demonstrated that protein fouling was largely restricted to a zone close to the membrane surface, which clearly indicates the role of the aggregates retained by sieving.

The most powerful application of confocal scanning laser microscopy is the on-line monitoring of fouling during filtration experiments. To date only two studies have applied this technique to observe deposition of foulant particles on membranes: Kromkamp *et al*. [47] and Brans *et al*. [48]. In the study by Kromkamp *et al*., the main goal was to examine the behavior of bidisperse suspensions in the shear-induced diffusive back-transport regime of microfiltration. The suspensions were filtered using a polyethersulfone membrane with a molecular weight cut-off of 100 kDa. CSLM images scanned at different depths of the membrane were used to monitor particle deposition in the transient flux regime, and the particle deposition on the membrane was calculated as the surface load, which corresponds to the volume of particles per surface area of the membrane. Brans *et al*. studied the deposition of particles on the top of the membrane and inside the pores during dead-end and cross-flow filtration with polymer membranes and polymer microsieves. They used CSLM to investigate the interaction of fluorescent polystyrene microspheres and fluorescent sulfate microspheres with the membranes by on-line monitoring of the particle transmission. The images obtained by CSLM allowed them to quantify the percentage of the membrane surface area covered by particles at different times.

1.1.5. Strengths and limitations of CSLM in the characterization of membranes and membrane processes

In the last few years interest in the use of CSLM for characterizing membranes and membrane processes has been growing, which has increased the number of publications on the topic. CSLM is now a highly beneficial complement to the most accepted microscopic techniques, and it has become the method of choice for those applications that require direct and accurate quantitative analysis of 3D microstructures.

CSLM can be a powerful non-destructive technique that allows in situ and ex situ visualization of various membrane structures as well as the deposition/adsorption of foulants on the membrane surface (cake formation) and inside the pores (internal fouling). The application of image analysis software and the development of suitable protocols provides, among other things, data on pore size, surface porosity, membrane and cake thickness, roughness and the size of defects. CSLM requires just minimal sample preparation and makes it possible to conduct in-situ and on-line experiments. One of the most innovative advantages of this technique is that several foulants can be located and identified at the same time, especially if on–line monitoring in real time is performed. Nowadays, Confocal Scanning Laser Microscopy has paved the way for new and exciting research as well as for routine applications in industry. However, to fully

UNIVERSITAT ROVIRA I VIRGILI
MEMBRANE FOULING CHARACTERIZATION BY CONFOCAL SCANNING LASER MICROSCOPY
Maria Malgorzata Zator
ISBN:978-84-693-0712-0/DL:T-422-2010

explore all the possibilities offered by confocal microscopy, the limitations of the technique have to be understood and, when possible, overcome [10].

The main limitation of CSLM is its low resolution, which is primarily a function of the numerical aperture of the optical system and the wavelength of light. Another important drawback that limits greater use of CSLM in the on-line monitoring of membrane processes is the lack of commercial objectives that combine values of small working distances, which make it possible to work with miniaturized filtration modules, with high numerical aperture (NA) [18]. It should also be pointed out that it is still not possible to monitor very fast processes since the speed of acquisition of a single optical section in most confocal scanning laser microscopes is about 1 second.

It is also of great importance to consider the possible interactions between fluorophores and all the components in the system, when working in the fluorescence mode. It would be advisable to minimize the amount of fluorophore in the target component by applying suitable staining protocols, and to validate the experimental results obtained with and without fluorophores.

1.1. Objectives

The development of a method for the characterisation, control and prevention of membrane fouling has been hindered by a lack of suitable fouling measurement techniques. CSLM is considered a non-invasive technique for monitoring the adsorption/deposition of macromolecules that exhibit fluorescence (natural or induced). The main aim of this study is to characterise membrane fouling caused by biological macromolecules using CSLM. To achieve this aim, we need to meet several other objectives. In the first part of this thesis we discuss the fundamentals of the CSLM technique and the conditions needed for proper visualization of the membrane and foulants. We also develop suitable strategies for obtaining quantitative information about the structure of the membrane and the extent of fouling using CSLM data combined with image analysis. In the second part of the thesis we combine the information obtained from CSLM analysis with macroscopic data to characterize the membranes and the membrane fouling/cleaning processes. The objectives of this thesis are:

- To develop suitable strategies for using CSLM together with image analysis for membrane fouling characterization during the microfiltration of biological streams.
    - ✓ To individually visualize and locate the foulants on the membrane surface and inside the pores.
    - ✓ To develop a protocol for obtaining quantitative information about the presence of individual foulants and their distribution both on the membrane surface and inside the membrane pores.
    - ✓ To obtain qualitative information about the distribution of foulants both on the surface and inside the pores by images based on the three-dimensional reconstruction of optical sections.
    - ✓ To analyse how fluorophore labelling affects membrane fouling.
    - ✓ To develop an operational procedure for obtaining on-line data on the progress of membrane fouling during microfiltration using CSLM; to obtain quantitative information on foulant deposition and/or adsorption on the membrane surface and inside the pores and on possible cake layer formation.
- To conduct the CSLM characterization of biofouling during the microfiltration of model solutions of extracellular polymeric substances (EPS) containing a protein and dextrans as the model for polymeric compounds through two kinds of microfiltration membranes with different surface porosities (polycarbonate and mixed esters).

UNIVERSITAT ROVIRA I VIRGILI
MEMBRANE FOULING CHARACTERIZATION BY CONFOCAL SCANNING LASER MICROSCOPY
Maria Malgorzata Zator
ISBN:978-84-693-0712-0/DL:T-422-2010

- ✓ To determine how the presence of polysaccharide and its molecular size affect membrane fouling.

- ✓ To study how the type of membrane affects the extent of fouling.

- To use CSLM analyses to determine the efficiencies of water rinsing cycles and a commercial cleaning agent in the removal of protein and polysaccharide from polycarbonate membranes.

  - ✓ To obtain, by CSLM analysis, quantitative information about the distribution of protein and dextran inside the membrane pores before and after rinsing or chemical cleaning cycles.

  - ✓ To develop suitable cleaning protocols for polycarbonate microfiltration membranes by combining macroscopic information on permeate flux recovery with qualitative and quantitative data obtained by CSLM.

- To characterize membrane fouling during the microfiltration of ternary solutions containing protein/polysaccharide/polyphenol using macroscopic data (flux and resistance) and microscopic data (CSLM analysis). To evaluate the effect of the chemical cleaning of polycarbonate membranes fouled by protein/polysaccharide/polyphenol solutions.

  - ✓ To study the influence of polyphenol addition on membrane fouling.

  - ✓ To obtain qualitative and quantitative information about internal and external fouling (P_s profiles, cake layer thickness, foulant distribution)

  - ✓ To evaluate the efficiency of chemical cleaning procedures for removing cake layer from the membrane surface and foulants deposited and/or adsorbed within the membrane pores.

1.2. Conclusions

In this thesis we have primarily focused on the use of CSLM for characterising membrane fouling during the microfiltration of biological streams. Many techniques exist for observing the fouling of membrane materials but CSLM seems to provide new opportunities for better understanding membrane fouling. Our main conclusions are listed in the following pages. Results to support these conclusions are presented in each chapter.

- On the suitability of CSLM for membranes and membrane fouling characterization we conclude that:
    - ✓ Information about internal and external fouling morphology can easily be accessed: the location and identification of fluorescently labelled fouling agents (e.g. proteins, polysaccharides) inside the membrane pores, on the top of the membrane and within the cake layer can be obtained from CSLM images and mainly by the three-dimensional reconstruction of the image stacks.
    - ✓ The prevailing fouling mechanisms and the contribution of each foulant to the overall fouling pattern can be identified by simultaneously evaluating the results from image analysis of CSLM data and macroscopic data (permeate flux and resistance evolution, retention and rejection profiles).
    - ✓ Applying image analysis algorithms and measuring parameters such as the fraction of the pore surface in which a particular foulant (protein or polysaccharide) is detected can provide quantitative information about the presence of fouling and its distribution inside the membrane pores.

- On the use of CSLM for on-line monitoring of the membrane fouling process we conclude that:
    - ✓ The main disadvantage of using CSLM for on-line characterization of membrane fouling during the microfiltration of protein solutions is the lack of commercially available CSLM objectives that combine short working distances with a high numerical aperture. The design of the cross-flow filtration module and running operational parameters should be optimized.

- On the use of CSLM for membrane fouling characterization of single, binary and ternary solutions using different kinds of microfiltration membranes, we conclude that:
    - ✓ Fluorescent dyes clearly influence the foulant-membrane and foulant-foulant interactions. However, under certain microfiltration conditions (e.g. a membrane with low surface porosity) this influence is almost negligible.

UNIVERSITAT ROVIRA I VIRGILI
MEMBRANE FOULING CHARACTERIZATION BY CONFOCAL SCANNING LASER MICROSCOPY
Maria Malgorzata Zator
ISBN:978-84-693-0712-0/DL:T-422-2010

- ✓ Proteins and different molecular weight dextrans from single and binary solutions cause extensive internal fouling. No cake layer formation was observed under the experimental conditions studied.
- ✓ The molecular size of the dextran used to prepare binary protein/dextran model solutions significantly affects the extent of fouling on mixed- esters membranes. Larger molecular size dextran leads to fouling reduction.
- ✓ Fouling caused by proteins (in single or binary solutions) on polycarbonate and mixed-esters membranes is largely irreversible under the experimental conditions tested.
- ✓ Adding tannic acid to a protein/dextran solution led to extensive external fouling, regardless of the concentration of polyphenol.

- On the characterization of rinsing and cleaning protocols using CSLM we conclude that:
  - ✓ CSLM analysis enables us to quantify the amount of protein and dextran residues on the membrane surface and inside the membrane pores after the application of rinsing and cleaning protocols.
  - ✓ Water and phosphate buffer rinsing are ineffective for membrane flux restoration because they caused foulant molecules to drive more deeply into the membrane pores (as shown in the P_s profiles), thus increasing blockage.
  - ✓ Applying cleaning protocols with an enzymatic cleaning agent (US53) to polycarbonate membranes after the microfiltration of binary (protein/dextran) and ternary (protein/dextran/polyphenol) solutions always resulted in the partial recovery of pure water flux.
  - ✓ The length of cleaning time and the concentration of the cleaning agent were key parameters in the recovery of pure water flux. A long cleaning time causes small pieces of foulant aggregates to drive more deeply into the membrane pores, which blocks the pores and reduces pure water flux. An increase in the concentration of the cleaning agent slightly improves the recovery of water permeate flux.
  - ✓ Chemical cleaning completely removed the cake layer from the membrane surface.

1.4. References

1. K.H Choo, C.H. Lee, Understanding membrane fouling in terms of surfacef energy Changes, Journal of Colloid and Interface Science 226 (2000) 367-370.
2. J.C. Chen, Q. Li, M. Elimelech, In situ monitoring techniques for concentration polarization and fouling phenomena in membrane filtration, Advances in Colloid and Interface Science 107 (2004) 83-108.
3. H. Choi, K. Zhang, D. Dionysiou, D.B. Oerther, G.A. Sorial, Effect of permeate flux and tangential flow on membrane fouling for wastewater treatment, Separation and Purification Technology 45 (2005) 68-78.
4. F.J. Benitez, J.L. Acero, A.I. Leal, M. Gonzales, The use of ultrafiltration and nanofiltration membranes for the purification of corc processing wastewater. Journal of Hazardous Materials (2008), doi:10.1016/j.jhazmat.2008.06.036.
5. S.T. Kelly, A.L. Zydney, Mechanisms for BSA fouling during microfiltration, Journal of Membrane Science 107 (1995)115-127.
6. E.M. Tracey, R.H. Davis, Protein fouling of track-eached polycarbonate microfiltration Membranes, Journal of Colloid and Interface Science 167 (1994) 104-116.
7. C. Güell, R.H. Davis, Membrane fouling during microfiltration of protein mixtures, Journal of Membrane Science 119 (1996) 269-284.
8. R.Jiraratananon, D. Uttapap, P. Sampranpiboon, Crossflow microfiltration of a colloidal suspension with the presence of macromolecules, Journal of Membrane Science 140 (1998) 57-66.
9. Ch. Duclos-Orsello, W. Li, Ch. Ho, A three mechanism model to describe fouling of microfiltration membranes, Journal of Membrane Science 280 (2006) 856-866.
10. M. Ferrando, A. Rózek, M. Zator, F. López, C. Güell, An approach to membrane fouling characterization by confocal scanning laser microscopy, Journal of Membrane Science 259 (2005) 283-293.
11. D. Wu, J.A. Howell, R.W. Field, Critical flux measurement for model colloids, Journal of Membrane Science 152 (1999) 89-98.
12. R. Chan, V. Chen, Characterization of protein fouling on membranes: opportunities and challenges, Journal of Membrane Science 242 (2004) 169-188.
13. J.C. Chen, Q. Li, M. Elimelech, In situ monitoring techniques for concentration polarization and fouling phenomena in membrane filtration, Advances in Colloid and Interface Science 107 (2004) 83-108.
14. A. Lamprecht, U. Schafer, C.M. Lehr, Structural analysis of microparticles by confocal scanner laser microscopy, American Association of Pharmaceutical Scientists – Pharmaceutical Science Technology, 1(3) (2000) article 17.
15. J.B. Pawley, Fundamental limits in confocal microscopy, Handbook of Biological Confocal Microscopy, Plenum Press, New York, 1995, pp 19-37.

UNIVERSITAT ROVIRA I VIRGILI
MEMBRANE FOULING CHARACTERIZATION BY CONFOCAL SCANNING LASER MICROSCOPY
Maria Malgorzata Zator
ISBN:978-84-693-0712-0/DL:T-422-2010

16. J.B. Xavier, A.Schnell, S. Wuertz, R.Palmer, D.C. White, J.S. Almeida, Objective threshold selection procedure (OTS) for segmentation of scanning laser confocal microscope images, Journal of Microbiological Methods 47 (2001) 169-180.
17. R.P. Haugland, Handbook of Fluorescent Probes and Research Products 5th edition. Eugene: Molecular Probes, Inc. 2002. On-line: www.probes.com.
18. M. Ferrando, **M. Zator**, F. López, C. Güell, (2008), Confocal Scanning Laser Microscopy: Fundamentals and uses on membrane fouling characterization and opportunities for on-line monitoring in "Monitoring and Visualizing Membrane –based Processes", Whiley-VCH Verlag GmbH & Co.KGcA Wanheim, Germany, pp. 57-77.
19. R.van den Berg, D. Schulze, J.A. Bolt-Westerhoff, F. de Jong, D.N. Reinhoult, D. Velinova, L. Buitenhuis, Influence of membrane microstructure on the diffusion barrier of supported liquid crystalline membranes, Journal of Physical Chemistry, 99 (1995) 7760-7765.
20. C. Charcosset, J.C. Bernengo, Comparison of microporous membrane morphologies using confocal scanning laser microscopy, Journal of Membrane Science 168 (2000) 53-62.
21. C. Charcosset, A. Cherfi, J.C. Bernengo, Characterization of microporous membrane morphology using confocal scanning laser microscopy, Chemical Engineering Science, 55 (2000) 5351-5358.
22. C. Charcosset, F. Yousefian, J.F. Thovert, P.M. Adler, Calculation of flow and solute deposition through three.dimensional reconstructed model of microporous membranes, Desalination 145 (2002) 133-138.
23. J.L. Thomas, M. Olzog, C. Drake, C-H. Shih, C. C. Gryte, Polyamide membrane precipitation studied by confocal backscattering microscopy, Polymer, 43 (2002) 4153-4157.
24. J.S.Turner, Y.L. Cheng, Morphology of PDMS-PMAA IPN membranes, Macromolecules 36 (2003) 1962-1966.
25. K. Zhang, H. Huang, G. Yang, J. Shaw, C. Yip, X. Y. Wu, Characterization of nanostructure of stimuli-responsive polymeric composite membranes, Biomacromolecules 5 (2004) 1248-1255.
26. D.L. Green, L. McAmish, A. V. McCormick, Three-dimensional pore connectivity in bi-axially stretched microporous composite membranes, Journal of Membrane Science 279 (2006) 100-110.
27. L. Yan, L. Hui, S. Xianda, L. Jianghong, Y. Shuili, Confocal laser scanning microscope analysis of organic-inorganic microporous membranes, Desalination 217 (2007) 203-211.
28. M.A. Snyder, D.G. Vlachos, V. Nikolakis, Quantitative analysis of membrane morphology, microstructure, and polycrystallinity via laser scanning confocal microscopy: Application to NaX zeolite membranes, Journal of Membrane Science 290 (2007) 1-18.

29. A. Ljunglöf, J. Thömmes, Visualising intraparticle protein transport in porous adsorbents by confocal microscopy, Journal of Chromatography A, 813 (1998) 387-395.
30. T. Linden, A. Ljunglöf, M.-R Kula, J Thömmes, Visualizing two component protein diffusion in porous adsorbents by confocal scanning laser microscopy, Biotechnology and Bioengineering 65 (1999) 622-628.
31. M. Ahmed, D.L. Pyle, Investigation of single protein adsorption on ion exchangers using confocal laser scanning microscopy, Journal of Chemical Technology and Biotechnology 74 (1999)193-198.
32. U. Reichert, T. Linden, G. Belfort, M.R. Kula, J. Thömmes, Visualizing protein adsorption to ion-exchange membranes by confocal microscopy, Journal of Membrane Science 199 (2002) 161-166.
33. M. Hayama, T. Miyasaka, S. Mochizuki, H. Asahara, K. Tsujioka, F. Kohori, K. Sakai, Y. Jinbo, M. Yoshida, Visualization of distribution of endotoxin trapped in an endotoxin-blocking filtration membrane, Journal of Membrane Science 210 (2002) 45-53.
34. M. Hayama, T. Miyasaka, S. Mochizuki, H. Asahara, K. Yamamoto, F. Kohori, K. Tsujioka, K. Sakai, Optimum dialysis membrane for endotoxin blocking, Journal of Membrane Science, 219 (2003) 15-25.
35. B. Doumeche, L. Galas, H. Vaudry, P. Di Martino, Membrane foulants characterization in a drinking water production unit, Food and Bioproducts Processing 85 (2007) 42-28.
36. M.Y. Chen, D.J. Lee, Z. Yang, X.F. Peng, J.Y. Lai, Fluorescent staining for study of extracellular polymeric substances in membrane biofouling layers, Environmental Science and Technology, 40 (2006) 6642-6646.
37. J. Tian, H. Liang, Y. Yang, S. Tian, G. Li, Membrane adsorption bioreactors (MABR) for treating slightly polluted surface water supplies: As compared to membrane bioreactor (MBR), Journal of Membrane Science 325 (2008) 262-270.
38. J. Tian, H. Liang, Y. Yang, S. Tian, G. Li, Membrane coagulation bioreactor (MCBR) for drinking water treatment, Water Research 42 (2008) 3910-3920.
39. Z. Yang, X.F. Peng, M.Y. Chen, D.J. Lee, J.Y. Lai, Intra-layer flow in fouling layer on membranes, Journal of Membrane Science, 287 (2006) 280-286.
40. B.K. Hwang, W.N. Lee, P.K. Park, C.H. Lee, I.S. Chang, Effect of fouling membrane reducer on cake structure and membrane permeability in membrane bioreactor, Journal of Membrane Science 288 (2007) 149-156.
41. F. Meng, H. Zhang, F. Yang, L. Liu, Characterization of cake layer in submerged membrane bioreactor, Environmental Science Technology 41 (2007) 4065-4070.
42. F. Meng, F.Yang, Fouling mechanisms of deflocculated sludge, normal sludge, and bulking sludge in membrane bioreactor, Journal of Membrane Science 305 (2007) 48-56.
43. F. Sun, X. Wang, X. Li, Visualization and characterization of biopolymer clusters in a submerged membrane bioreactor, Journal of Membrane Science 325 (2008) 691-697.

UNIVERSITAT ROVIRA I VIRGILI
MEMBRANE FOULING CHARACTERIZATION BY CONFOCAL SCANNING LASER MICROSCOPY
Maria Malgorzata Zator
ISBN:978-84-693-0712-0/DL:T-422-2010

44. P. Le-Clech, Y. Marselina, Y. Ye, R.M. Stuetz, V. Chen, Visualizing of polysacharide fouling on microporous membrane using different characterization techniques, Journal of Membrane Science 290 (2007) 36-45.
45. D.Spettmann, S. Eppmann, H-C. Flemming, J.Wingender, Visualization of membrane cleaning using confocal scanning laser microscopy, Desalination 224 (2008) 195-200.
46. D.M.Kanani, X.Sun, R.Ghosh, Reversible and irreversible membrane fouling during in-line microfiltration of concentrated protein solutions, Journal of Membrane Science 315 (2008) 1-10.
47. J. Kromkamp, F. Faber, K. Schroen, R. Boom, Effects of particle size segregation on cross-flow microfiltration performance: Control mechanism for concentration polarization and particle fractionation, Journal of Membrane Science 268 (2006) 189–197.
48. G. Brans, A. van Dinther, B. Odum, C.G.P.H. Schroën, R.M. Boom, Transmission and fractionation of micro-sized particles suspensions, Journal of Membrane Science 290 (2007) 230-240.

UNIVERSITAT ROVIRA I VIRGILI
MEMBRANE FOULING CHARACTERIZATION BY CONFOCAL SCANNING LASER MICROSCOPY
Maria Malgorzata Zator
ISBN:978-84-693-0712-0/DL:T-422-2010

UNIVERSITAT ROVIRA I VIRGILI
MEMBRANE FOULING CHARACTERIZATION BY CONFOCAL SCANNING LASER MICROSCOPY
Maria Malgorzata Zator
ISBN:978-84-693-0712-0/DL:T-422-2010

2

OFF-LINE AND ON-LINE CHARACTERIZATION OF MEMBRANE FOULING BY CONFOCAL SCANING LASER MICROSCOPY.

This chapter has been published as:

M. Ferrando, A. Różek, M. Zator, F. López, C. Güell, An approach to membrane fouling characterization by confocal scanning laser microscopy, Journal of Membrane Science 250 (2005) 283-293.

UNIVERSITAT ROVIRA I VIRGILI
MEMBRANE FOULING CHARACTERIZATION BY CONFOCAL SCANNING LASER MICROSCOPY
Maria Malgorzata Zator
ISBN:978-84-693-0712-0/DL:T-422-2010

UNIVERSITAT ROVIRA I VIRGILI
MEMBRANE FOULING CHARACTERIZATION BY CONFOCAL SCANNING LASER MICROSCOPY
Maria Malgorzata Zator
ISBN:978-84-693-0712-0/DL:T-422-2010

2.1. Introduction

A major limitation restricting overall performance of membrane filtration is fouling and the resulting progressive decline of permeate flux with time. By adjusting proper filtration conditions, flux decline can be minimized by reduction of concentration polarization and fouling. It is greatly important to understand the mechanisms which influence the performance of the membranes. Identification of the location of fouling and the ability to follow the development of the foulant layer with time is a crucial step in understanding the fouling phenomena [1-8].

As extensively reviewed in the previous section of this work (1.1), the knowledge of the mechanisms involved in membrane fouling has risen significantly. In the last years the losses due to sample preparation, inability to discriminate between the different species on the surface in order to ascertain which dominate the fouling process, and location of the foulant are the main restrictions of the current techniques for protein fouling characterization. Therefore, progress in developing a means for characterizing, controlling and preventing membrane fouling should be directed to suitable non-invasive fouling measurement techniques [9,10]

In recent decades confocal scanning laser microscopy (CSLM) has become a powerful tool in biology to examine fixed specimens that have been stained with fluorescent dyes. CSLM offers promising opportunities for membrane characterization in no invasive manner and also as a tool for on line monitoring of the filtration processes. One of the main advantages of CSLM over most of the other characterization techniques mentioned is that it can distinguish among different species (depending on their fluorescent emission) .

CSLM is an optical microscopic technique that was commercially developed in the early nineties and has several advantages over conventional optical microscopy and electronic microscopy. CSLM has better resolution through the observation axis than conventional optical microscopy, and at the same time it provides high resolution images obtained at different depths of a three-dimensional object. This optical sectioning of the sample means that invasive techniques need not be used in sample preparation, since physical slicing is no longer necessary. Therefore, CSLM makes it possible to visualize a variety of structures (cellular organules and membranes, emulsion drops, microorganisms) and macromolecules without modifying their environment, which is a clear advantage over electronic microscopy [11].

CSLM can be used in transmission and reflection modes, but fluorescence imaging proves to be the most powerful technique in biological applications and in the microscopy of food materials. Figure 2.1 shows the confocal principle in fluorescence optical microscopy. An excitation beam from the laser is reflected by the dichroic mirror and focussed by the objective lens on a limited spot or microvolume in the specimen. Flourescence light emitted from the irradiated spot passes

through the dichroic mirror and an adjustable imaging aperture or pinhole, which is placed confocally to the illumination aperture, and is collected by a photomultiplier. The instantaneous response of the light detector at all points of this scan must be displayed with the equivalent spatial position and relatively brightness on a monitor screen. To build-up a two-dimensional image, either the beam or the microscope stage has to be scanned in a raster pattern, with simultaneous accumulation of a digitized image [12,13]. One of the main advantages of the confocal microscope is the exclusion of out-of-focus blur. The fluorescence emissions from the illuminated regions of the specimen above and below the in-focus point are not allowed to reach the photomultiplier, as a pinhole in front of the detector ensures that only light from the in-focus point is collected (Figure 2.1). Different focus levels make optical sectioning possible and a thick specimen can be imaged in three dimensions, one of the most useful properties of CSLM. By combining the information on several focal planes that is on optical slices stored in a computer a three-dimensional image that describes the object can be built up [14].

Figure 2.1. Confocal schematic. Light from the laser is reflected by the dichroic mirror into the objective lens. The lens focuses the light beam at a spot within the specimen. The fluorescent light, because of its longer wavelength, passes through the dichroic mirror and it comes to a focus at the plane of the detector pinhole. Only that fluorescence emission from the in-focus spot is able to pass through the pinhole detector.

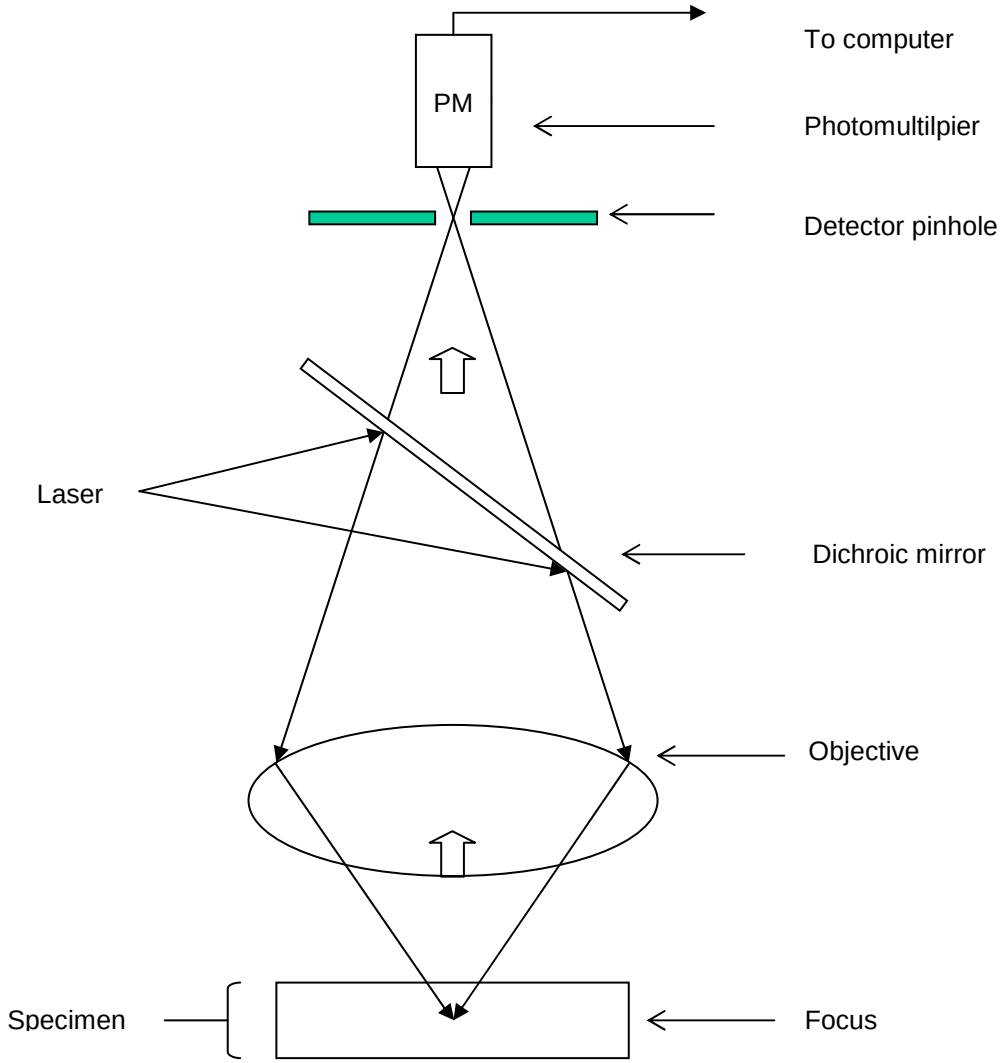

UNIVERSITAT ROVIRA I VIRGILI
MEMBRANE FOULING CHARACTERIZATION BY CONFOCAL SCANNING LASER MICROSCOPY
Maria Malgorzata Zator
ISBN:978-84-693-0712-0/DL:T-422-2010

The limits of CSLM are related to its resolution. Resolution in CSLM is primarily function of the numerical aperture of the optical system and the wavelength of the light, but it can be also limited if the signal levels represent so few quanta that the signal lacks the statistical precision to produce a 'visible' feature or if the data is not correctly sampled because the pixels are two large [11]. In the best case, the CSLM resolves 180 nm in the focal plane (x,y) and only 500-800 nm along the optic axes (z) [15]. According to this, the use of CSLM to characterize surface porosity is restricted to microfiltration membranes.

Some macromolecules present autofluorescence or have an inherent fluorescence capacity but, mostly, the fluorescence has to be induced by chemical treatment. This is also known as secondary fluorescence, and can be achieved in two ways: a) by treating the sample with specific stains (fluorochromes) or producing specific fluorescent reaction products in the sections of interest; b) by applying fluorescent-labeled biological molecules with binding affinity for specific constituents. The number of fluorophores with an absorption wavelength close to the emission wavelengths of the available lasers is quite limited. Fluorescein, rhodamine nitrobenzoxadiazole (NBD) and acridines are some of the classical fluorophores that are commonly used in CSLM. Afterwards, cyanines, borate-dipyrromethane, Texas red and cascade blue are some of the main groups of molecules that have been developed. The general requirements that a fluorescent probe has to fulfil to be used in CSLM are the following: a) the maximum absorption of the fluorescent has to be close to the emission wavelength of the laser; b) the fluorescent emission must be intense; c) multi-labeling experiments in which more than one structure is stained require fluorescent compounds whose excitation/emission wavelengths overlap minimally. On the other hand, it is important to note that the size of the fluorophores does not alter the adsorption/interaction behavior of the molecules.

The main aim of this chapter is to develop the appropriate strategies so that CSLM can be used to characterize fouling during the microfiltration of biological solutions. As a first step single and binary solutions of BSA conjugated with fluorescein and ovalbumin conjugated with Texas red will be filtered using polycarbonate microfiltration membranes. Samples of the membranes at the end of the filtration cycle will be analyzed by CSLM. A standardized protocol in the sample analysis by CSLM and in the image analysis using the appropriate software will be presented. In this chapter we will mainly focus on how basic information related to membrane fouling can be obtained by CSLM. Secondly, on-line monitoring by CSLM of the protein particles adsorption/deposition on the polycarbonate membrane will be carried out, using a cross flow filtration module specially designed to adjust to CSLM configuration.

2.2. Materials and Methods

2.2.1. Microfiltration plant and experiments

The first step was to develop working protocols to run off-line membrane characterization by CSLM. When the off-line protocols had been developed, fully tested and optimized, a special cross-flow filtration module to carry out on-line membrane fouling characterization by CSLM was designed. The specific feature of the cross-flow filtration module was that it could be mounted above the CSLM objective. The cross-flow filtration plant was also adapted to the CSLM equipment to allow all the on-line experiments to be conducted.

Off-line: Microfiltration experiments were carried out using a lab scale filtration plant (Figure 2.2) which consisted of a 10 cm^3 Nucleopore stir cell connected to a feed vessel containing the protein solution. A peristaltic pump (Watson Marlow 3135) was used to feed the solution. All runs were conducted at room temperature (20-23 ℃), with a constant flow rate of 0.48 mL/s during an 180 minute period (transmembrane pressure ranging from 0.2×10^5 Pa to 1.2×10^5 Pa). Permeate mass data were taken every 10 seconds. Fresh protein solution (0.25 g/L) and a new membrane were loaded into the apparatus before each experiment. Three different protein solutions (fluorescent and non-fluorescent) were used in the experiments: single BSA, single ovalbumin (OVA) and a binary mixture of BSA and ovalbumin. Total protein concentration was maintained in all the solutions at 0.25 g/L. The permeate was collected in a reservoir placed on an electronic microbalance (Denver Instruments XL 3100) interfaced to a personal computer to collect and record mass versus time data. All experiments were run in duplicate. After each run, the apparatus was thoroughly cleaned using a 2% sodium hydroxide solution, and then rinsed in prefiltered deionized water.

Figure 2.2. Lab scale filtration plant to run off-line experiments, 1 - feed vessel, 2 - peristaltic pump, 3 - manometer, 4 - dead-end filtration module, 5 - sampling of permeate to determine fluxes 6 – electronic microbalance connected to the computer.

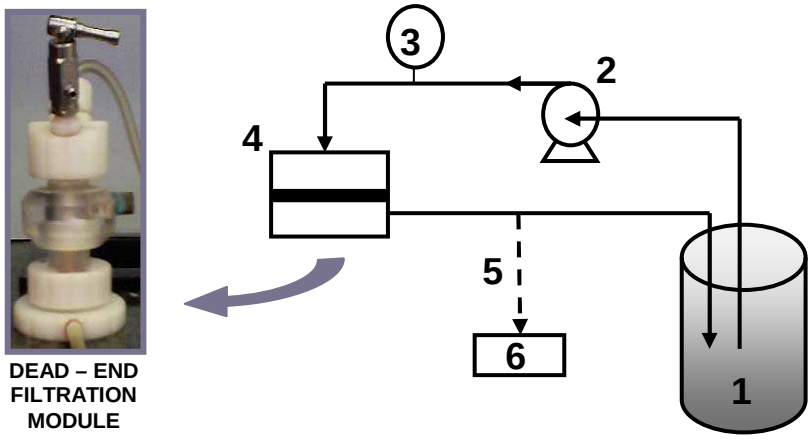

UNIVERSITAT ROVIRA I VIRGILI
MEMBRANE FOULING CHARACTERIZATION BY CONFOCAL SCANNING LASER MICROSCOPY
Maria Malgorzata Zator
ISBN:978-84-693-0712-0/DL:T-422-2010

On-line: Microfiltration experiments were carried out using a lab scale filtration plant (Figure 2.3) which consisted of a cross-flow filtration module specially designed to fit the CSLM microscope, connected to a feed vessel containing the protein solution. A peristaltic pump (Watson Marlow 3135) was used to feed the solution. All runs were carried out at room temperature (20-23 ℃), under maximum working pressure of 0.15×10^5 Pa. The runs lasted 20, 60, 180 and 240 minutes. In all cases, firstly phosphate buffer solution (PBS) pH 7.4 was run through the system for a few minutes. Then the circulation was stopped, the membrane surface was localized and a z-stack of images was collected. Afterwards, the buffer solution was completely flushed out of the system by pumping in the BSA-FITC solution, which took around two minutes (initial concentration of BSA-FITC was 0.5 g/L or 1 g/L). A z-stack of the same field of the membrane after the protein solution was introduced into the system was also obtained. This was taken to represent the membrane at initial conditions. Z-stacks of the fouled membrane with protein were obtained at 15, 30, 45, and 60 minutes and then every 30 minutes until the end of the run. Membrane samples of the fouled membrane obtained at 240 minutes and using 1 g/L initial concentration of BSA-FITC were also analyzed using two different confocal microscope objectives (40 x and 100 x). Fresh protein solution (0.5 g/L and 1 g/L), and new membrane were loaded into the apparatus before each experiment.

Figure 2.3. Lab scale filtration plant to run on-line experiments, 1- feed vessel, 2 - peristaltic pump, 3 - manometer, 4 - cross-flow filtration module, 5 – back pressure regulator, 6 - sampling of permeate and retentate to determine fluxes, 7 - electronic microbalance connected to the computer.

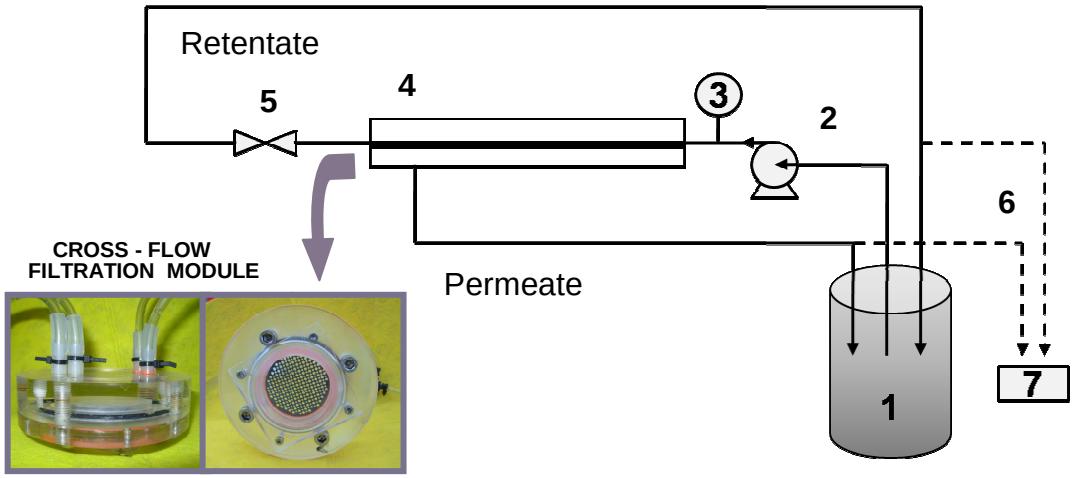

2.2.2. Membranes, proteins and chemicals

Off-line: Microfiltration experiments were conducted using polycarbonate track etched 25 mm membrane discs from Micron Klear (K02BR02500) with a nominal pore size of 0.22 μm, and from Whatman (110659) with nominal pore size of 0.8 μm, with a clean water flux of 1.83 L/(m^2s) at 1 × 10^5 Pa . BSA was purchased from Sigma (A-3803) and ovalbumin (400450500) from Across Organics. BSA-fluorescein conjugate (494 nm/520 nm) was from Sigma (A-9771) and ovalbumin-Texas red conjugate (596 nm/615 nm) was from Molecular Probes (O-23021). A phosphate buffer was used to adjust the pH of all protein solutions to 7.4.

On-line: Microfiltration experiments were conducted using polycarbonate track etched 47 mm membrane discs from Osmonics INC (K04BP810FX) with nominal pore size 0.8 μm with a clean water flux of 5.71 L/(m^2s) at 0.51 × 10^5 Pa. BSA-fluorescein conjugate (494 nm/520 nm) was from Sigma (A-9771) and a phosphate buffer was used to adjust the pH of all protein solutions to 7.4.

2.2.3. Microscopes and sample preparation

Off-line: Scanning Electron Microscopy (SEM) (JEOL JSM-35C, UK) and CSLM (Leica TCDS 4D) where used to obtain pictures of clean and fouled membranes. For SEM analysis, the original membranes were coated with a 1.5 x 10^{-2} mm layer of gold before the photographs were taken. The voltage ranged from 15 to 25 kV and magnification was 1000 x. For CSLM analysis, all the membranes (original or fouled) were cut to the appropriate size to fit a holder, and a drop of Mowiol (Calbiochem 475903) was added to preserve fluorescence. This mounting medium has a refraction index close to the immersion oil (1.518), is able to solidify avoiding problems with the movement of the sample (or the coverslip) relative to the slide and contains anti-fading agents for unstable reagents. Membranes used in the experiments with fluorescent and non-fluorescent proteins were prepared in the same way. The samples from off–line experiments were magnified by 100 x or 40 x objective (NA 1.3, WD 0.2 mm), and the zoom magnification was set at 2.6.

On-line: CSLM (Nikon D - Eclipse C1) with specially designed filtration module was used to obtain images of the membrane before, during and after filtration. In all cases the 40 x magnification objective (CFI Plan Fluor ELWD NA 0.6, WD 3.7-2.7 mm) was used, and the zoom magnification was set at 2.31.

UNIVERSITAT ROVIRA I VIRGILI
MEMBRANE FOULING CHARACTERIZATION BY CONFOCAL SCANNING LASER MICROSCOPY
Maria Malgorzata Zator
ISBN:978-84-693-0712-0/DL:T-422-2010

2.2.4. CSLM analysis in reflection and fluorescence modes

A protocol was developed to carry out the CSLM analysis of the membrane samples. This made it possible to obtain suitable information for membrane characterization and protein deposition on the membrane. All the membrane samples were first analyzed in reflection mode, since it helped to select the position of the z-axes corresponding to the membrane surface (Figure 2.4).

Then, all the fouled membranes were analyzed using the fluorescence mode with the appropriate laser wavelength (488 nm for fluorescein and 586 nm for Texas red). In off-line experiments, specimens were magnified by a 100x or/and 40x objective (NA 1.3), and zoom magnification was set at 2.6. For on-line experiments the working distance had to be increased to 2.7 mm and therefore the magnification reduced to 40x objective (NA 0.6), the zoom magnification used was 2.31.The resolution of a confocal image depends not only on the contrast intrinsic to the feature but also on the number of photons detected. The number of photons used was increased by averaging four scans in all cases, which led to better-resolved images. The membrane after the filtration of the buffer solution and the membrane fouled with non-fluorescent proteins (BSA and OVA) were used as a control to set the detection conditions for the fluorescent signals. The detection conditions were kept constant for samples obtained at the same filtration conditions.

Optical sectioning of the membranes was performed to obtain a stack of through-focus images (z-series), which were used to carry out the z-projection and 3D reconstruction (orthogonal and volumetric) of the membrane. Z-projection is created by comparing the successive images from a through-focus series and storing the brightest value at each pixel position. Images were taken from the surface of the membrane to the inside and to the outside each 0.16 μm, resulting a series of images. This optical sectioning provided data on protein penetration into the membrane up to 3 μm (25% of the total membrane thickness), and into a 3 μm cake of protein deposited on top of the membrane (Figure 2.5).

UNIVERSITAT ROVIRA I VIRGILI
MEMBRANE FOULING CHARACTERIZATION BY CONFOCAL SCANNING LASER MICROSCOPY
Maria Malgorzata Zator
ISBN:978-84-693-0712-0/DL:T-422-2010

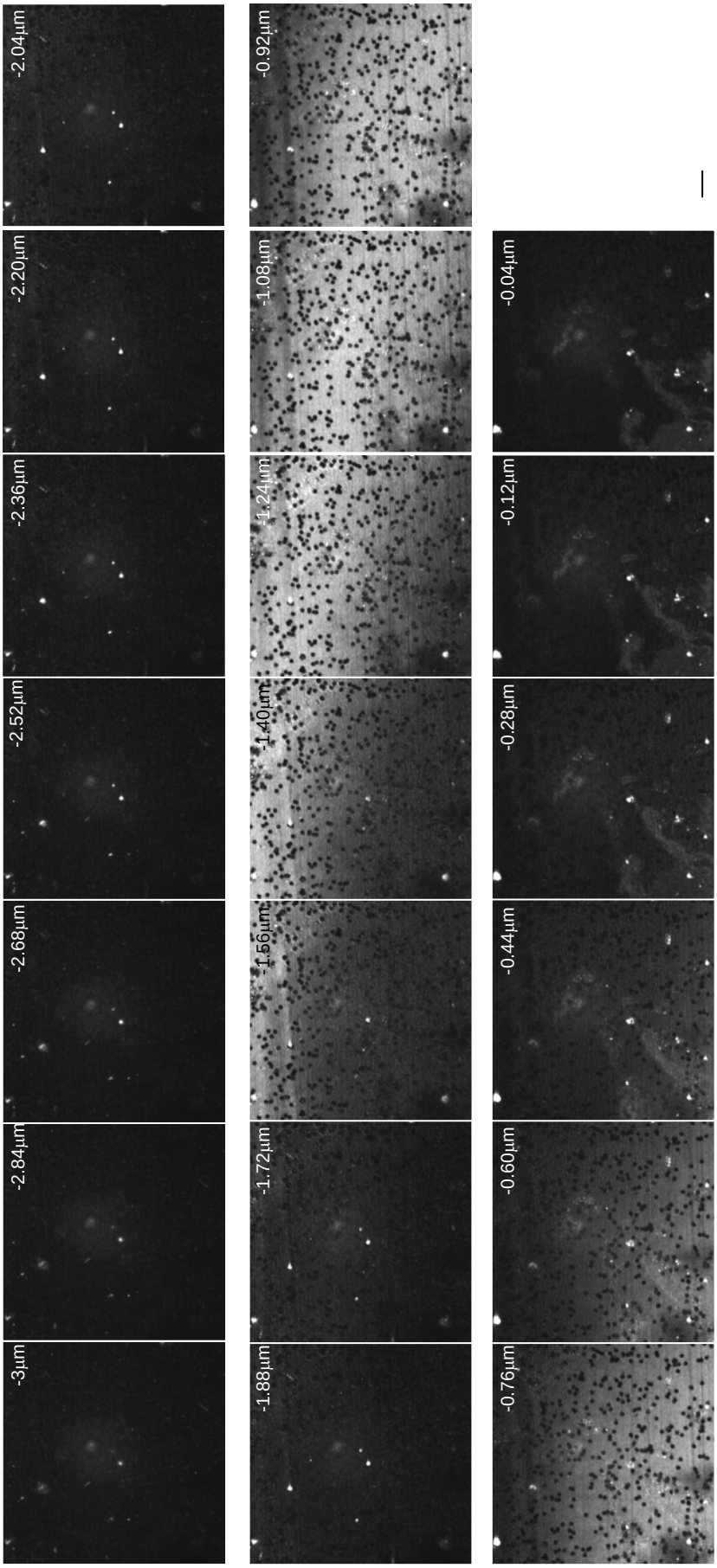

Figure 2.4. Z-series of a 0.8 µm polycarbonate membrane. Images in reflection mode. In images from z = -1.56 µm to z = -0.76 µm it can be visualized the membrane surface with a lack of signal from out-of-focus parts of the surface. Scale bar = 5 µm.

UNIVERSITAT ROVIRA I VIRGILI
MEMBRANE FOULING CHARACTERIZATION BY CONFOCAL SCANNING LASER MICROSCOPY
Maria Malgorzata Zator
ISBN:978-84-693-0712-0/DL:T-422-2010

Figure 2.5 Z-series projection of CSLM images taken in reflection (grey signal) and fluorescent (green signal) modes.

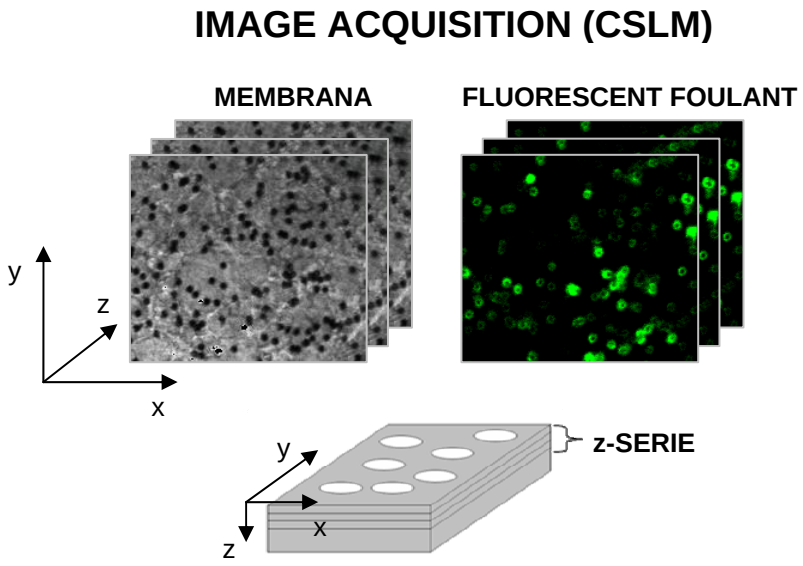

2.2.5. Image analysis

Images were analysed by ImageJ 1.30v (National Institutes of Health, USA) and Imaris (Bitplane). ImageJ 1.30v was used to measure the surface occupied by pores (A_p) and the fraction of the pore surface in which protein has been detected (P_s):

$$P_S = \frac{A_f}{A_p} \tag{2.1}$$

where A_f is the surface of the pore in which protein has been detected.

The processing of the CSLM images included identifying the features to be analysed, and segmenting and extracting the measurements of interest. The digital images had 1024 x 1024 pixels with an integer value ranging from 0 to 255. The image was segmented into foreground and background by setting a threshold, which separated the pixels of interest from the rest of the image (Figure 2.6). The threshold was the same for the samples from the same filtration conditions i.e. protein-fluorophore conjugate and concentration. Colocalization is the presence of two or more types of fluorescent molecules at the same physical location. Within the context of membrane fouling, the molecules may fill the same pore, while in the context of digital imaging the colours emitted by the fluorescent molecules occupy the same pixel in the image. Colocalization was determined using arithmetic operations with the binary images. Imaris is a software for 3D-reconstruction that provides simple and advanced 3D views from optical sections (z-series) acquired with CSLM. In these 3D-reconstructions, the optical sections acquired in the reflection and fluorescence modes were viewed simultaneously.

Figure 2.6. ImageJ processing of the CSLM images that consist in establishing a threshold for digital CSLM images, which separate the pixels of interest from the rest of the image. A_f values are obtained from binarized reflection images while A_p values are obtained by arithmetic operations of binarized reflection and fluorescent images.

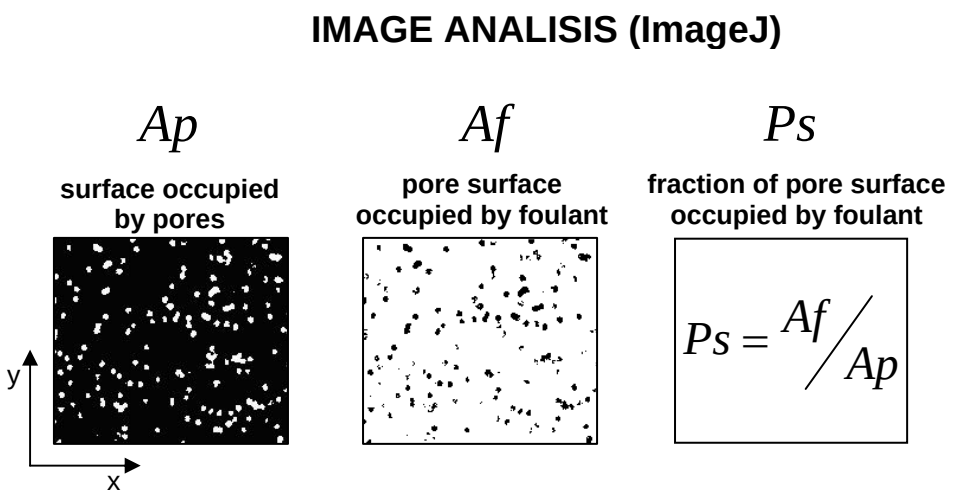

UNIVERSITAT ROVIRA I VIRGILI
MEMBRANE FOULING CHARACTERIZATION BY CONFOCAL SCANNING LASER MICROSCOPY
Maria Malgorzata Zator
ISBN:978-84-693-0712-0/DL:T-422-2010

2.3. Results and Discussion

2.3.1. CSLM for membrane characterization and protein visualization

As stated by Charcosset et al. [16-17] CSLM can be used to obtain surface porosity data. In order to validate the use of CSLM for this purpose, 0.22 µm original polycarbonate membranes (Micron Klear) were analyzed by both SEM and CSLM (reflection mode). Using the images obtained by the two microscopic techniques, the surface porosities were calculated to be 6.5%±0.5 and 7.1%±0.6 for SEM and CSLM in reflection mode, respectively. These results quantitative validate the use of CSLM in reflection mode to determine surface porosity with respect SEM. Figure 2.4 shows how CSLM makes it possible to clearly distinguish the pores on the membrane surface. When the membrane is scanned axially (a z scan) through the focal plane, the photodetector receives the maximum amount of light when the surface is on focus. As the polycarbonate membrane posses a sort of regular surface morphology, most or all of the detected signal can be attributed to scattering from the surface and the black signal to the relative non-reflectivity of the pores [13]. Since the membrane did not keep completely flat when mounted on the slide, several images from the surface were obtained in which there is a lack of signal from out-of-focus parts (see Figure 2.4, images from z = -1.56 µm to z = -0.76 µm). The surface porosity of polycarbonate membranes from Whatman with a nominal pore size of 0.8 µm obtained by CSLM ranged from 12.8% to 14.1%.

CSLM can be used for protein fouling characterization if the proteins on the top and inside the membrane can be visualized using the fluorescence mode. It must also be possible to visualize more than one protein simultaneously in order to study how each one contributes to membrane fouling. Therefore, single BSA and ovalbumin 0.25 g/L solutions (fluorescent and non fluorescent) were filtered through the 0.8 µm polycarbonate membrane for 3 hours. Membrane samples were prepared as explained above and were analyzed by CSLM (reflection and fluorescence modes) using the protocol explained in detail in the section above.

Membrane samples from the experiments with fluorescent proteins showed fluorescence for both BSA-fluorescein and ovalbumin-Texas red. However, membrane samples from the experiments with non-fluorescent proteins showed no fluorescence when analyzed in the same conditions (laser intensity and detection parameters) in the CSLM. Figures 2.7 a and 2.7 b show CSLM images of 0.8 µm polycarbonate membranes after the filtration of a 0.25 g/L BSA-fluorescein and ovalbumin-Texas red, respectively. The images correspond to a z-projection of 20 images stack along the axis perpendicular to image plane, inside the membrane. The green in Figure 2.7 a clearly shows the presence of BSA, which in some cases partially fills some of the existing pores. The red in Figure 2.7 b indicates the presence of ovalbumin, which also fills some of the pores. The two previous figures make it clear that CSLM can locate and identify the proteins conjugated with the fluorescent dyes, so the ability of the technique to simultaneously

locate and identify both proteins when they are together in a mixture had to be tested. Figure 2.7 c presents a 0.8 µm polycarbonate membrane after the filtration of a binary protein mixture. The individual fouling caused by BSA (green signal) and ovalbumin (red signal) can be seen. Some pores seem to be filled by only one protein, but in some pores the deposition of both proteins, BSA and ovalbumin, can be detected.

Figure 2.7. CSLM image of a 0.8 µm polycarbonate membrane fouled by: a) BSA-fluorescein conjugate, b) OVA-Texas red conjugate, and c) a mixture of BSA-fluorescein and OVA-Texas red conjugate. Green and red signals indicate the presence of BSA-fluorescein conjugate and OVA-Texas red conjugate, respectively. The images correspond to a z-projection of 20 image stack along the axis perpendicular to image plane, inside the membrane. Scale bar = 5 µm.

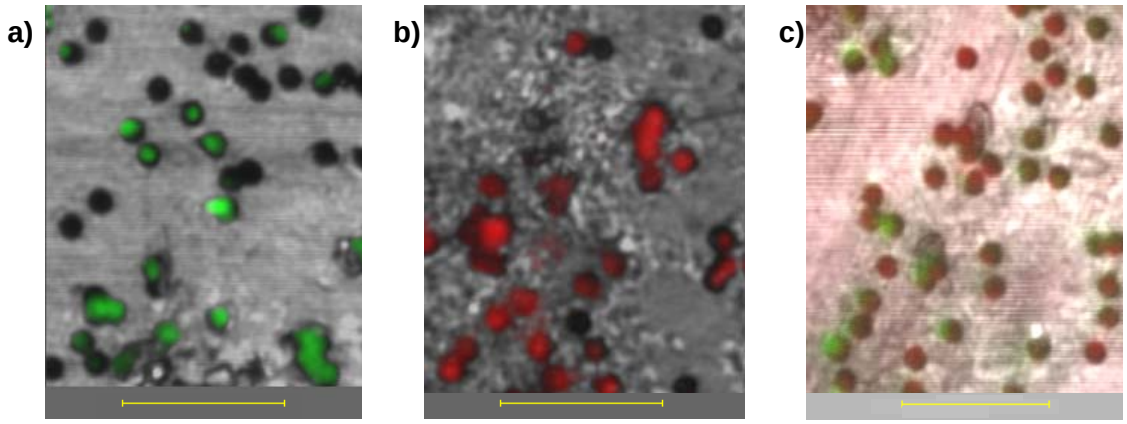

2.3.2. Protein detection in membrane pores

As presented in the previous section, CSLM in the fluorescence mode can be used to identify and locate proteins adsorbed/deposited on top and inside the membrane. This technique is very sensitive and can detect and identify small amounts of fluorophore molecules. With the methodology previously described, the fluorescent signal indicates protein adsorption/deposition. However, at this stage, this methodology cannot quantitatively correlate the amount of protein adsorbed/deposited with the signal intensity. CSLM images obtained in the fluorescence mode can be analyzed using the appropriate image analysis software to obtain quantitative information on the fraction of pore surface in which protein was detected (P_S).

In the present study, ImageJ has been used to analyze CSLM images from membranes fouled by BSA, ovalbumin and a mixture of both proteins. A colocalization algorithm was used to determine P_S when single and binary solutions of BSA and ovalbumin were filtered through a 0.8 µm polycarbonate membrane. P_S was calculated at depths of up to 3 µm inside the membrane. At higher z-values BSA-fluorescein conjugate was not detected. As observed in Figure 2.4, when visualizing the membrane surface with CSLM in reflection mode, several images from the surface in which only some parts of the image are properly detected were obtained (see the range from z = -1.56 µm to z = -0.76 µm). Therefore, using CSLM in reflection mode the position of the membrane surface was established (z = 0), but there is always a 0.5-

UNIVERSITAT ROVIRA I VIRGILI
MEMBRANE FOULING CHARACTERIZATION BY CONFOCAL SCANNING LASER MICROSCOPY
Maria Malgorzata Zator
ISBN:978-84-693-0712-0/DL:T-422-2010

0.75 µm interval that corresponds to the focussed images in the reflection mode. Thus, this interval is considered as the position of the membrane surface in the analysis and discussion of the following data.

Figures 2.8 and 2.9 plot P_S through the membrane due to fouling of the BSA-fluorescein conjugate and OVA-Texas red conjugate in single protein solutions, respectively. The negative values on the z-axes indicate the position inside the membrane. Each figure shows the pattern of P_s in two different fields of the same membrane. The curves in figures 2.8 and 2.9 present a maximum of P_s next to the membrane surface. In the case of the BSA-fluorescein conjugate, this maximum varies notably (80% or 40%) depending on the membrane field used for the analysis, while the P_s in case of ovalbumin-Texas red conjugate ranges from 92% to 97% independently of the field. This may be due to the fact that BSA does not homogeneously foul the membrane. In any case, if quantitative data from CSLM analysis is going to be used for fouling modeling, a thorough statistical study should be made of the number of fields required and their size.

The profile of P_s through the membrane shows that it significantly decreases as the distance from the membrane surface increases (Figures 2.8-2.9). At z-values of –2 µm, the pore fraction in which BSA-fluorescein conjugate is detected decreases to 7% or 20%, depending on the field, while the pore fraction in which ovalbumin-Texas red conjugate is detected decreases to 36% and 49%.

Figure 2.8. Fraction of pore surface in which BSA-fluorescein conjugate is detected (P_s after the filtration of a single protein solution. Negative z-values show the position inside the membrane.

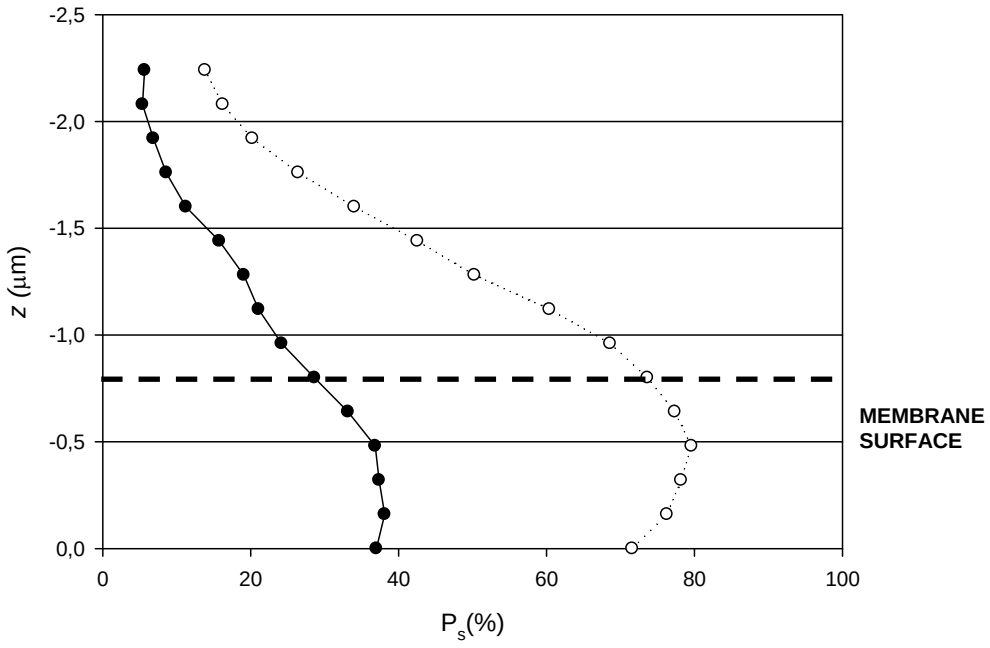

UNIVERSITAT ROVIRA I VIRGILI
MEMBRANE FOULING CHARACTERIZATION BY CONFOCAL SCANNING LASER MICROSCOPY
Maria Malgorzata Zator
ISBN:978-84-693-0712-0/DL:T-422-2010

Figure 2.9. Fraction of pore surface in which ovalbumin-Texas red conjugate protein is detected (P_s) after the filtration of a single protein solution. Negative z-values show the position inside the membrane.

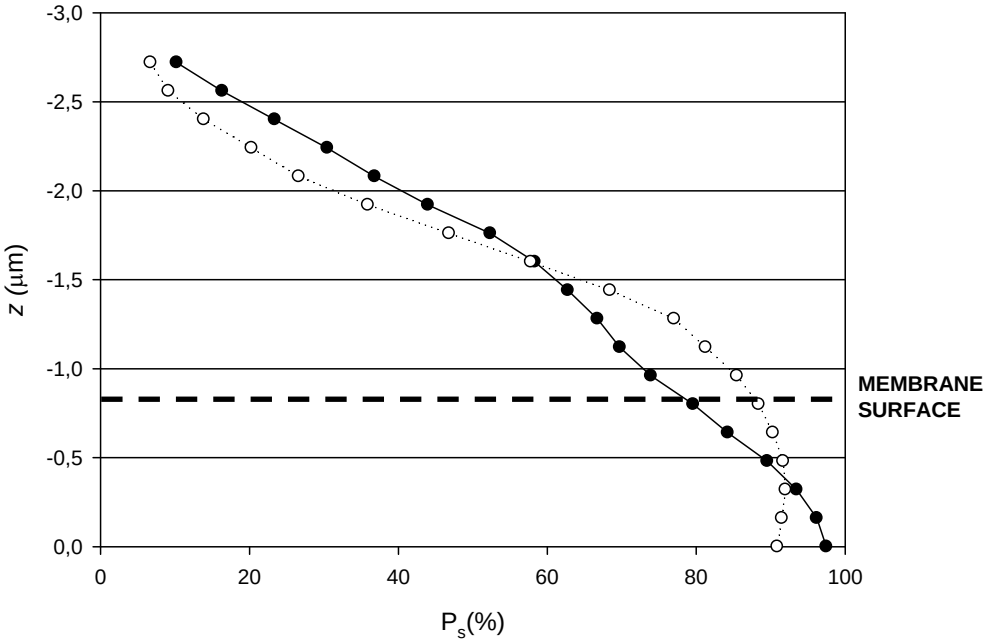

Protein detection of a binary protein solution of BSA-fluorescein and OVA-Texas red conjugates was also carried out. Colocalization algorithms enabled the individual fouling (P_s^{ind}) to be determined i.e. the fraction of pore surface in which each protein is detected. P_s^{ind} can range from 0 to 100%, as the pixel size at the conditions used was (0.04 x 0.04) μm^2 and in one pixel it is possible to detect both proteins simultaneously. The individual fouling pattern of each protein in the binary mixture (Figure 2.10) was very similar to the one observed in single solutions. The P_s^{ind} due to ovalbumin-Texas red was always higher than the P_s^{ind} due to BSA-conjugate. The maximum P_s^{ind} due to ovalbumin-Texas red was 100% at z positions close to the membrane surface, whereas the maximum P_s^{ind} due to BSA-fluorescein conjugate was between 34% and 70%.

The pattern of total fouling (Figure 2.11), defined as the fraction of pore surface in which both BSA-fluorescein and ovalbumin-Texas red are detected, is controlled by the adsorption/deposition of ovalbumin-Texas red conjugate. As can be seen in both curves of Figure 2.11, the profile of fraction of pore surface in which both proteins are detected follows the same trend as the one in Figure 2.10 due to the individual fouling (P_s^{ind}) of ovalbumin-Texas red. This is in good agreement with previous results in which single protein solutions of ovalbumin fouled more intensively than single BSA solutions [9], even though the molecular weight of ovalbumin is smaller than the molecular weight of BSA.

UNIVERSITAT ROVIRA I VIRGILI
MEMBRANE FOULING CHARACTERIZATION BY CONFOCAL SCANNING LASER MICROSCOPY
Maria Malgorzata Zator
ISBN:978-84-693-0712-0/DL:T-422-2010

Figure 2.10. Fraction of pore surface in which BSA-fluorescein and OVA-Texas red conjugates have been detected (P_s^{ind}) after the filtration of a binary protein solution. Negative z-values show the position inside the membrane.

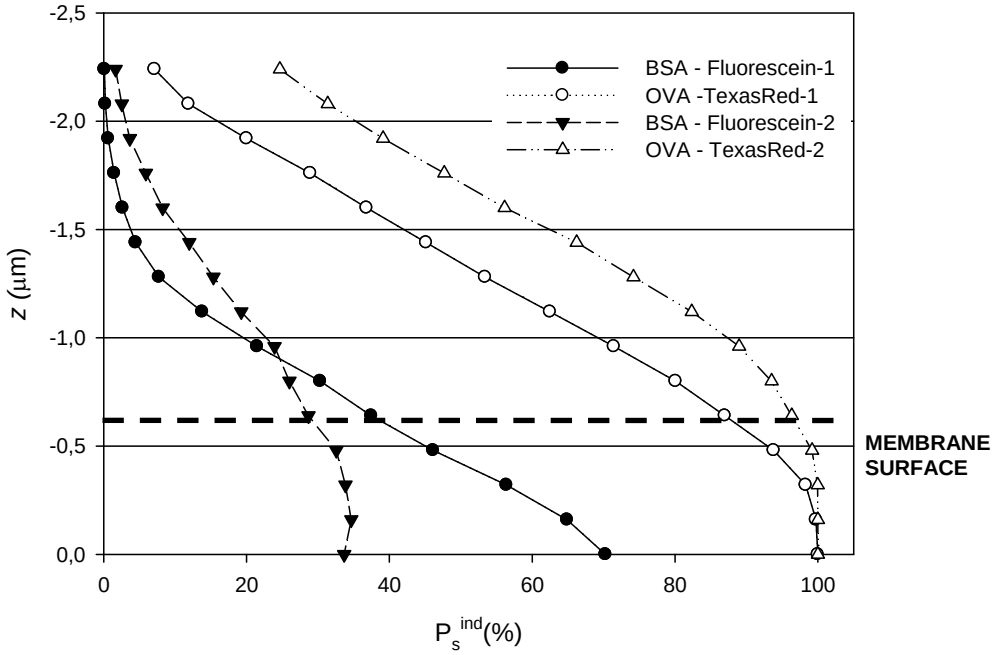

Figure 2.11. Fraction of pore surface in which protein has been detected (P_s) after the filtration of a binary protein solution of BSA-fluorescein and OVA-Texas red conjugates. Negative z-values show the position inside the membrane.

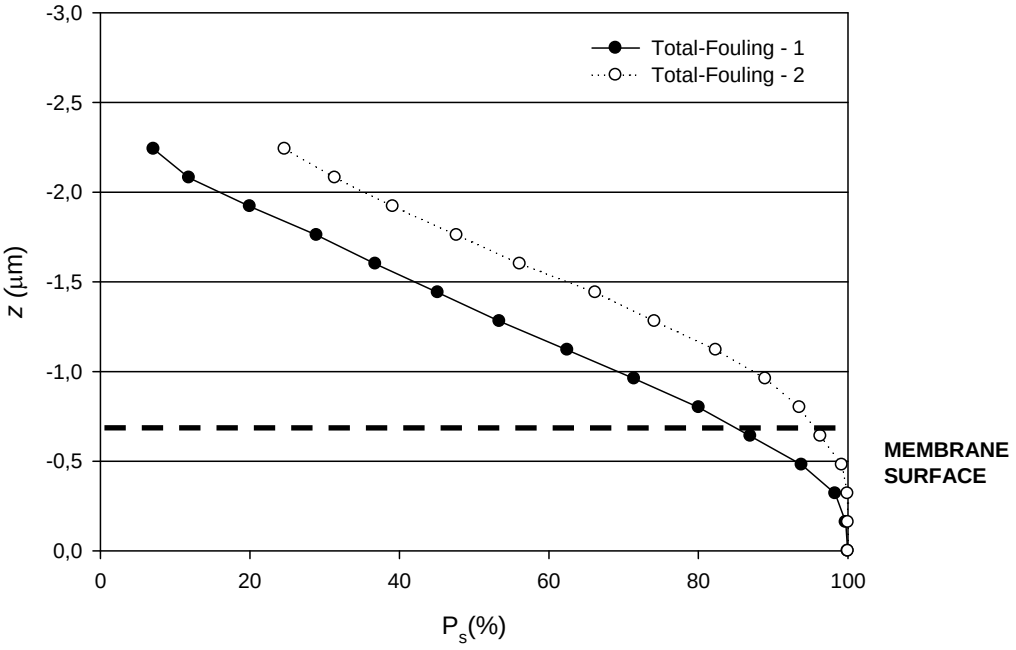

UNIVERSITAT ROVIRA I VIRGILI
MEMBRANE FOULING CHARACTERIZATION BY CONFOCAL SCANNING LASER MICROSCOPY
Maria Malgorzata Zator
ISBN:978-84-693-0712-0/DL:T-422-2010

To compare protein fouling obtained by CLSM (P_s and P_s^{ind}) with macroscopic results on membrane fouling, permeate flux evolution during 3 hour filtration runs of single and binary protein mixtures was obtained. Figure 2.12 a, b and c show permeate flux evolution of single BSA-fluorescein, single ovalbumin-Texas red and the binary protein mixture, respectively. Macroscopic results show that low fouling was occurring, since permeate fluxes were almost constant during a 3 hour period. However, P_s in single and binary protein solutions reached values up to 97% and 100%, respectively. First of all, it has to be noted that the highest P_s values are only obtained next to the membrane surface, secondly, the high sensitivity of microscopy in fluorescence mode allows to detect that proteins are present inside the pores even in low fouling scenarios.

Figure 2.12. Permeate flow obtained during microfiltration of 0.25 g/L protein solution on 0.8 µm polycarbonate membranes: a) fluorescent and non fluorescent BSA, b) fluorescent and non fluorescent ovalbumin, and c) mixtures of fluorescent and non fluorescent BSA and ovalbumin.

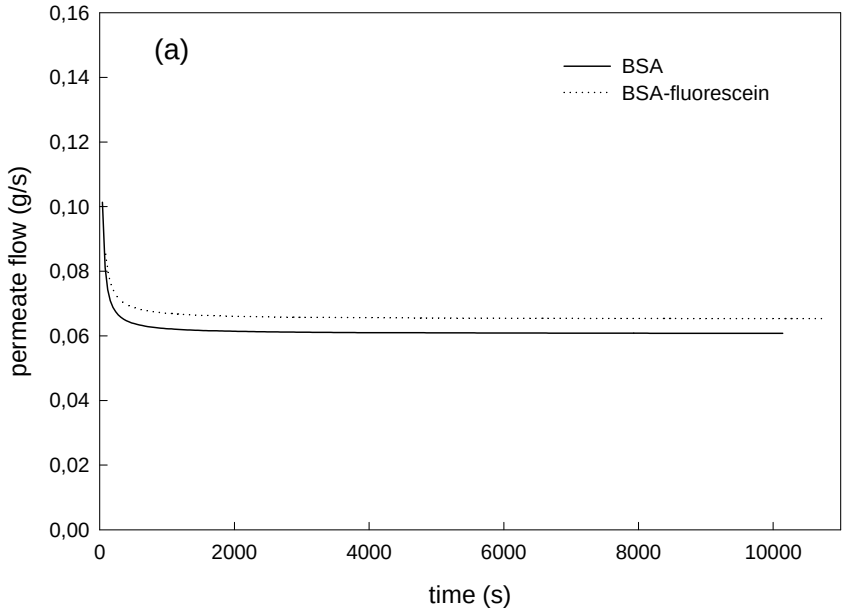

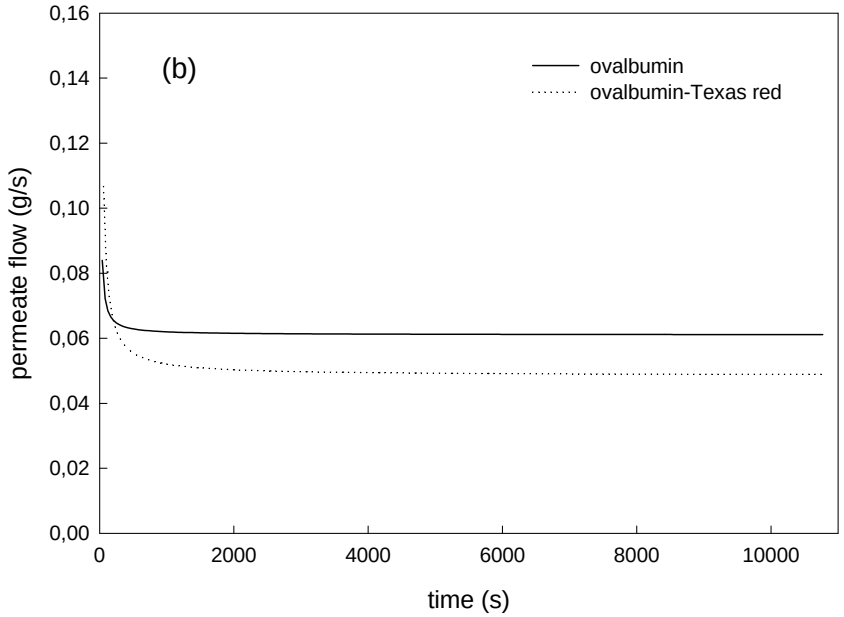

UNIVERSITAT ROVIRA I VIRGILI
MEMBRANE FOULING CHARACTERIZATION BY CONFOCAL SCANNING LASER MICROSCOPY
Maria Malgorzata Zator
ISBN:978-84-693-0712-0/DL:T-422-2010

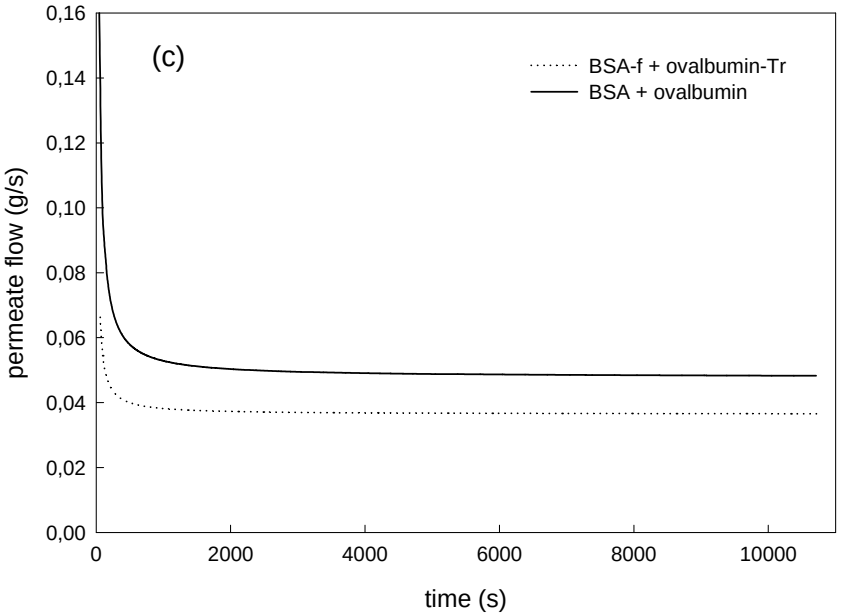

2.3.3. 3D reconstruction

With CSLM, the fouled membranes were optically sectioned to obtain information about the fouling pattern of proteins inside the membrane. The results of CSLM analysis were z-series or stacks of twenty images taken at a z-axis distance of 0.16 µm. Imaris was the software used to generate 3D reconstructions. There are several ways to visualize these 3D reconstructions, and the ones used in the present study are the following:

- orthogonal planes, which make it possible to examine cross-sectional slices through the image volume in XZ, YZ and XY planes. This helps to view three-dimensional structural information about the specimen. Sliders are used to select the X, Y and Z coordinates and the views in the image windows give the cross-sections at that position.

- volumetric three dimensional reconstruction, consisting of rotated views from a stack of through-focus images.

Figure 2.13 shows an orthogonal view of the 3D reconstruction of a polycarbonate membrane fouled by a binary solution of BSA-fluorescein conjugate and ovalbumin-Texas red conjugate. In this figure, images in reflection (gray) and fluorescent mode (green and red) have been combined and reconstructed to visualize the fouling distribution inside the membrane. The gray image gives information about the membrane surface and the pore distribution. The coordinates of the membrane to be visualized have been selected by the sliders. The XY section shows that this point is located in the middle of a pore. The ZX and ZY sections show the penetration of fouling into the membrane due to BSA and ovalbumin: the transversal section of the pore channel is not completely filled with proteins. These images suggest that there is more

UNIVERSITAT ROVIRA I VIRGILI
MEMBRANE FOULING CHARACTERIZATION BY CONFOCAL SCANNING LASER MICROSCOPY
Maria Malgorzata Zator
ISBN:978-84-693-0712-0/DL:T-422-2010

ovalbumin (red signal) than BSA (green signal) on the top of the membrane. This qualitative impression agrees with the quantitative results obtained by image analysis of P_s.

Figure 2.13. Orthogonal view of the 3D reconstruction of a 0.8 μm polycarbonate membrane fouled by a protein binary solution of BSA-fluorescein conjugate and OVA-Texas red conjugate. Green and red signal show adsorption/deposition of BSA-fluorescein conjugate and OVA-Texas red conjugate. Black and gray colors show pores and membrane surface, respectively. (Scale bar = 2μm).

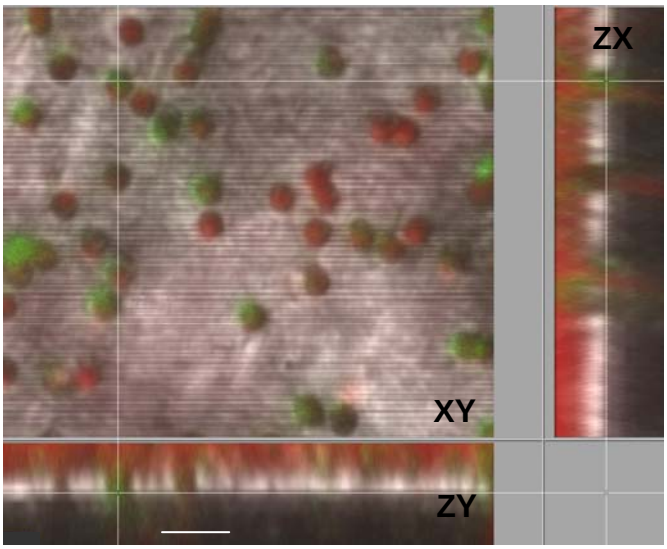

Figure 2.14 shows a volumetric three–dimensional reconstruction of membrane fouled by BSA-fluorescein conjugate. Two different perspectives of the same 3D reconstruction can be seen in Figure 2.14. In this way, it is possible to obtain information about the morphology of the protein fouling on the top of the membrane (Figure 2.14 a) and inside the membrane pores (Figure 2.14 b). This kind of visualization shows how proteins penetrate some pores but do not completely fill the channels. These images illustrate that there was no fouling layer on the top of the membrane, which indicates that internal fouling is the prevailing mechanism.

Figure 2.14. A volumetric 3D reconstruction of a 0.8 μm polycarbonate membrane fouled by BSA-fluorescein conjugate. Image a) shows a view of the top of the membrane and image b) shows a view of the pores inside of the membrane. (Scale bar = 3.5 μm).

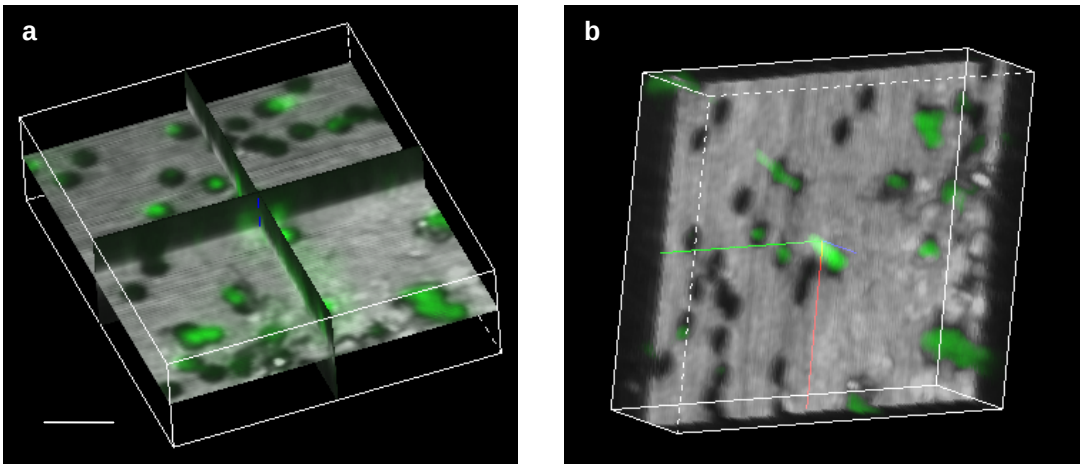

UNIVERSITAT ROVIRA I VIRGILI
MEMBRANE FOULING CHARACTERIZATION BY CONFOCAL SCANNING LASER MICROSCOPY
Maria Malgorzata Zator
ISBN:978-84-693-0712-0/DL:T-422-2010

2.3.4. On-line monitoring

During the on-line monitoring experiments using 40x (NA 0.6, WD 3.7-2.7mm) objective, we were able to obtain the z-stacks of the polycarbonate membrane, however the deposition of protein particles on the membrane surface was not detected, independently of the foulant concentration (0.5 g/L or 1 g/L) and time of exposure to the fouling solution (up to 240 minutes). Figure 2.15 shows the 3D orthogonal reconstruction of the polycarbonate membrane during filtration of 0.5 g/L BSA-FITC solution. The stack of images was taken at different time points: when all the system was filled with phosphate buffer (before filtration), when the buffer was replaced by protein solution (t=0), after ten minutes filtration of protein solution (t=10) and after sixty minutes filtration of protein solution (t=60). Gray and black signals on the images correspond to the membrane and the membrane pores, respectively; green signal that should correspond to the fluorescently labeled protein is not detected at any filtration time. Therefore, no protein fouling could be observed on the polycarbonate membranes during the cross-flow microfiltration of BSA-FITC solutions while performing on-line characterization.

As polycarbonate membranes coming from previous off-line experiments using lower BSA-FITC concentration (0.25 g/L) showed significant protein fouling when analyzed by CSLM, membranes from on-line experiments were also analyzed by CSLM once the on-line experiment was over. To verify the effect of the adsorption/deposition of BSA-FITC on the membrane surface and within the pores, off-line analysis of the membrane samples, prepared according to protocols describe in section 2.1.3 of this chapter were carried out. As the confocal microscope used for the analysis was the same, the main differences between off-line and on-line analysis of the membranes was the addition of the preserving reagent (Mowiol) and the use of an objective with a higher numerical aperture (NA = 0.6 for on-line, NA = 1.3 for off-line). Figure 2.16 shows the 3D reconstruction of a polycarbonate membrane after 240 minutes filtration of 0.5 g/L BSA-FITC solution analyzed using microscope objective 40x with NA 1.3 and WD 0.2 mm (two magnifications). As can be clearly distinguished in both images, gray signal corresponds to the membrane surface, black signal (circle shape) indicates membrane pores and green signal comes from protein deposits on the membrane surface and inside the pores. Comparing the CSLM images in Figures 2.15 and 2.16 it is possible to assume that lack of the green signal in the images taken during on-line monitoring experiments (Figure 2.15) is mainly due to the objective limitations, such as small numerical aperture (NA 0.6). Objectives with NA lower than 1 are not considered confocal, and therefore light emitted from out-off focus planes can reach the detector, resulting in a high degree of blurring in the images (Figure 2.15). During the development of the present thesis it was not possible to obtain an oil immersion confocal objective with a numerical aperture higher that 1, and with a working distance of about 1 mm. If these technical constrains can be overcome, CSLM could be used to successfully characterize protein fouling on-line.

UNIVERSITAT ROVIRA I VIRGILI
MEMBRANE FOULING CHARACTERIZATION BY CONFOCAL SCANNING LASER MICROSCOPY
Maria Malgorzata Zator
ISBN:978-84-693-0712-0/DL:T-422-2010

Figure 2.15. Orthogonal view of the 3D reconstruction of a 0.8 µm polycarbonate membrane during filtration of 0.5 g/L BSA-FITC solution at different filtration times. (Scale bar = 20µm)

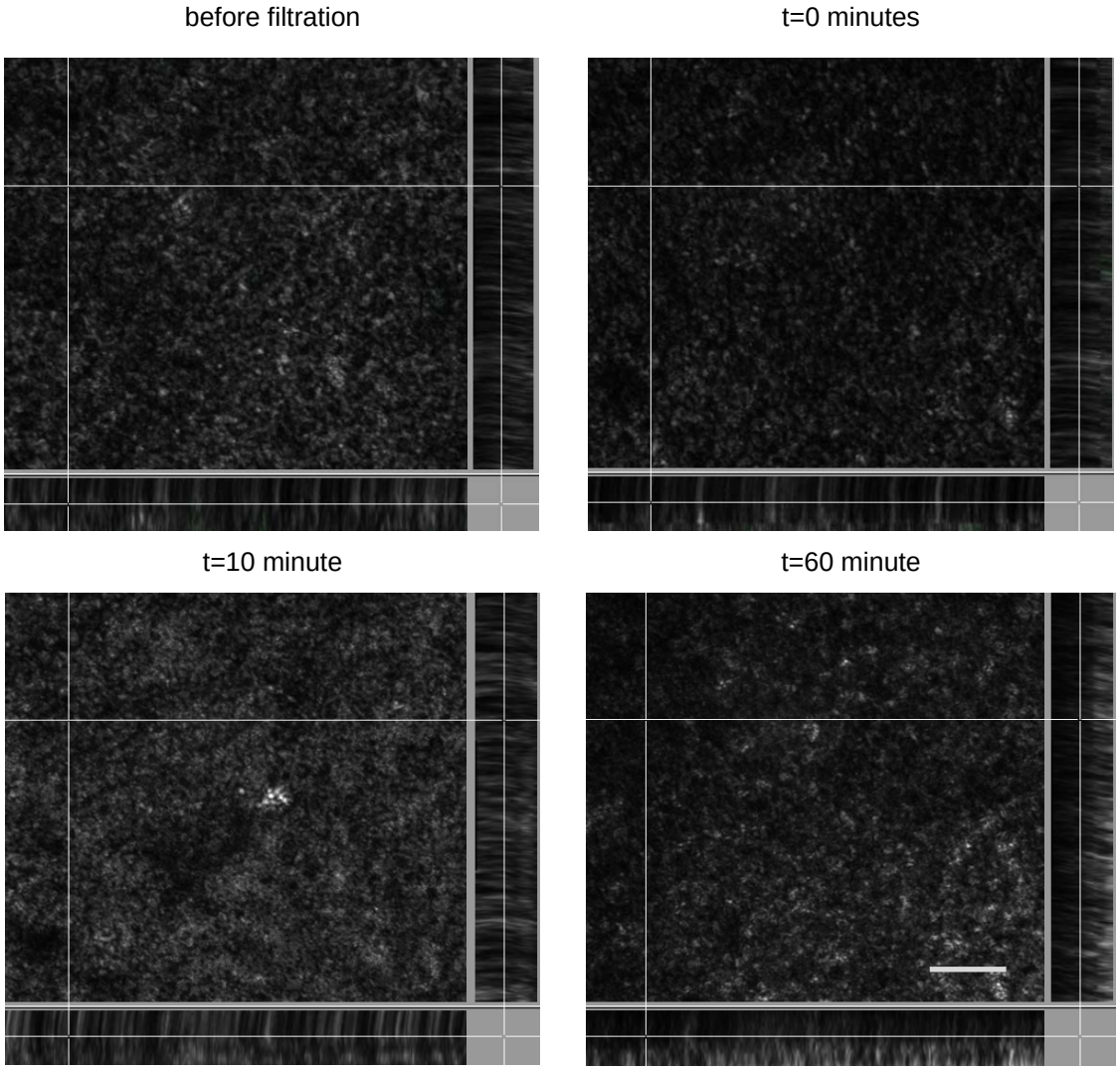

Figure 2.16. Orthogonal view of the 3D reconstruction of a 0.8 µm polycarbonate membrane after 240 minutes filtration of 0.5 g/L BSA-FITC. (Scale bar = 20µm).

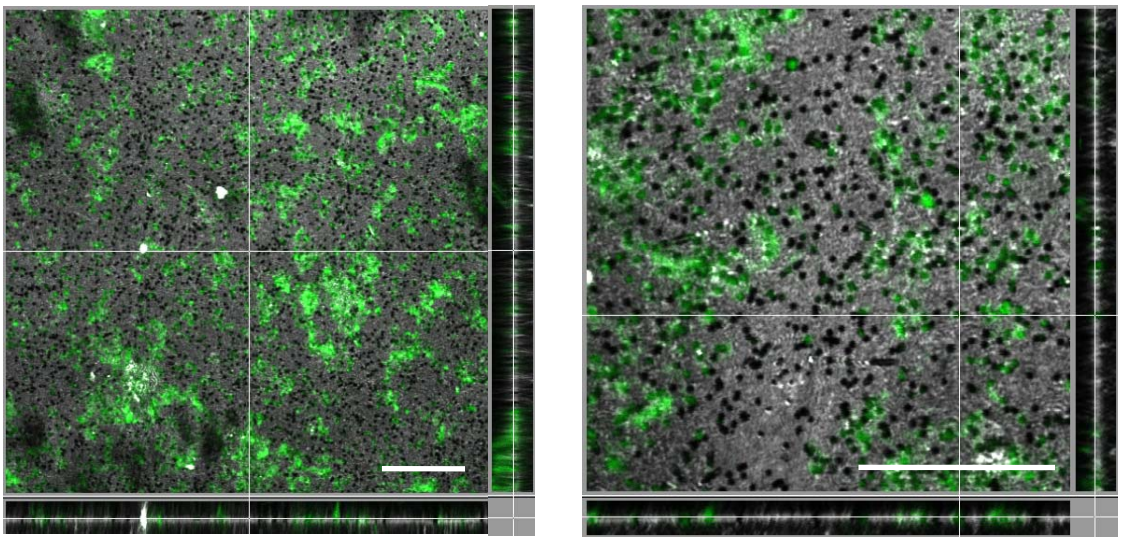

UNIVERSITAT ROVIRA I VIRGILI
MEMBRANE FOULING CHARACTERIZATION BY CONFOCAL SCANNING LASER MICROSCOPY
Maria Malgorzata Zator
ISBN:978-84-693-0712-0/DL:T-422-2010

2.4. Conclusions

CSLM can be used to characterize membrane fouling and makes it possible to visualize and identify several agents in a mixture that cause fouling (for instance, several proteins). Quantitative information about the presence of proteins on the surface of and inside the membrane can also be obtained by applying image analysis algorithms and measuring parameters such as the fraction of pore surface in which protein is detected. The use of these results for modeling, however, requires a statistical analysis of the number and size of the fields in the membrane to be visualized. This is particularly important when the fouling pattern of the protein is not homogeneous but has preferential deposition/adsorption sites on the membrane.

The simultaneous analysis of the results obtained through CSLM imaging combined with image analysis and macroscopic filtration data (permeate flux) enables both the identification of the prevailing mechanism during fouling and that of the major fouling agent. The results of the present study reveal internal fouling and demonstrate that ovalbumin causes considerably more fouling in single and binary protein solutions than BSA. The three dimensional reconstruction of the optical sections obtained with CSLM provides information about the morphology of the adsorption/deposition of proteins inside or on the surface of the membrane pores. This technique makes it possible to visualize the formation of a cake on the top of the membrane and/or the pore constriction caused by deposition or adsorption of foulant agents.

In order to better understand the mechanisms that govern protein fouling, CSLM was used to obtain information on fouling progress during cross-flow microfiltration experiments by on-line monitoring of the process. The results obtained in this work show that on-line visualization of protein adsorption/deposition on the membrane surface and/or within the membrane pores was not possible mainly because of technical limitations, e.g. microscope objective limitations related to the numerical aperture (NA) and working distance (WD).The distance between the membrane surface and the objective lens, which in our experimental set up was around 1 mm, required the use of a commercially available objective with low a numerical aperture (NA=0.6), low magnification (40x) and a high working distance (2.7mm), resulting in low resolution images.

This chapter describes some of the possible applications of CSLM in membrane fouling characterization: determination of surface porosity, location and identification of the adsorbed/deposited proteins, quantitative data about the pore surface in which protein was detected, and fouling morphology. However, if CSLM is to be used more extensively to characterize membrane fouling, quantitative relationships will have to be established between adsorbed/deposited proteins and the fluorescent signal. In order to obtain qualitative and quantitative information on fouling progress during on-line monitoring of the filtration processes, problems related to objective parameters (NA, WD) must be overcome.

2.5. References

1. Vernhet A., Moutounet M., Fouling of organic microfiltration membranes by wine constituents: importance, relative impact of wine polysaccharides and polyphenols and incidence of membrane properties, Journal of Membrane Science 201 (2002) 103-1
2. Eagles W.P, Wakeman W.P, Interactions between dissolved material and fouling layer during microfiltration of a model beer solution, Journal of Membrane Science 206 (2002) 253-64.
3. Palacio L., Ho C.-C., Prádanos P., Hernández A., Zydney A.L., Fouling with protein mixtures in microfiltration: BSA-lysozyme and BSA-pepsin, Journal of Membrane Science 222 (2003) 41-51.
4. Mänttäri M., Nyström M., Critical flux in NF of high molar mass polysaccharides and effluents from the paper industry, Journal of Membrane Science 170 (2000) 257–273.
5. Mänttäri M., Nuortila-Jokinen J., Nyström M., Influence of filtration conditions on the performance of NF membranes in the filtration of paper mill total effluent, Journal of Membrane Science 137 (1997) 187-199.
6. Mänttäri M, Puro L., Nuortila-Jokinen J., Nyström M., Fouling effects of polysaccharides and humic acid in nanofiltration, Journal of Membrane Science 165 (2000) 1–17.
7. Pignon F., Magnin A., Piau J.M., Cabane B., Aimar P., Meireles M., Lindner P., Structural characterization of deposits formed during frontal filtration, Journal of Membrane Science 174 (2000) 189-204.
8. Vernhet, A. and Moutounet, M., Fouling of organic microfiltration membranes by wine constituents: importance, relative impact of wine polysaccharides and polyphenols and incidence of membrane properties, J. Membr. Sci. 201 (2002) 103-122.
9. McCarthy, A.A.; Walsh, P.K. and Foley, G., Experimental techniques for quantifying the cake mass, the cake and membrane resistances and the specific cake resistance during crossflow filtration of microbial suspensions, Journal of Membrane Science, 201 (2002) 31-45.
10. Kuiper, S.; van Rijn, C.; Nijdam, W.; Raspe, O.; van Wolferen, H.; Krijnen, G. and Elwenspoek, M., Filtration of lager beer with microsieves: flux, permeate haze and in-line microscope observations, Journal of Membrane Science, 196 (2002) 159-170.
11. Pawley, J.B. (1995). Fundamental limits in confocal microscopy. In J.B. Pawley (Ed.), Handbook of biological confocal microscopy. New York: Plenum Press pp. 19-37.
12. Shotton, D.M., Confocal scanning optical microscopy and its applications for biological specimens, J. Cell Sci., 94 (1989) 175-206.
13. Wilson, T., Confocal Microscopy, in T. Wilson (Ed.), Confocal Microscopy. London: Academic Press Limited (1990) 1-64.
14. Sheppard, C.J.R. and Cogswell, C.J., Three-dimensional imaging in confocal microscopy, in T. Wilson (Ed.), Confocal Microscopy. London: Academic Press Limited (1990) 143-170.

UNIVERSITAT ROVIRA I VIRGILI
MEMBRANE FOULING CHARACTERIZATION BY CONFOCAL SCANNING LASER MICROSCOPY
Maria Malgorzata Zator
ISBN:978-84-693-0712-0/DL:T-422-2010

15. Hell, S.W., Toward fluorescence nanoscopy, Nature Biotechnology, 21 (2003) 1347-1355.
16. C. Charcosset, J.C. Bernengo, Comparison of microporous membrane morphologies using confocal scanning laser microscopy, Journal of Membrane Science 168 (2000) 53-62.
17. C. Charcosset, A. Cherfi, J.C. Bernengo, Characterization of microporous membrane morphology using confocal scanning laser microscopy, Chemical Engineering Science, 55 (2000) 5351-5358.

UNIVERSITAT ROVIRA I VIRGILI
MEMBRANE FOULING CHARACTERIZATION BY CONFOCAL SCANNING LASER MICROSCOPY
Maria Malgorzata Zator
ISBN:978-84-693-0712-0/DL:T-422-2010

UNIVERSITAT ROVIRA I VIRGILI
MEMBRANE FOULING CHARACTERIZATION BY CONFOCAL SCANNING LASER MICROSCOPY
Maria Malgorzata Zator
ISBN:978-84-693-0712-0/DL:T-422-2010

3

MEMBRANE FOULING CHARACTERIZATION BY CONFOCAL MICROSCOPY DURING FILTRATION OF PROTEIN/POLYSACCHARIDE SOLUTIONS.

This chapter has been published as:
M. Zator, M. Ferrando, F. López, C. Güell, (2007), Membrane Fouling Characterization by confocal microscopy during filtration of BSA/dextran mixtures, Journal of Membrane Science 301, pp. 57-66.

UNIVERSITAT ROVIRA I VIRGILI
MEMBRANE FOULING CHARACTERIZATION BY CONFOCAL SCANNING LASER MICROSCOPY
Maria Malgorzata Zator
ISBN:978-84-693-0712-0/DL:T-422-2010

UNIVERSITAT ROVIRA I VIRGILI
MEMBRANE FOULING CHARACTERIZATION BY CONFOCAL SCANNING LASER MICROSCOPY
Maria Malgorzata Zator
ISBN:978-84-693-0712-0/DL:T-422-2010

3.1. Introduction

In recent years membrane bioreactors (MBRs) have gained increasing attention in the field of waste water technology. MBRs remove dissolved organics that cause biological oxygen demand (BOD), and suspended materials in wastewater from beverages, livestock, dairy, food, residential sources, pulp and paper, and other industrial sources, as well as from municipal wastewater. The combination of bioreactors and membrane technology enables an innovative and effective cleaning process in waste water technology. This technology for the treatment of highly concentrated waste water flows has a broad potential. Despite its many advantages, the major obstacle to a more widespread application of MBR systems is membrane fouling resulting in rapid decline on the permeation flux. Membrane fouling is inevitable due to the complexity of biological feedstreams, but can be limited by operating the system under appropriate conditions, thus it is the key problem that should be solved [1-5].

Extracellular polymeric substances (EPS) have been identified as the major cause of fouling in MBRs. EPS mainly consist of polysaccharides (PS), proteins or nucleic acids which can originate from cell-lysis, microbial metabolites or unmetabolised wastewater components [2, 6-7]. Not least due to the large variety of (non-standardized) analytical tools, knowledge on EPS/membrane interactions and conditions leading to either the uptake or formation of EPS are scarce. A number of research works have been performed using model solutions to study the mechanisms of protein fouling in MBRs, while research on the impact of polysaccharides is relatively limited. Membrane fouling of proteins/dextrans model solutions is affected by three major factors, namely membrane material properties (pore size, pore shape, porosity, hydrophobicity, hydrophilicity, charge density), the feed characteristics (size of the molecules, aggregation) and the operating parameters (cross flow velocity, transmembrane pressure). Irreversible fouling can be facilitated by altering interactions among solvent, solute and membrane. Membrane-solute and solute-solute interactions are the key to understanding the fouling phenomena. Membrane solute interactions will determine fouling through the adsorption of solute on the membrane surface. Furthermore, this interaction will enhance or modify the particle deposition and pore blocking whereas the solute-solute interactions will facilitate fouling by solute aggregation in solution and/or the surface preadsorbed with solutes [2-5, 8-9].

To allow greater understanding of membrane fouling mechanisms, many research works focus on modeling the flux decline during filtration. The classic fouling models are: complete pore blockage (CBM), intermediate pore blockage (IBM), pore constriction (standard blocking model-SBM) and cake formation (CFM). In CBM, the flux decline is caused by particles which arrive at the membrane, deposit on its surface and block some of the pores with no superposition of particles. In this case the filtrate can only pass through the unblocked pore area, and the filtrate flow rate decreases exponentially over time. The intermediate pore blocking model is similar to

CBM but less restrictive, in that not every particle necessarily blocks the pores and particles can settle on top of other deposited particles. SBM assumes that every particle arriving at the membrane is deposited onto the internal pore walls, leading to a decrease in the pore volume. Cake filtration model (CFM) is used to explain the case of large particles which cannot enter most pores and assumes that a uniform cake layer deposits on the entire membrane surface [10, 11].

Recently, among the various techniques that exist for the visualization of mechanisms involved in the fouling of biocomponents, Confocal Scanning Laser Microscopy (CSLM) was found to be a powerful tool used on the micrometer scale [12-17]. A Confocal Laser Microscope is an optical microscope that presents several advantages over conventional optical microscopic techniques. CSLM provides information on the fouling pattern at different depths of a three-dimensional object as a result of non-invasive optical sectioning of the sample. CSLM makes it possible to visualize a variety of structures and macromolecules without modifying their environment, which is a clear advantage over other techniques.

In order to distinguish macromolecules under CSLM they need to show fluorescence, with a maximum absorption close to the emission wavelength of the laser. For multi-labeling experiments in which more than one structure is stained, fluorescent compounds whose excitation/emission wavelengths do not overlap are required. Nowadays, there are a great number of fluorophores that fulfill such requirements. Some of the most common dyes for protein and polysaccharides labeling are Fluorescein (FITC-green), Tetramethyl rhodamine (TRITC-red) and Rhodamine B (RITC-red). Fluorescent tags FITC, TRITC and RITC have aromatic rings, which make them hydrophobic [18 - 20]. There are some recent studies that use CSLM to characterize membrane fouling in MBRs [21-24]. Chen et al. [24] used a quadruple staining protocol combined with CSLM to study the contribution to membrane fouling of nucleic acids, proteins, α- and β-polysaccharides. They found a first deposit layer on top of the membrane with a mixture of the four foulants. Above this initial deposit layer, they found a distribution of EPS highly stratified. Hwang et al. [22] used three fluorescent dyes to stain bacterial cells, polysaccharides and proteins to study the effect of a membrane fouling reducer (a cationic polymeric material). CSLM images enabled to perform analysis of the 3D architecture of the cakes and spatial distribution of cellular and polymeric constituents. Yang et al. [21] used a six-fold staining protocol combined with CSLM to study the biofouling layer formed on top a mixed cellulose ester membrane.

The main aim of this work was to characterize biofouling during microfiltration by confocal scanning laser microscopy. The results can be applied on, but they are not limited to, study fouling caused by extracellular polymeric substances. As has been previously reported [2, 6-7] the main fractions of EPS are polysaccharides, proteins, nucleic acids and humic substances arising from cell lysis, secretion or already present in the influent. Therefore, the model solution for the EPS selected in the present work combines bovine serum albumin (BSA) and two

UNIVERSITAT ROVIRA I VIRGILI
MEMBRANE FOULING CHARACTERIZATION BY CONFOCAL SCANNING LASER MICROSCOPY
Maria Malgorzata Zator
ISBN:978-84-693-0712-0/DL:T-422-2010

dextrans (as model polysaccharides) with different molecular weight. The final selection for the compounds of the model solution was based on the type of compounds present in EPS and also on the available commercial fluorescent proteins and polysaccharides. The effect of polysaccharide molecular size on membrane fouling was studied using solutions of BSA and dextrans of two molecular sizes (70 and 150 kDa) and two different organic microfiltration membranes: polycarbonate (PC) and mixed esters (Metricel). When CSLM analysis was applied to characterize membrane fouling, the model solutions were prepared with BSA-FITC conjugate (green), Dextran 150 kDa-TRITC conjugate (red) and Dextran 70 kDa- RITC conjugate (red). The use of mixtures containing protein/dextrans labeled with fluorescent probes enables the simultaneous identification of protein and dextran molecules on the membrane surface and inside the pores. Since CSLM analysis must use fluorescent compounds, the possible influence of labeling proteins and dextrans on the fouling extent was also studied, which has not been carried out by other previous studies, where staining protocols were applied to dye the different components of the cake layer. For this purpose, microfiltration experiments with different fluorescent and non-fluorescent protein/polysaccharide mixtures were carried out. Macroscopic data from permeate flux evolution, which has been adjusted to fit the classical fouling models, and CSLM characterization of membrane samples fouled with fluorescent molecules have been performed.

UNIVERSITAT ROVIRA I VIRGILI
MEMBRANE FOULING CHARACTERIZATION BY CONFOCAL SCANNING LASER MICROSCOPY
Maria Malgorzata Zator
ISBN:978-84-693-0712-0/DL:T-422-2010

3.2. Materials and methods

3.2.1. Microfiltration plant and experiments

Microfiltration experiments were carried out using a lab scale filtration plant which consists of a flat filtration module connected to a feed vessel containing the protein/dextran solution (Figure 3.1). A peristaltic pump (Watson Marlow 3135) was used to feed the solution. All runs were carried out at room temperature (23 ± 2°C), with a constant pressure of 0.51×10^5 Pa. Fresh protein and polysaccharide solutions and a new membrane were loaded into the apparatus for each experiment. To minimize photo-bleaching (reduction of the fluorescent signal due to light exposure) of the fluorescent protein and dextrans, the filtration set-up was completely covered with aluminum foil. Retentate and permeate were returned to the feed vessel to maintain a constant volume in the system, and also in the interest of economy of fluorescent molecules usage. After each run, the apparatus was thoroughly cleaned using 25% sodium hydroxide solution, and then rinsed by pre-filtered deionized water until neutral pH.

Permeate fluxes were obtained by collecting permeate samples for 10 sec and weighing them. Samples were obtained every 20 min during the first hour of filtration, and every 30 min until the end of the run. Different protein and polysaccharide solutions (fluorescent and non-fluorescent) were buffered with phosphate buffer solution (PBS) pH 7.4. Different combinations of fluorescent and non-fluorescent solutes were used for the experiments. Table 3.1 lists all the solutions tested in this work as well as the type of membrane employed during the filtration. The initial total solute concentration was always maintained at 0.5 g/L, and all experiments were run in duplicates.

Figure 3.1. Lab scale filtration plant, 1- feed vessel, 2 - peristaltic pump, 3 - manometer, 4 - cross-flow filtration module, 5 - back pressure regulator, 6 - sampling of permeate and retentate to determine fluxes 7 - electronic microbalance connected to the computer.

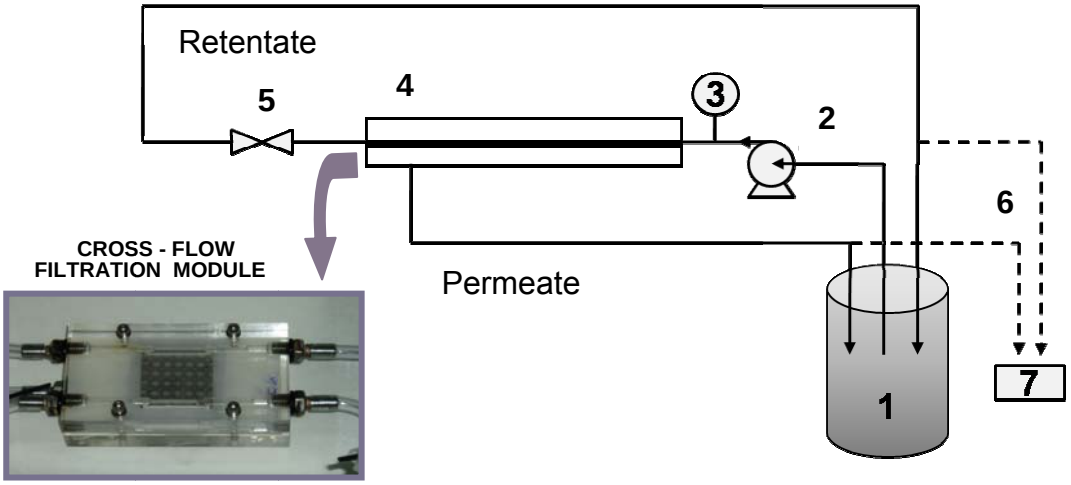

UNIVERSITAT ROVIRA I VIRGILI
MEMBRANE FOULING CHARACTERIZATION BY CONFOCAL SCANNING LASER MICROSCOPY
Maria Malgorzata Zator
ISBN:978-84-693-0712-0/DL:T-422-2010

Table 3.1. Composition of the feed solutions and membranes tested.

Solution	Membrane
BSA FITC / DEX 70 kDa RITC	METRICEL(1)
BSA FITC / DEX 70 kDa	METRICEL
BSA / DEX 70 kDa RITC	METRICEL
BSA / DEX 70kDa	METRICEL
BSA FITC / DEX 150 kDa TRITC	METRICLE / PC(2)
BSA FITC / DEX 150 kDa	METRICEL / PC
BSA / DEX 150 kDa TRITC	METRICEL / PC
BSA / DEX 150 kDa	METRICEL / PC

(1) Mixed esters
(2) Polycarbonate

3.2.2. Membranes, proteins and chemicals

Microfiltration experiments were carried out using two types of 47 mm microfiltration membrane discs, Metricel® black (mixed esters; nominal pore size 0.45 μm), with a clean water flux of 14719 L/(hm^2) at 0.51 × 10^5 Pa, and black polycarbonate tracked etched membrane (nominal pore size 0.40 μm) from Osmonics, INC (K04BP810FX) with a clean water flux 15108 L/(hm^2) at 0.51 × 10^5 Pa. The two membranes selected have been previously treated by the manufacturer to have no fluorescent emission. The selection of this type of black membranes eliminates interferences in the detection of the fluorescent compounds used in the model solution. The use of CSLM requires a thorough knowledge of the fluorescent properties of the membrane material, to avoid interferences with the target compounds. However, staining procedures can be also used to render fluorescent membranes in a particular wavelength.

BSA is one of the most common representative protein molecules used for membrane fouling studies. The molecular weight of BSA is 66.3 kDa with a hydrodynamic radius from 3 to 6 nm, depending on the solvent ionic activity. The molecule is negatively charged at pH 7 due to the presence of surface hydroxyls. It is believed that the surface hydroxyls minimize protein-membrane attractions [25, 26]. BSA was purchased from Across Organics (A019127801), BSA-fluorescein conjugate (491nm/520 nm) (A-9771) was purchased from Sigma. Dextrans are hydrophilic polysaccharides which can be found in a wide variety of molecular weights; they present good water solubility, low toxicity, and relatively inactivity. The high proportion of α-1, 6

polyglucose linkages make them resistant to acid and alkaline hydrolysis. Non fluorescent dextrans were purchased from Fluka (Dextran 70 kDa (32390) and 150 kDa (31422)) and fluorescent dextrans Dextran 70 kDa – rhodamine B conjugate (540 nm/625 nm) (R9379) and Dextran 150 kDa – tetramethylrodamine conjugate (557 nm/576 nm) (T1287) were purchased from Sigma. Regarding the possible interaction between the two fluorophores or any quenching effects, there is no reference regarding this fact. Phosphate buffer was used to adjust the pH of all protein solutions to 7.4.

3.2.3. SEM and CSLM analysis

Scanning Electron Microscopy (SEM) (JEOL JSM-35C,UK) and CSLM (Leica TCDS 4D) were used to obtain images of clean membranes. For SEM analysis the original membranes were coated with a 1.5×10^{-2} mm layer of gold before the photographs were taken. The voltage ranged from 15 to 25 kV and magnification was 8000 and 4000 ×. The preparation of samples for CSLM analysis of membranes obtained during experiments is explained in detail in Chapter 2. Membranes used in the experiments with fluorescent and non-fluorescent proteins and polysaccharides were prepared in the same way. Two fields of view for each membrane sample were specified and analyzed. The protocols used to carry out the CSLM analysis are described in detail in Chapter 2. In all cases the specimens from all experiments were magnified by 100 × objective (NA 1.3), and the zoom magnification was 2.8.

The detection conditions were kept constant for samples obtained under the same filtration conditions. Images were taken from the surface of the membrane to inside and to outside each 0.16 μm, producing a series of 20 images in each case. This optical sectioning provided data on foulant penetration in the membrane and the cake layer up to 2.5-3 μm.

Images were analyzed by ImageJ 1.30v (National Institutes of Health, USA) and Imaris (Bitplane). ImageJ 1.30v was used to measure the surface occupied by pores (A_p) and the fraction of the pore surface in which protein/polysaccharide was detected (P_s), as described in Chapter 2. The digital images had 512 × 512 pixels with an integral value ranging from 0 to 255. The processing of the images included identifying the features to be analyzed, segmenting and extracting the measurements of interest, as described in a previous chapter.

UNIVERSITAT ROVIRA I VIRGILI
MEMBRANE FOULING CHARACTERIZATION BY CONFOCAL SCANNING LASER MICROSCOPY
Maria Malgorzata Zator
ISBN:978-84-693-0712-0/DL:T-422-2010

3.3. Results and discussion

In the present study, CSLM was employed to allow greater understanding of the contribution of organic biofoulants on membrane fouling during microfiltration. For this purpose, the use of molecules with a conjugated fluorescent probe was required. As mentioned in the previous section, model solutions were prepared with BSA – FITC/Dextran 70 kDa RITC and BSA – FITC/Dextran 150 kDa TRITC, and membrane fouling was studied during the filtration of these solutions using two different organic membranes: polycarbonate (PC) and Mixed esters (Metricel). The surface porosity obtained by CSLM for PC (0.4 μm) and metricel (0.45 μm) membranes was 16.25%±0.44 and 31.95%±1.62, respectively.

3.3.1. Influence of fluorescent probes on membrane fouling

As shown in chapter 2, where protein fouling was characterized by CSLM using BSA-FTIC/ovalbumin-Texas red solutions on polycarbonate membranes, it was found that the permeate fluxes evolution for the fluorescent and non-fluorescent protein solutions behaved quite similarly, and it was concluded that membrane fouling was not influenced by the presence of a fluorescent probe conjugated with the proteins. Since the characterization of membrane fouling by means of CSLM requires a fluorescent probe to allow identification and location of the species, the first step must be to understand the effect of the presence of the fluorescent dye on the fouling behavior. For this reason, experiments with different fluorescent and non-florescent protein/dextran solutions were run with both types of membranes, and the evolution of permeate flux during filtration is plotted in Figures 3.2 a to 3.2 c. The results correspond to the average value of all performed replicates, and standard deviations are plotted for some values for clarity purposes. As additional information, permeate fluxes at a fixed time and the steady state values are given for all the experiments in Table 3.2.

UNIVERSITAT ROVIRA I VIRGILI
MEMBRANE FOULING CHARACTERIZATION BY CONFOCAL SCANNING LASER MICROSCOPY
Maria Malgorzata Zator
ISBN:978-84-693-0712-0/DL:T-422-2010

Table 3.2. Average fluxes for the protein/dextran solutions after 3.5 h of filtration (metricel membrane), after 2.5 h of filtration (polycarbonate membrane) and the steady state value.

	t = 3.5 h J [kg/(m^2 h)]	Steady state J [kg/(m^2 h)]
Metricel		
BSA/dextran 70 kDa	507	507
BSA FITC/dextran 70 kDa	121	118
BSA/dextran RITC 70 kDa	73	71
BSA FITC/dextran RITC 70 kDa	680	88
BSA/dextran 150 kDa	759	143
BSA FITC/dextran 150 kDa	336	246
BSA/dextran TRITC 150 kDa	150	124
BSA FITC/dextran TRITC 150 kDa	11500	53
	t = 2.5 h J [kg/(m^2 h)]	Steady state J [kg/(m^2 h)]
Polycarbonate		
BSA/dextran 150 kDa	84	84
BSA FITC/dextran 150 kDa	92	82
BSA/dextran TRITC 150 kDa	103	100
BSA FITC/dextran TRITC 150 kDa	83	89

UNIVERSITAT ROVIRA I VIRGILI
MEMBRANE FOULING CHARACTERIZATION BY CONFOCAL SCANNING LASER MICROSCOPY
Maria Malgorzata Zator
ISBN:978-84-693-0712-0/DL:T-422-2010

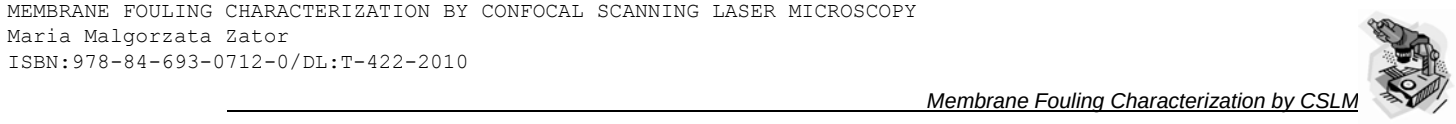

Figure 3.2. Permeate flux obtained during microfiltration of 0.5 g/L protein/dextran solution on 0.45 μm Metricel and 0.4 μm PC membranes: (a) fluorescent and non fluorescent BSA/dextran 70 kDa and a Metricel membrane; (b) fluorescent and non fluorescent BSA/dextran 150 kDa and a Metricel membrane; (c) fluorescent and non fluorescent BSA/ dextran 150 kDa and a PC membrane.

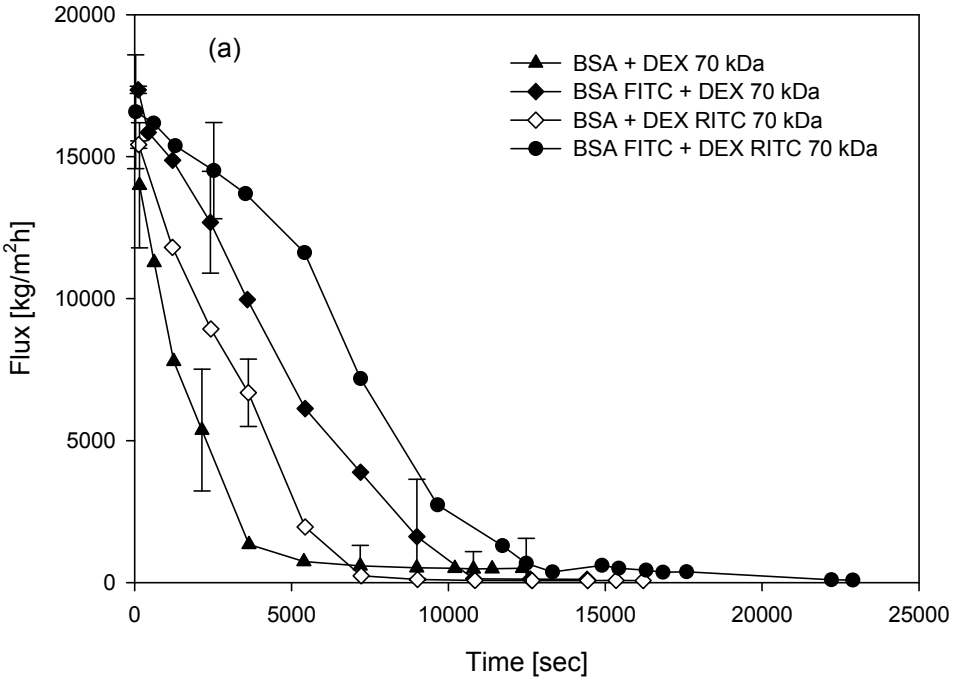

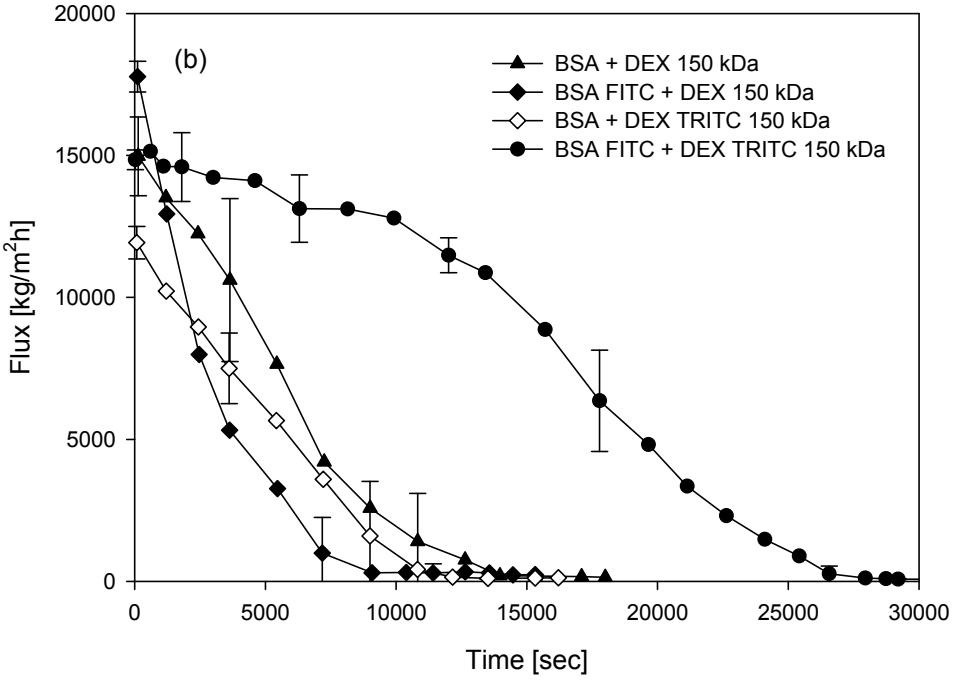

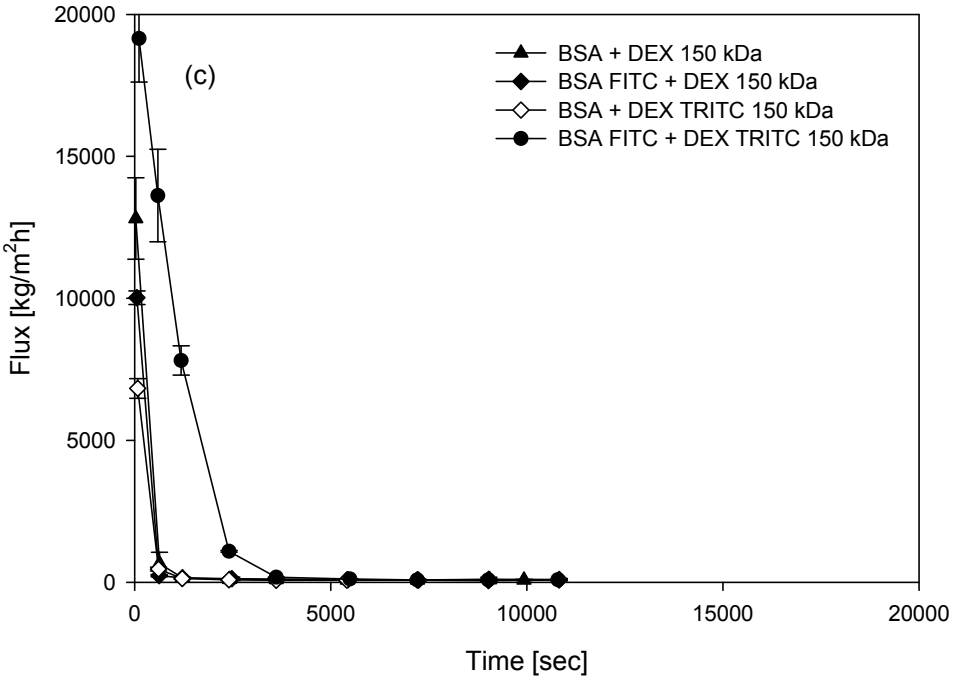

For the mixed esters (Metricel) membrane it can be clearly seen (Figures 3a-b) that the fluorescent dye has a significant effect on the fouling that occurs during the filtration of a protein/dextran solution. During the filtration of the solution with the smallest dextran (70 kDa) there was always a reduction of the fouling if at least one of the two molecules was conjugated with a fluorescent probe (Figure 3.2a). When the solution filtered contained a 150 kDa dextran mixed with BSA, the reduction of the fouling is only seen if both the protein and the dextran are fluorescent labeled (Figure 3.2b). However, in this situation the time needed to reach the steady state was almost double than with non-fluorescent compounds. Bingaman et al. [27] reported that addition of fluorescent dyes, and particularly FITC, alter physicochemical characteristics of BSA such as molecular size and relative charge, which may affect the fouling behavior of the protein. In their study they found that the same commercial BSA-FITC as the one used in the present study showed a significant increase in the negative charge. Person et al. [28] concluded that the charge of the molecules affects the repulsive force among the molecules decreasing aggregation rate, and also between the membrane and the molecules causing their repulsion from the membrane surface. When the molecules are neutral they can come closer to each other, and the aggregation rate increases causing a faster build up of cake layer. They can also come closer to the membrane and pass through the pores more easily.

The results obtained in the present study, plus the findings reported in the literature may suggest that the effect of the fluorescent probe has to be accounted for when it is employed as a tool to allow the detection/visualization of certain species. However, when a PC membrane was used, the presence of a fluorescent probe conjugated with either the protein or the dextran (or both) has a minor effect (Figure 3.2c). From these results it is clear that before using CSLM

UNIVERSITAT ROVIRA I VIRGILI
MEMBRANE FOULING CHARACTERIZATION BY CONFOCAL SCANNING LASER MICROSCOPY
Maria Malgorzata Zator
ISBN:978-84-693-0712-0/DL:T-422-2010

to characterize membrane fouling, it is of key importance to study the behavior of the fluorescent solutions, and compare it to the non-fluorescent ones. The membrane type also plays an important role, since the mixed esters membrane, with the highest surface porosity and a net like structure is fouled to a different extent depending on the size of the dextran mixed with BSA and on the presence of a fluorescent probe, whereas the polycarbonate membrane, with a low surface porosity and pore structure closer to cylindrical pores, exhibits similar fouling independently of the nature of the molecules.

3.3.2. Influence of dextran molecular weight on membrane fouling

When comparing the permeate flux evolution for mixtures containing dextrans of different molecular weight (BSA/dextran 70 kDa and BSA/dextran 150 kDa) during filtration on a mixed esters membrane, it can be observed that the presence of larger size dextran reduces the extent of membrane fouling (Figures 3.2 a and 3.2 b). When the protein and the polysaccharide were conjugated with a fluorescent probe, the fouling behavior depended on the molecular size and on the presence of a fluorescent probe. For the smallest dextran (70 kDa), its labeling with a fluorescent probe (RITC) results in less fouling during the first hour and a half, but a much lower steady state permeate flux is reached after 3.5 h (Figure 3.2 a, Table 3.2). When both the protein and the dextran are fluorescently labeled, the highest values for permeate flux were obtained and the time required to reach the steady state was almost doubled, compared with the non-fluorescent mixture. When a 150 kDa dextran is mixed with BSA, the presence of TRITC has a different effect depending on whether the protein is also fluorescently labeled. When both the protein and the dextran are fluorescent, the extent of membrane fouling was clearly reduced, since the permeate flux was maintained at higher values (Figure 3.2 b, Table 3.2), and for the BSA-FITC/dextran 150 kDa TRICT solution, the time required to reach the steady state was almost doubled compared to the BSA/dextran 150 kDa solution, and also much higher than for the BSA/dextran 70 kDa solution.

These observations are in good agreement with the results obtained by other researchers. Lim et al. [4] and Bai et al. [5, 29] found that smaller particles played a more important role in membrane fouling. They showed that permeation fluxes for granular (bigger) sludge wastewater were significantly bigger that those for the bulking (smaller) sludge wastewater, during microfiltration. It could be expected that smaller particles would contribute to membrane fouling through internal and external pore blocking mechanisms. When Meng et al. [1] investigated EPS (total sum of proteins and carbohydrates) as a dominant factor in MBR fouling, they concluded that the particle size of activated sludge has a strong effect, since smaller particles can be deposited more easily on the membrane surface than larger particles. The results obtained in the present work seem to agree with those findings, since permeate fluxes decrease more rapidly when the smallest dextran tested (70 kDa) was present in the solution. Even though BSA-FITC/dextran 150 kDa shows a much sharper decrease in the permeate flux than BSA-FITC/dextran 70 kDa (Figures 3.2 a and 3.2 b), it is important to mention that the steady state

permeate flux for the solution containing the biggest dextran is double than the one obtained with the solution containing the smallest dextran (Table 3.2). In the following sections, microscopic results obtained by CSLM will also be in agreement with a higher extent of fouling for the solutions containing a protein and a 70 kDa dextran.

3.3.3. CSLM analysis: protein and dextran profiles inside the membrane

The use of CSLM to visualize membrane samples at the end of the filtration period, and the image analysis of the results obtained using CSLM make it possible to correlate qualitatively the fluorescent signal to the presence of protein or dextran adsorbed/deposited on the top and inside the membrane. In this case the correlation was made through the fraction of pore surface in which the protein/dextran has been detected (P_s). Image J has been used to analyze CSLM images from membranes fouled by solutions of BSA/dextran 70 kDa, and BSA/dextran 150 kDa on 0.45 μm mixed esters and 0.4 μm polycarbonate membranes (Figure 3.3). The samples analyzed by CSLM came from experiments where at least one of the components in the solution was fluorescently conjugated. The P_s values were calculated using a co-localization algorithm described in Chapter 2. The profiles in Figure 3.3 are presented for each fluorescent molecule separately, and P_s values were calculated until depths of 3 μm inside the membrane. P_s values in Figure 3.3 a-c correspond to the average value of all replicates, and standard deviations are plotted in few values for clarity purposes. It is important to mention that when BSA-FITC and dextran-TRITC are detected in the binary solutions, colocalization algorithms enabled the individual fouling (P_s) to be determined i.e. the fraction of pore surface in which the protein and the dextrans are detected. P_s for each compound can range from 0 to 100%, as in one pixel it is possible to detect both the protein and the dextrans simultaneously.

From Figure 3.3 it can be observed that the presence of protein or dextran inside the membrane varies depending on whether both compounds are fluorescent or just one. This behavior, which has to be related to the macroscopic results presented in Figure 3.2, was observed for both dextrans independently of their molecular weight, and also for both membranes.

UNIVERSITAT ROVIRA I VIRGILI
MEMBRANE FOULING CHARACTERIZATION BY CONFOCAL SCANNING LASER MICROSCOPY
Maria Malgorzata Zator
ISBN:978-84-693-0712-0/DL:T-422-2010

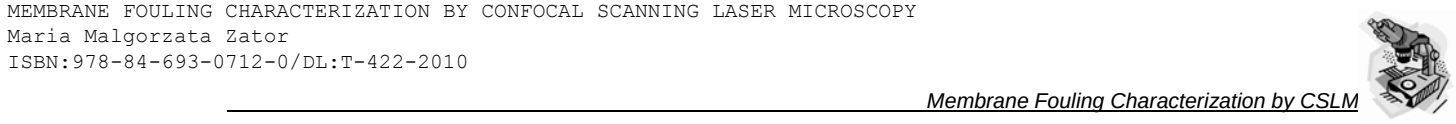

Figure 3.3. Fraction of pore surface on which BSA FITC or dextran TRITC/RITC conjugate is detected (P_s) after filtration of binary protein/dextran solutions: (a) fluorescent and non fluorescent BSA/dextran 70 kDa with mixed esters membrane; (b) fluorescent and non fluorescent BSA/dextran 150 kDa with mixed esters membrane; (c) fluorescent and non fluorescent BSA/dextran 150 kDa with polycarbonate membrane; Negative z values show the position inside the membrane.

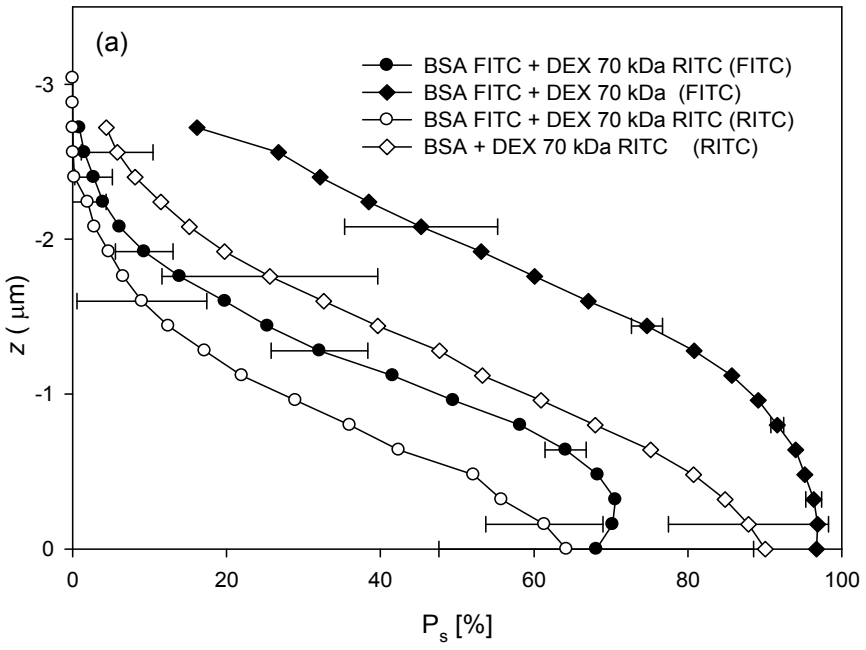

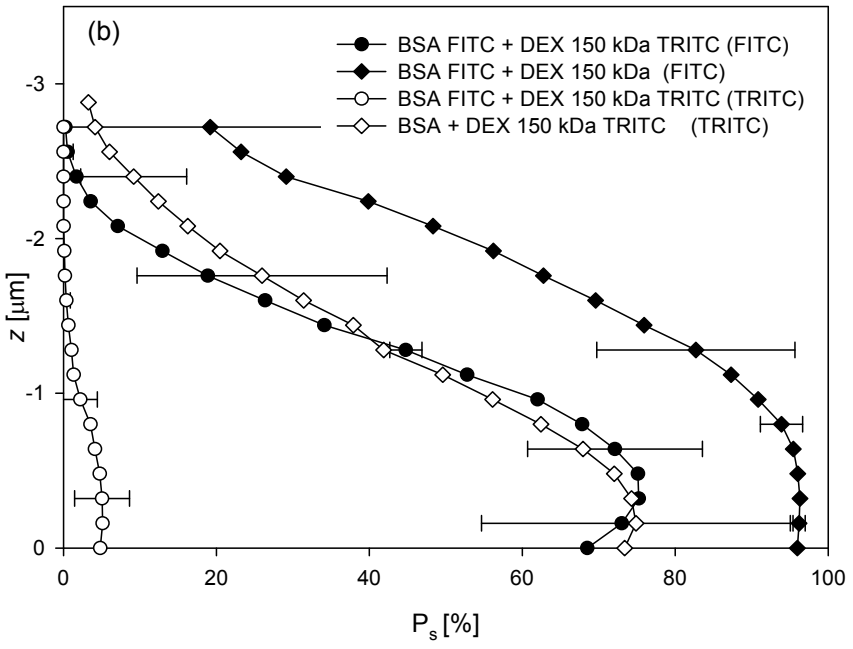

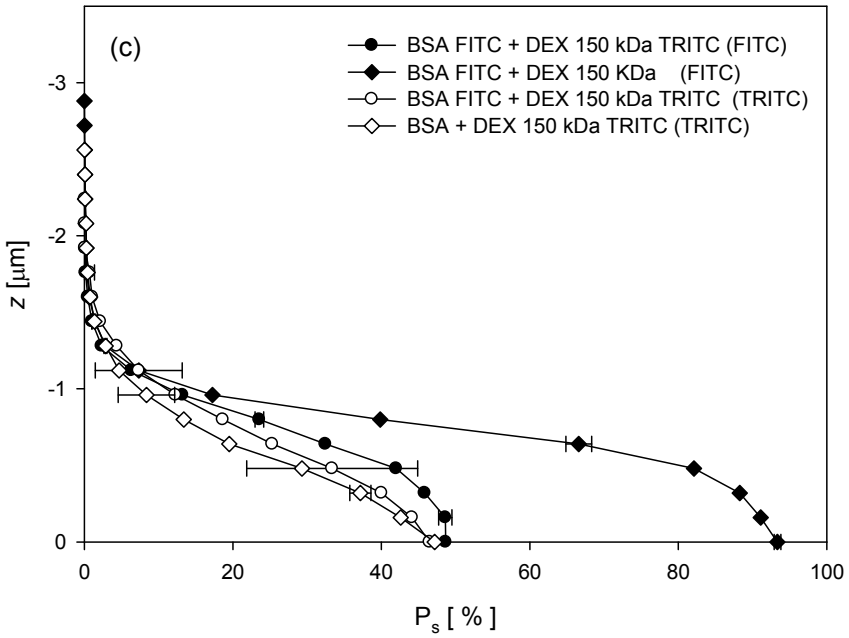

Figure 3.3 a shows P_s values obtained for three different solutions: BSA-FITC/dextran 70 kDa RITC, BSA-FITC/dextran 70 kDa and BSA/dextran 70 kDa RITC after the filtration using a mixed esters membrane. In this case it can be observed that when the solution contained both molecules fluorescently labeled, the maximum P_s of BSA FITC was about 70% on the top of membrane and it decreases when the penetration inside the membrane increases (at a depth of -1μm, P_s is about 50 %). The maximum P_s value obtained for dextran 70 kDa RITC from the same solution is about 60% on the membrane surface and 30% at a depth of -1 μm inside the membrane. A different deposition/adsorption trend can be observed for BSA-FITC when mixed with non-fluorescent 70 kDa dextran. In this case, the P_s values of BSA-FITC are very high, with a maximum of 95% on the membrane surface. This P_s value was maintained almost constant when measured inside the membrane up to a depth of -1 μm. These results suggest that the protein molecules could enter most pores and deposit/adsorb on the pore walls causing reduction/complete blocking of pore volume. When 70 kDa dextran RITC was filtered with non-fluorescent BSA the observed P_s value is higher on the membrane surface than the one obtained for the same compound when BSA-FITC was also present in the solution (90 and 60%, respectively). However, when P_s values for dextran 70 kDa RITC were obtained at different depths inside the membrane, they decreased very rapidly independently of whether the BSA present in the solution was fluorescent or not. If the microscopic results (P_s values) are compared with the macroscopic results in Figure 3.2, the lowest permeate fluxes exhibited for the BSA FITC/dextran 70 kDa are correlated to a higher blockage of the pores.

UNIVERSITAT ROVIRA I VIRGILI
MEMBRANE FOULING CHARACTERIZATION BY CONFOCAL SCANNING LASER MICROSCOPY
Maria Malgorzata Zator
ISBN:978-84-693-0712-0/DL:T-422-2010

Figure 3.3 b shows the evolution of P_s profiles for mixtures of BSA FITC/dextran 150 kDa TRITC, BSA FITC/dextran 150 kDa and BSA/Dextran 150 kDa TRITC after the filtration using a mixed esters membrane. The same tendency observed for the solution with protein and dextran 70 kDa can be observed in this case. When both compounds are fluorescently labeled, the maximum P_s value for BSA FITC is about 70% and decreases when measured inside the membrane up to 60% at -1μm, while the P_s values obtained for the dextran were very small, around 5% on the membrane surface and they are kept constant inside the membrane up to a depth of -1μm. The P_s profile for BSA FITC for the solution with the non-fluorescent 150 kDa dextran is very similar to the one obtained for BSA FITC with non fluorescent 70 kDa dextran, showing a P_s value of 95% on the membrane surface which is maintained practically constant inside the membrane up to a depth of -1 μm.

Figure 3.3 c shows the P_s profiles obtained for mixtures of BSA FITC/dextran 150 kDa TRITC, BSA FITC/dextran 150 kDa and BSA/dextran 150 kDa TRITC after the filtration using a polycarbonate membrane. The effect of the fluorescent probe on the pattern of P_s is similar to that obtained for the mixed esters membrane. When both the protein and the dextran were fluorescent, the P_s values were about 50% on the membrane surface for both components and a very fast decrease is observed with an increase in the distance from the membrane surface (5% at depth of - 0.5 μm). It has to be pointed out that polycarbonate membrane with roughly the same nominal pore size (0.4 μm) than the mixed esters (0.45 μm) has much smaller surface porosity. Moreover, the pore structure is totally different, since for the PC membranes the pores are considered to be almost cylindrical; therefore if the molecules or aggregates are big enough to block the pore entrances, this prevents other molecules from entering. This would explain why the P_s values inside the PC membrane are much lower than those for Metricel.

The fouling exhibited for BSA FITC mixed with a non-fluorescent dextran filtered using a PC membrane shows the same trend as for the Metricel one, reaching a P_s value of 90% on the membrane surface and decreasing to 80% at a depth of - 0.5 μm, followed by a sharp decrease to 5% at - 1 μm. For the mixture of dextran 150 kDa TRITC with non-fluorescent BSA, the observed P_s (50%) is very similar to the one obtained for the mixture of fluorescent dextran/protein.

3.3.4. Models for membrane fouling

In order to obtain more information on the fouling exhibited by the different BSA/dextran mixtures studied in this work, the experimental macroscopic results were fitted to the simple linear equations derived for constant pressure filtration by Hermia [30]. For each experiment, values of filtrate flow rate, volume and time were fitted to the equations derived for CBM, SBM, IBM and CFM to obtain k_{CBM}, k_{SBM}, k_{IBM} and k_{CFM}. The constants k_{CBM} and k_{IBM} are directly related to blocked surface area per unit filtrate volume; k_{SBM} is dependent upon the volume of

particles retained per unit filtrate volume, while k_{CFM} depends on both the cake resistance and the concentration of the suspension. The best correlations were obtained when data were fitted to CBM and IBM for all the conditions studied in the present work (data not shown), indicating that internal fouling was the prevailing fouling mechanism and a combination of complete blocking of the pores and a progressive deposition of BSA and dextrans inside the pores lead to the permeate flux reduction.

To understand the effect of the presence of a fluorophore probe conjugated with BSA or dextran on membrane fouling, a comparison of k_{CBM} and k_{IBM} values will be discussed. When k_{CBM} values obtained for the four different BSA/dextran solutions studied in the present work (BSA/dextran, BSA FITC/dextran, BSA/dextran TRITC and BSA FITC/dextran TRITC) using the same membrane (metricel) and two dextran molecular sizes (70 and 150 kDa) are compared, it is possible to observe that the influence of the fluorophore on the extent of membrane fouling strongly depends on the molecular size of the dextran present in the solution (Table 3.3). For the smallest dextran, it can be seen that the highest k_{CBM} is obtained for the non-fluorescent protein dextran mixture, while for the biggest dextran the highest k_{CBM} value is obtained for a fluorescent BSA mixed with non-fluorescent dextran. Moreover, independently of the dextran size, the lowest k_{CBM} value was always found when both the protein and the dextran where fluorescently conjugated. From the results in Table 3.3 it is clear that the highest values of k_{CBM} obtained for BSA/dextran 150 kDa solutions using different membranes (metricel and polycarbonate) correspond to the polycarbonate membrane, being two or three orders of magnitude higher than for the metricel one. However, the same trend regarding which solution exhibits maximum and minimum k_{CBM} values is maintained: the highest value for the BSA FITC/dextran and the lowest value for the solutions with both fluorescent protein and dextran. As can also be observed in Table 3.3, the same trend shown by k_{CBM} can be found when values for k_{IBM} are compared

The comparison between the results obtained using CSLM data (P_s) and k_{CBM} and k_{IBM} is rather difficult, since the P_s values were obtained from the membranes at the end of the filtration period, and the constants were obtained fitting the macroscopic results gathered during the filtration period. However, P_s values provide very useful insights on the nature and extent of the penetration of each species inside the membrane, showing less blocking of the internal structure of the membrane when the k_{CBM} and k_{IBM} are also small.

UNIVERSITAT ROVIRA I VIRGILI
MEMBRANE FOULING CHARACTERIZATION BY CONFOCAL SCANNING LASER MICROSCOPY
Maria Malgorzata Zator
ISBN:978-84-693-0712-0/DL:T-422-2010

Table 3.3. Values of the constants obtained when data of permeate flow rate, filtrate volume and time were fitted to the Complete Blocking Model and Intermediate Pore blocking Model.

	(k_{CBM}± std error) x 10^4[1/s]	R	(k_{IBM}± std error) x 10^4 [1/mL]	R
Metricel				
BSA/dextran 70 kDa	6.00±0.29	0.9975	2.00±0.12	0.9950
BSA FITC/dextran 70 kDa	2.00±0.14	0.9880	0.36±0.04	0.9805
BSA/dextran RITC 70 kDa	3.00±0.33	0.9999	0.75±0.06	0.9927
BSA FITC/dextran RITC 70 kDa	0.65±0.04	0.9911	0.14±0.01	0.9845
BSA/dextran 150 kDa	1.00±0.05	0.9971	0.24±0.02	0.9927
BSA FITC/dextran 150 kDa	4.00±0.03	0.9958	1.00±0.17	0.9804
BSA/dextran TRITC 150 kDa	1.00±0.07	0.9968	0.53±0.05	0.9848
BSA FITC/dextran TRITC 150 kDa	0.22±0.02	0.9714	0.053±0.005	0.9624
Polycarbonate				
BSA/dextran 150 kDa	310*		75*	
BSA FITC/dextran 150 kDa	729*		226*	
BSA/dextran TRITC 150 kDa	258*		118*	
BSA FITC/dextran TRITC 150 kDa	10±1	0.9938	2.0±0.4	0.9825

* Values obtained from two data points

UNIVERSITAT ROVIRA I VIRGILI
MEMBRANE FOULING CHARACTERIZATION BY CONFOCAL SCANNING LASER MICROSCOPY
Maria Malgorzata Zator
ISBN:978-84-693-0712-0/DL:T-422-2010

3.3.5. 3D reconstruction

More qualitative information on how BSA and dextrans were present in the membrane at the end of each filtration run can be obtained using 3D reconstructions of the image stacks collected during CSLM analysis. In Figure 3.4, orthogonal 3D reconstructions performed with Imaris show metricel membranes fouled with a BSA/fluorescent dextran of 70 and 150 kDa (figures 3.4 a and b, respectively). Regarding the penetration of 70 and 150 kDa dextrans inside the membrane, it has to be considered that the pictures correspond to a 3D reconstruction of a single field in one membrane, which shows how the dextrans can be visualized. The data concerning dextran penetration inside the membrane is presented in Figure 3.3, where P_s values are plotted. Those values correspond to averages of two fields per membrane and two membranes, therefore being much more representative of the actual situation. P_s values in Figure 3.3 show that there is a higher coverage of the pores up to 1.5 μm inside the membrane for the smaller dextran, which is can also be seen comparing Figures 3.4 a and b.

Regarding membrane samples after the filtration of a BSA FITC/dextran solutions, it can be observed from Figures 3.5 a and b, that the penetration of BSA inside the membrane is higher than the dextran (since it was already obtained with the P_s values) and also that, independently of the molecular size of the dextran, the BSA deposit on top of the membrane is also significant.

Figure 3.4. Three D reconstruction of image stacks obtained after filtration of BSA/dextran TRITC using a Metricel membrane. 70 kDa a); 150 kDa b) (red signal corresponds to dextran TRITC).

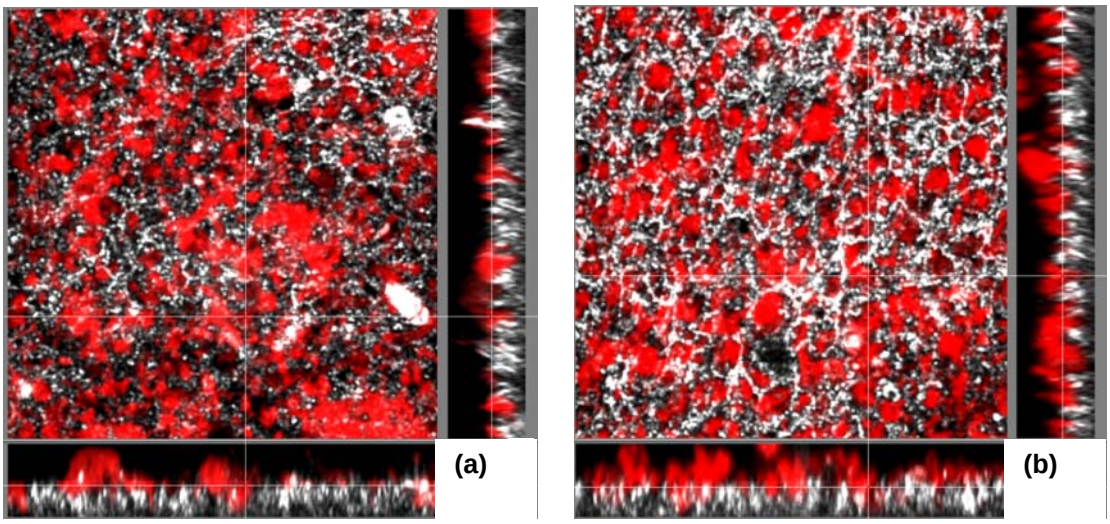

UNIVERSITAT ROVIRA I VIRGILI
MEMBRANE FOULING CHARACTERIZATION BY CONFOCAL SCANNING LASER MICROSCOPY
Maria Malgorzata Zator
ISBN:978-84-693-0712-0/DL:T-422-2010

Figure 3.5. Three D reconstruction of image stacks obtained after filtration of BSA FITC/dextran using a Metricel membrane. 70 kDa a); 150 kDa b) (green signal corresponds to BSA FITC

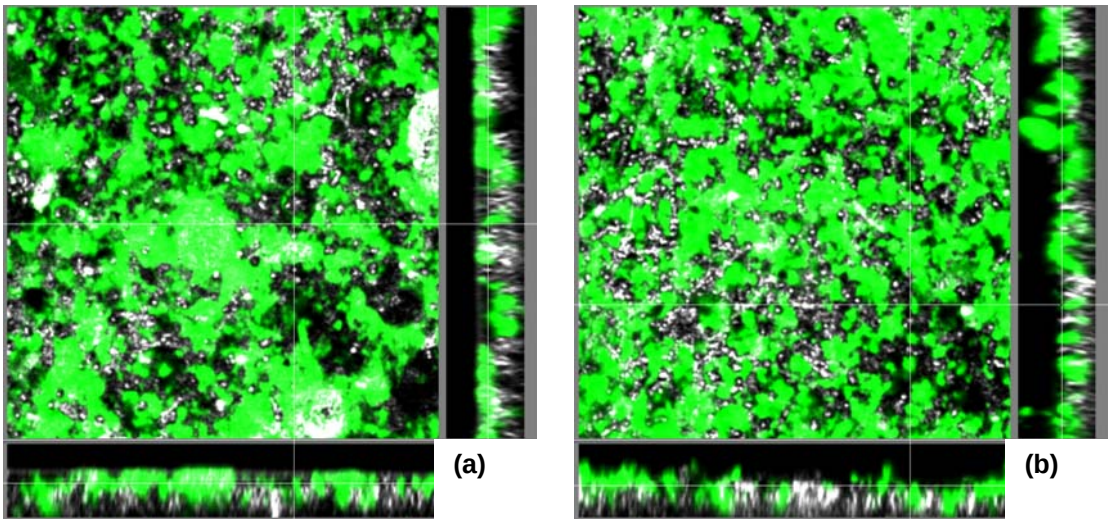

Figure 3.6. Three D reconstruction of image stacks obtained after filtration of BSA FITC/dextran TRITC using a Metricel membrane. 70 kDa a); 150 kDa b) (green corresponds to BSA FITC signal, red corresponds to dextran TRITC signal).

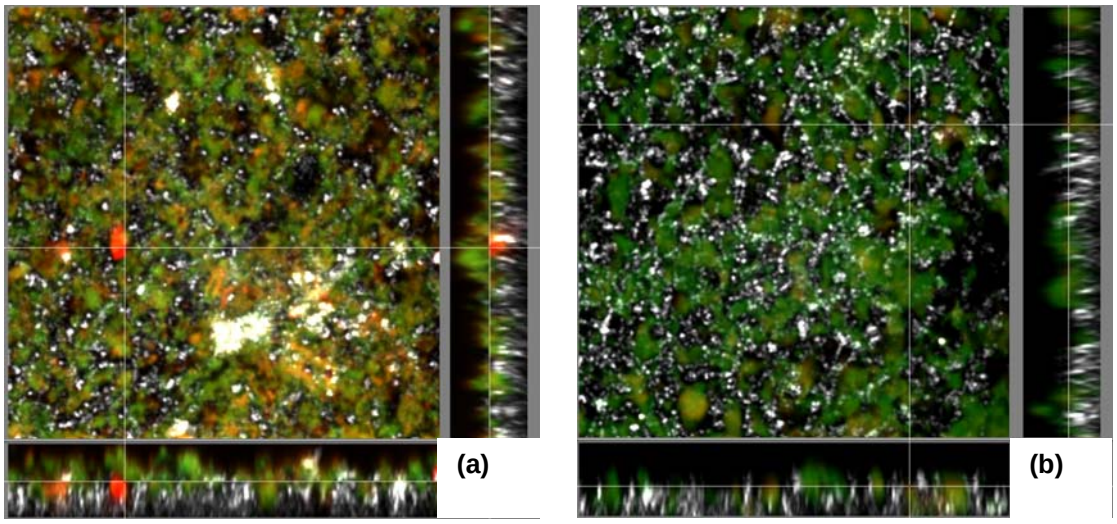

When both the protein and the dextran were fluorescently labeled, the 3D orthogonal reconstructions show almost no presence of dextran inside or on top of the membrane for the biggest dextran (Figure 3.6 b), while some red signal can be detected from the picture obtained after the 3D reconstruction using the image stack for the metricel membrane at the end of the filtration of the protein/dextran 70 kDa solution (Figure 3.6 a).

3.4. Conclusions

From the results presented in this chapter it is clear that CSLM can provide very useful information during the characterization of membrane fouling. Images obtained by CSLM from membranes at the end of several filtration runs made it possible to locate the foulants and to quantify the pore surface occupied by each of them.

However, from the results discussed in this work, it becomes clear that the influence of fluorescent dyes on membrane fouling can be significant, especially for membranes with a high surface porosity or net like structure, such as the mixed esters ones. The use of fluorescein and tetramethyl rhodamine conjugated with BSA and dextrans, respectively, results in a reduction in membrane fouling when compared with the mixtures of non-fluorescent compounds. This behavior could be related to the fact that the fluorescent probes give a slight negative charge to the dextrans and increases the negative charge of BSA at pH 7.4, and therefore charge repulsion between BSA and the dextran may prevent fouling. For PC membranes, with much smaller surface porosity, membrane fouling is fast enough to result in a negligible influence of fluorescent dyes.

The analysis of the results obtained for mixtures of BSA with dextrans of different molecular weight filtered using mixed esters membranes, shows that when the biggest dextran (150 kDa) is present in the mixture, filtration time is significantly extended and fouling reduced. The study of 3D reconstructions of images from CSLM, together with P_s values and the modeling of flux decline during filtration, provided information about adsorption-deposition of particles inside the pores and/or on the top of the membrane. All the results suggest that internal fouling is the prevailing mechanism for all the cases studied in this work. A combination of complete blocking of the pores with a progressive pore diameter reduction, mainly though to be due to protein adsorption, seems to be more in agreement with the results obtained using the Hermina models to fit the macroscopic data, and also agrees with the CSLM results. Therefore, CSLM together with macroscopic analysis has proven to present promising opportunities for the characterization and visualization of fouling on microfiltration membranes. A detailed analysis of the fluorescent probe influence on membrane fouling has to be carried out as a first step.

UNIVERSITAT ROVIRA I VIRGILI
MEMBRANE FOULING CHARACTERIZATION BY CONFOCAL SCANNING LASER MICROSCOPY
Maria Malgorzata Zator
ISBN:978-84-693-0712-0/DL:T-422-2010

3.5. References

1. F. Meng, H. Zhang, Y. Li, X. Zhang, F. Yang, Application of fractal permeation model to investigate membrane fouling in membrane bioreactor, Journal of Membrane Science 262 (2005) 107-116.
2. Y. Ye, P. Le Clech, V. Chen, A.G. Fane, Evolution of fouling during crossflow filtration of model EPS solutions, Journal of Membrane Science 164 (2005) 190-199.
3. A. Drews, M. Vocks, V. Iversen, B. Lesjean and M. Kraume, Influence of unsteady membrane bioreactor operation on EPS formation and filtration resistance, Desalination 192 (2006) 1-9.
4. A.L Lim, R. Bai, Membrane fouling and cleaning in microfiltration of activated sludge wastewater, Journal of Membrane Science 216 (2003) 279-290.
5. R. Bai, H.F. Leow, Microfiltration of activated sludge wastewater – the effect of system operation parameters, Separation and Purification Technology 29 (2002) 189-198.
6. C. Nuengjamnong, J.H. Kweon, J. Cho, C. Polprasert, K.H. Ahn, Membrane fouling by extracellular polymeric substances during microfiltration processes, Desalination 179 (2005) 117-124.
7. A. Drews, C.H. Lee, M. Kraume, Membrane fouling, a review on the role of EPS, Desalination 200 (2006) 186-188.
8. H. Susanto, M. Ulbricht, Influence of ultrafiltration membrane characteristics on adsorptive fouling with dextrans, Journal of Membrane Science 266 (2005) 132-142.
9. S. T. Kelly, W. S. Opong, A. .L Zydney, The influence of protein aggregates on the fouling of microfiltration membranes during stirred cell filtration, Journal of Membrane Science 80 (1993) 175-187.
10. R. Jiraratananon, D. Uttapap, P. Sampranpiboon, Crossflow microfiltration of colloidal suspension with the presence of macromolecules, Journal of Membrane Science 140 (1998) 57-66.
11. Ch. Duclos-Orsello, W. Li, Ch. Ho, A three mechanism model to describe fouling of microfiltration membranes, Journal of Membrane Science 280 (2006) 856-866.
12. M. Zator, M. Ferrando, F. López, C. Güell, Characterization of foulant removal by Confocal scanning laser microscopy, Desalination 200 (2006) 203-204.
13. M. Ferrando, A. Różek, M. Zator, F. López, C. Güell, An approach to membrane fouling characterization by confocal scanning laser microscopy, Journal of Membrane Science 250 (2005) 283-293.
14. F. Velde, F. Weinbreck, M. W. Edelman, E. Linden, R. H. Tromp, Visualisation of biopolymer mixtures using confocal scanning laser microscopy (CSLM) and covalent labeling techniques, Colloid and Surfaces B: Biointerfaces 31 (2003) 159-168.

15. C. Charcosset, F. Yousefian, J. F. Thovert, P. M. Adler, Calculation of flow and solute deposition through three-dimensional reconstructed model of microporous membranes, Desalination 145 (2002) 133-138.
16. T. Linden, A. Ljunglöf, M. R. Kula, J. Thommes, Visualizing two-component protein diffusion in porous adsorbents by confocal scanning laser microscopy, Biotechnology and Bioengineering 65 (1999) 622-630.
17. R. Chan, V. Chen, Characterization of protein fouling on membranes: opportunities and challenges, Journal of Membrane Science 242 (2004) 169-188.
18. P. Mulherkar, R. Reis, Flex test: a fluorescent dextran test for UF membrane characterization, Journal of Membrane Science 236 (2004) 171-182.
19. J. P. S. G Crespo, M. Trotin, D. Hough, J. A. Howell, Use of fluorescent labeling to monitor protein fractionation by ultrafiltration under controlled permeate flux, Journal of Membrane Science 155 (1999) 209-230.
20. R. Hovius, P. Vallotton, T. Wohland, H. Vogel, Fluorescent techniques: shedding light on ligand-receptor interactions, TiPS 21 (2002) 266-273.
21. Z. Yang, X.F. Peng, M.Y. Chen, D.J. Lee, J.Y. Lai, Intra-layer flow in fouling layer on membranes, Journal of Membrane Science 287 (2007) 280-286.
22. B.K. Hwang, W.Y. Lee, P.K. Park, C.H. Lee, I.S. Chang, Effect of membrane fouling reducer on cake structure and membrane permeability in membrane bioreactor, Journal of Membrane Science 288 (2007) 149-156.
23. P. Le-Clech, Y. Marselina, Y. Ye, R.M. Stuetz, V. Chen, Visualization of polysaccharide fouling on microporous membrane using different characterization techniques, Journal of Membrane Science 290 (2007) 36-45.
24. M.Y. Chen, D.J. Lee, Z. Yang, F. Peng, J.Y. Lai, Fluorescent staining for study of extracellular polymeric substances in membrane biofouling layers, Environmental Science and Technology 40 (2006) 6642-6646.
25. A. M. Sokolnicki, R. J. Fisher, T. P. Harrah, D. L. Kaplan, Permeability of bacterial cellulose membranes, Journal of Membrane Science 272 (2006) 15-27.
26. Y. Ye, V. Chen, Reversibility of heterogeneous deposits formed from yeast and protein during microfiltration, Journal of Membrane Science 265 (2005) 20-28.
27. S. Bingaman, V. H. Huxley, R. E. Rumbaut, Fluorescent dyes modify properties of proteins used in microvascular research, Microcilculation 10 (2003) 221-231.
28. A. Persson, A. S. Jonsson, G. Zacchi, Transmission of BSA during cross-flow microfiltration: influence of pH and salt concentration, Journal of Membrane Science 223 (2003) 11-2.
29. R. Bai, H. F. Leow, Microfiltration of polydispersed suspension by a membrane screen/hollow-fiber composite module, Desalination 140 (2001) 2277-287.
30. J. Hermia, Constant pressure blocking filtration law applications to power-law non-newtonian fluid, Transaction of the American Institute of Chemical Engineering 60 (1982) 183-187.

UNIVERSITAT ROVIRA I VIRGILI
MEMBRANE FOULING CHARACTERIZATION BY CONFOCAL SCANNING LASER MICROSCOPY
Maria Malgorzata Zator
ISBN:978-84-693-0712-0/DL:T-422-2010

4

CHEMICAL CLEANING OF POLYCARBONATE MEMBRANES FOULED BY BSA/DEXTRAN MIXTURES

This chapter has been published as:
M. Zator, M. Ferrando, F. López, C. Güell, (2006), Characterization of foulant removal by confocal scanning laser microscopy, Desalination 200 pp. 203-204.
M. Zator, J. Warczok, M. Ferrando, F. López, C. Güell, (2009), Chemical cleaning of polycarbonate membranes fouled by BSA/dextran mixtures, Journal of Membrane Science 327 pp. 59-68.

UNIVERSITAT ROVIRA I VIRGILI
MEMBRANE FOULING CHARACTERIZATION BY CONFOCAL SCANNING LASER MICROSCOPY
Maria Malgorzata Zator
ISBN:978-84-693-0712-0/DL:T-422-2010

UNIVERSITAT ROVIRA I VIRGILI
MEMBRANE FOULING CHARACTERIZATION BY CONFOCAL SCANNING LASER MICROSCOPY
Maria Malgorzata Zator
ISBN:978-84-693-0712-0/DL:T-422-2010

4.1. Introduction

The use of membrane technologies is currently widespread in most industrial production processes. Even in the most optimized operation conditions, membrane fouling will eventually occur, and as an immediate effect a reduction of permeate flux is observed, therefore, membrane fouling has to be kept to a minimum. Several strategies have been developed and applied to reduce membrane fouling, such as the development of new membrane materials, the redesign of membrane modules, the modification of the feed flow pattern or the incorporation of in situ or ex situ cleaning regimes in the membrane module [1].

As a long-term effect, membrane fouling will reduce membrane lifetime and eventually the membrane will need to be cleaned to recover its initial permeate flux. Chemical cleaning methods depend upon chemical reactions to weaken the cohesion forces between the foulants and the adhesion forces between the foulants and the membrane surface [2]. There are numerous commercially available cleaning compounds, including acidic or alkaline solutions which may or may not contain enzymes and/or surfactants. According to Väisänen et al. [3] the selection of a cleaning agent must take into account: the fouling substances present, the process conditions, the nature of the membrane material, the formulation and the concentration of the cleaning agent and the operating conditions (temperature, transmembrane pressure and cross-flow velocity). Selected materials should be chemically stable, safe, cheap, and washable with water. However, chemical cleaning to reduce irreversible fouling should be limited to avoid changes in membrane performance and to minimize the amount of chemical reagents spent on the process [4-6].

Proteins have been reported as the main cause of irreversible fouling and consequently the main target of cleaning, whereas polysaccharides belong to the class of low fouling molecules [7-8]. Kuzmenko et al. [9] report that organic fouling is caused by many factors related to both the foulants and the membrane surface, such as the structure and charge of the foulants, composition, the hydrophobicity and surface potential of the membrane.

Cleaning agents can be defined as substances that can effectively remove matter that is not an integral part of the membrane surface [10]. One of the most popular types of protein removers are neutral enzymatic detergents that contain complexing agents and a combination of approved organic and inorganic surfactants. According to Wais et al. [11-12] the interactions between foulants and cleaning agents can affect fouling material present on a membrane surface in the three following ways (i) the foulants may be removed, (ii) the morphology of the foulants may be changed, (iii) the surface chemistry of the deposit may be altered causing changes in hydrophobicity or charge. To recover the initial flux effectively, the bonds between the foulants and the membrane must be broken down; however the treatment should have no side effects. Water rinsing can be an effective method for removing loose foulant pieces that

occur during the cleaning procedure, although in some conditions it can cause compaction of the fouling layer or drive some particles inside the membrane [7].

The most common parameter for assessing the effectiveness of a chemical cleaning treatment is measuring the recovery of water permeate flux. However, as different foulants may influence permeation characteristics, other methodologies should also be considered, such as microscopic techniques or surface characterization. Väisänen et al. [3] studied the cleaning efficiency of selected cleaning agents on ultrafiltration membranes using a combination of complementary surface characterization methods. Data from FTIR-ATR spectra allowed them to determine the foulants present and the changes in foulant composition after the cleaning step. Using SEM pictures, they concluded that the foulants were located primarily inside the membrane structure. Lim and Bai [1] studied the prevailing fouling mechanisms during microfiltration of activated sludge wastewater and the efficiency of various cleaning methods using SEM, particle size distribution measurements and permeate flux data. SEM images were used to obtain information on how the different cleaning methods affected the membrane surface and the cake formed during filtration. However, the percentage of flux recovery was used as an important parameter to compare the effectiveness of the treatments. Bird and Barteltt [13] described protocols and developed a mathematical model of MF and UF membrane cleaning and determined the effect of cleaning agent concentration, temperature, cross-flow velocity (CFV) and transmembrane pressure (TMP). They showed that the greatest effect on flux recovery was related to cleaning agent concentration and temperature applied. In addition, to describe the structure of the deposit and morphological changes during cleaning they used SEM and light microscopy. Platt and Nyström [14] studied the effectiveness of cleaning on membranes fouled by proteins under similar conditions using different hydrodynamics. They based their evaluation on the flux recovery parameter, turbidity and absorbance of BSA after water rinsing and chemical cleaning. Chen et al. [15] investigated the cleaning efficiency of four types of cleaning agents in order to optimize cleaning performance and provide information for cleaning modeling and performance prediction. They evaluated flux recovery and resistance decrease, also employing SEM and MALDI-MS techniques to determine protein components on the fouling layer before and after cleaning. Recently Rebiller-Baudry at al. [16] investigated the fundamental mechanisms of cleaning PES membranes fouled by skimmed milk in ultrafiltration in order to optimize cleaning. To report the kinetics of the cleaning process they used contact angle measurements for cleaned membranes versus the time for different cleaning agents. The FTIR-ATR method was then used to quantify protein residues.

Recently confocal scanning laser microscopy (CSLM) has been applied to characterize biofouling patterns during the microfiltration of single and binary protein/dextran solutions. Images of membranes obtained with CSLM provide very useful information about the localization of foulants and allow the pore surface occupied by each of them to be quantified [17-18]. The use of CSLM to characterize mechanical cleaning of membranes was reported by Spettmann et al. [19]. They found CSLM in conjunction with image analysis to be a suitable

UNIVERSITAT ROVIRA I VIRGILI
MEMBRANE FOULING CHARACTERIZATION BY CONFOCAL SCANNING LASER MICROSCOPY
Maria Malgorzata Zator
ISBN:978-84-693-0712-0/DL:T-422-2010

technique for evaluating the efficiency of ultrasonic treatment by comparing fouled membranes before and after removal of the deposit. Other widely reported methods for analyzing cleaning results and flux recovery are (i) determining pore size distribution before and after cleaning, (ii) analyzing the foulant in the cleaning solution, and (iii) characterizing the charge differences between virgin and cleaned membranes using the streaming potential method [20-24].

The main goal of this chapter is apply CSLM to determine the efficiency of a water rinsing cycle and the use of a chemical cleaning agent on the removal of foulants deposited on polycarbonate membranes after the filtration of a model solution containing a protein (BSA) and a polysaccharide (dextran). A rinsing cycle, different cleaning times and different concentrations of the cleaning agent will be used. Results on flux recovery, resistance reduction, amount of protein/polysaccharide detected inside the pores (calculated from CSLM images) and 3D reconstructions of CSLM images will be used to compare the effect and efficiency of the cleaning protocols. CSLM is selected to quantify protein and polysaccharide profiles inside the membrane before and after the rinsing and chemical cleaning cycles because it allows the effect of the treatments on each compound to be compared separately.

UNIVERSITAT ROVIRA I VIRGILI
MEMBRANE FOULING CHARACTERIZATION BY CONFOCAL SCANNING LASER MICROSCOPY
Maria Malgorzata Zator
ISBN:978-84-693-0712-0/DL:T-422-2010

4.2. Materials and methods

4.2.1. Membrane, fouling solutions and chemicals

Microfiltration experiments were carried out using 47 mm membrane discs, black polycarbonate membrane with a nominal pore size of 0.80 μm, (Table 4.1), with a clean water flux of 20565 L/(hm^2) at 51 kPa and Metricel® black , mixed esters membranes with nominal pore size 0.45 μm), with a clean water flux of 14719 L/hm^2 at 0.51 × 10^5 Pa, both supplied by Sterlitech . Black membranes were selected to eliminate interferences in the detection of the fluorescent compounds present in the model solution [18]. BSA-fluorescein (FITC) conjugate (A-9771) and the fluorescent dextrans Dextran 70 kDa rhodamine B (RITC) conjugate (R9379) and Dextran 150 kDa tetramethylrodamine (TRITC) conjugate (T1287) were purchased from Sigma. Besides the fact that BSA and dextrans act as model compounds for proteins and polysaccharides, the selection was also based on the fact that they exhibit a maximum absorption close to the emission wavelength of the lasers in the CSLM, and their excitation/emission wavelengths do not overlap. A phosphate buffer was used to adjust the pH of all protein solutions to 7.4. ECOLAB-Henkel provided P3 Ultrasil 53 (US53), a neutral enzymatic powder detergent containing a combination of organic and inorganic surfactants. US53 does not attack membranes or filtration installations and is especially recommended for use in the food industry.

Table 4.1. Polycarbonate (PCTE) 0.8 μm and Metricel 0.4 μm membranes characteristics and performance*.

	PCTE	Metricel
Max. Operating Temp	140°C	130°C
Hydrophilic	Yes	Yes
pH	4-8	neutral
Thickness	9 μm	135 μm
Porosity (%)	15	78
Acids	Resistant	---
Alcohols	Resistant	---
Bases	Not Resistant	---

* data supplied by the manufacturer.

UNIVERSITAT ROVIRA I VIRGILI
MEMBRANE FOULING CHARACTERIZATION BY CONFOCAL SCANNING LASER MICROSCOPY
Maria Malgorzata Zator
ISBN:978-84-693-0712-0/DL:T-422-2010

4.2.2. Filtration plant and operating conditions for membrane fouling and cleaning

All experiments were conducted using a lab-sized microfiltration plant described in more detail in Chapter 3, section 3.2. The filtration area of the cross-flow module was 0.0016 m^2. The operating conditions were: room temperature (23±2°C), constant pressure of 51 kPa and cross-flow velocity of 6.63 m/s. At the beginning of each experiment a new polycarbonate or metrical membrane was placed and fresh protein/dextran solution buffered at pH 7.4 was loaded and filtered until the flux reached a constant value. The average length of the filtration experiments was three hours for BSA-FITC/dex RITC 70 kDa solution and five hours for BSA-FITC/dex TRITC 150 kDa. Total initial concentrations of 0.5 and 1 g/L of the protein/dextran solutions (0.25 g/L BSA and dextran for the 0.5 g/L and 0.5 g/L BSA and dextran for the 1g/L) were used, unless noted otherwise. Feed volume was kept constant by returning retentate and permeate in a closed loop. After the filtration of the model solution had finished, the whole system was rinsed in situ with miliQ water, or buffer solution, or chemically cleaned in situ with 0.1 or 0.5% US53 (Ecolab-Henkel). Water or buffer rinsing and chemical cleaning were always performed in a forward direction. Flow rate and transmembrane pressure during rinsing and cleaning were maintained at the same values as during the filtration experiments. Before each experiment the filtration rig was thoroughly cleaned with a 20% sodium hydroxide solution, and then rinsed with prefiltrated deionized water until neutral pH was reached. The whole set-up was completely covered with aluminum foil in order to minimize photo-bleaching of the fluorescent reagents.

4.2.3. CSLM analysis

The protocols for performing the CSLM analysis are described in detail in Chapter 2, section 2.2. The microscope used was a Nikon Eclipse TE200 and in all cases specimens were magnified by 100 × objective (numerical aperture 1.4), and the zoom magnification was 2.8. The microscope's detection conditions were kept constant for all the membrane samples taken under the same filtration conditions. The optical sectioning was done by taking twenty images every 0.16 μm from the surface towards the interior of the membrane, and twenty images every 0.16 μm from the surface towards the cake layer. This optical sectioning provided data on foulant penetration in the membrane and the cake layer up to 2.5-3 μm.

ImageJ 1.30v (National Institute of Health, USA) and Imaris (Bitplane) were used to analyze CSLM images from the membranes after filtration, water rinsing and the applied chemical cleaning cycle. ImageJ 1.30v was used to measure the surface occupied by pores (A_p) and the fraction of the pore surface in which protein/polysaccharide was detected (P_s), according to equation (4.1) as described in Chapter 2.

$$P_S = \frac{A_f}{A_p} \tag{4.1}$$

The digital images had 512 × 512 pixels with an integral value ranging from 0 to 255. The processing of the images included identifying the features to be analyzed, segmenting and extracting the measurements of interest, as described Chapter 2, section 2.2. The P_s values are always presented for each fluorescent molecule separately (BSA-FITC, dextran-RITC 70 kDa or dextran-TRITC 150 kDa). The P_s profiles have been calculated up to depths of 3 μm inside the membrane, and they correspond to the average value of nine replicates (experiments were run in triplicates and 3 fields of each membrane were visualized using CSLM). Standard deviations are plotted in a few values to indicate reproducibility. It is important to mention that when BSA-FITC and the dextran (dextran-RITC 70 kDa or dextran-TRITC 150 kDa) were detected in the same voxel, colocalization algorithms enabled the individual fouling (P_s) to be determined, that is, the fraction of the pore surface in which the protein and the dextran were detected. P_s for each compound can range from 0 to 100%, as it is possible to detect both the protein and the dextran simultaneously in one pixel.

The primary limitations of CSLM are related to its resolution, which in the best case may be 180 nm in the focal plane (x,y) and only 500-800 nm along the optic axes (z). Due to this limitation, the use of CSLM to characterize surface porosity is restricted to microfiltration membranes. The fact that detection of species using CSLM relies on their fluorescence could also be considered a limitation. From the results of a previous chapters regarding the influence of fluorescent labeling on membrane fouling, it becomes clear that the use of compounds labeled with fluorescent dyes significantly influences membrane fouling. However, for membranes with low surface porosity such as PC membranes, it has been shown that membrane fouling occurs fast enough that the influence of using fluorescent labeled compounds is negligible.

UNIVERSITAT ROVIRA I VIRGILI
MEMBRANE FOULING CHARACTERIZATION BY CONFOCAL SCANNING LASER MICROSCOPY
Maria Malgorzata Zator
ISBN:978-84-693-0712-0/DL:T-422-2010

4.3. Results and discussion

4.3.1. Pure water flux recovery

To study the extent of reversible fouling, a rinsing cycle was performed on the fouled membranes after the filtration of fluorescent BSA/dextran solutions. The membranes were rinsed with water by pumping MiliQ water into the module for 30 min. Before and after the rinsing cycle, water permeate flux was determined and the results are compared in Table 4.2. As can be seen, a 30 minutes water rinsing cycle caused a reduction in the water permeate flux (FRED) for all the solutions, regardless of the molecular size of the dextran and the total concentration of solutes present.

$$FRED = \frac{J_{filtration} - J_{rinsing}}{J_{filtration}} * 100\% \qquad (4.2)$$

where $J_{filtration}$ is the pure water or buffer flux after filtration and J_{rising} is the pure water or buffer flux after rising

Table 4.2. Pure water flux after filtration of BSA/dextran solutions and after 30 min rinsing with MiliQ water.

	$J_{filtration}$ [L/h m^2]	$J_{rinsing}$ [L/h m^2]	FRED [%]
BSA-FITC/dextran-RITC 70 kDa, 0.5 g/L	1148±158	789±145	31
BSA-FITC/dextran-RITC 70 kDa, 1 g/L	986±349	418±137	58
BSA-FITC/dextran-TRITC 150 kDa, 0.5 g/L	252±59	180±67	28
BSA-FITC/dextran-TRITC 150 kDa, 1 g/L	394±121	229±67	42

[1]J: water flux

UNIVERSITAT ROVIRA I VIRGILI
MEMBRANE FOULING CHARACTERIZATION BY CONFOCAL SCANNING LASER MICROSCOPY
Maria Malgorzata Zator
ISBN:978-84-693-0712-0/DL:T-422-2010

Figure 4.1. Permeate flux evolution during filtration of a 0.5 g/L BSA-FITC/dextran-RITC 70 kDa solution and water flux during rinsing.

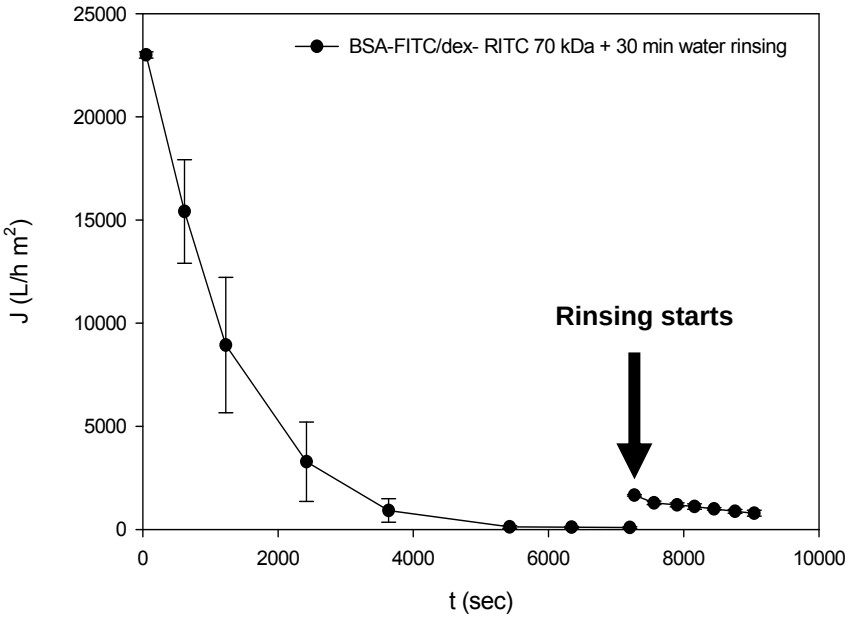

Figure 4.1 shows, as an example of the type of filtration curves obtained, the permeate flux evolution during filtration of a 0.5 g/L BSA-FITC/dextran-RITC solution followed by water permeate flux during the rinsing step. It can be clearly seen that the water permeate flux is slightly higher than the steady-state protein/dextran permeate flux at the beginning of the rinsing (Figure 4.1, Table 4.2), and it decreases along its course. It is thought that rinsing slightly helps cleaning the membrane at the very beginning, removing some reversible fouling (even though in this case it is very small) but after a very short initial stage, the effect is the opposite since it pushes the foulants inside the membrane pores, blocking them. Seeing the water permeate flux evolution in Figure 4.1, it is thought that it will eventually reach the same value obtained during the filtration of the solution. These results will be further commented when presenting the results of the confocal microscopy analysis of the membrane samples. Although there was a lesser reduction in flux after the rinsing period for the BSA-FITC/dextran-TRITC 150 kDa solutions than for the BSA-FITC/dextran-RITC 70 kDa solutions, it must be noted that the pure water flux at the end of the filtration runs was always much reduced for the solutions with the biggest dextran, as a result of a higher blockage of the pores. As the results in Table 4.2 show, it is clear that a rinsing step using water does not improve membrane permeability, and a chemical cleaning agent should be applied to remove fouling. Kuzmenko et al. working with polyethersulfone (PES) membranes fouled by BSA [9] concluded that cleaning with deionized water for 30 minutes was a very ineffective treatment in terms of flux recovery.

In order to evaluate the possible influence of pH changes from 7.4 fixed for all the filtration solutions to 5.5 for miliQ water rising, rising using phosphate buffer (PBS) solution with a pH 7.4 was performed. PBS fluxes were obtained for the clean and fouled membranes, and

UNIVERSITAT ROVIRA I VIRGILI
MEMBRANE FOULING CHARACTERIZATION BY CONFOCAL SCANNING LASER MICROSCOPY
Maria Malgorzata Zator
ISBN:978-84-693-0712-0/DL:T-422-2010

also after a 30 min pumping of PBS buffer to the module. These values were used to evaluate the reduction in buffer flux (FRED), which is assumed to be a measure of the irreversible fouling, according to equation (4.2).

Table 4.3 presents the permeate fluxes obtained for BSA-fluorescein and phosphate buffer (PBS) for the clean and fouled membranes (a 0.8 μm polycarbonate and a 0.45 μm mixed esters), and after the rinsing step, as well as the flux reduction which is assumed to be a measure of the irreversible fouling.

Table 4.3. Permeate fluxes for clean membrane, fouled with 0.5 g/L BSA solution, and after PBS rinsing.

Membrane	J^1_{PBS} for clean membrane [L/h m^2]	J^2 after BSA-FITC filtration [L/h m^2]	J^1_{PBS} after BSA-FITC filtration [L/h m^2]	J^1_{PBS} after rinsing [L/h m^2]	FRED [%]
Polycarbonate	4390±544	41±3	179±11	45±2	75 %
Mixed esters	15059±878	71±9	91±7	66±6	27 %

[1] J_{PBS}: buffer flux;
[2] J: permeate flux at the end of filtration run

In this study, US53 was used as the chemical cleaning agent. Two different concentrations were tested (0.1 and 0.5%) and the cleaning times applied were 5, 15 and 30 min. Table 4.4 shows the pure water fluxes obtained at the end of the filtration runs, after chemical cleaning, as well as flux recovery (*FREC*), calculated according to equation (4.3), for BSA-FITC 0.5 g/L and solutions of BSA-FITC/dextran-RITC 70 kDa 0.5 g/L.

$$FREC = \frac{J_{cleaning}}{J_{original}} * 100\% \qquad (4.3)$$

where $J_{cleaning}$ is the pure water flux after cleaning and $J_{original}$ is the pure water flux of the clean membrane

Table 4.4. Pure water flux after filtration of BSA 0.5 g/L and BSA/dextran 70 kDa 0.5 g/L solutions and after chemical cleaning with US53.

	J^1 after filtration [L/h m^2]	$J_{cleaning}$ after 5 min US53 [L/h m^2]	FREC.[2] [%]	$J_{cleaning}$ after 15 min US53 [L/h m^2]	FREC.[2] [%]	$J_{cleaning}$ after 30 min US53 [L/h m^2]	FREC.[2] [%]
BSA-FITC , US53 0.1%	848±375	8757±384	43	6205±145	30	N/A	N/A
BSA-FITC/dextran-RITC 70 kDa, US53 0.1%	1148±158	5726±157	28	8019±88	39	6333±85	31
BSA-FITC/dextran-RITC 70 kDa, US53 0.5%	1148±158	6099±277	30	5746±225	28	N/A	N/A

[1] J: water flux
[2] FREC: flux recovery, calculated according to equation (4.3)

UNIVERSITAT ROVIRA I VIRGILI
MEMBRANE FOULING CHARACTERIZATION BY CONFOCAL SCANNING LASER MICROSCOPY
Maria Malgorzata Zator
ISBN:978-84-693-0712-0/DL:T-422-2010

As can be seen in Table 4.4, cleaning with US53 0.1 % for five minutes resulted in the highest water flux recovery for the BSA-FITC solution, while for the 0.5 g/L BSA-FITC/dextran-RITC 70 kDa solution maximum flux recovery was obtained after 15 minutes of chemical cleaning. When the concentration of US53 was raised to 0.5%, the maximum flux recovery for the BSA-FITC/dextran-RITC 70 kDa solution was obtained after five minutes, although in this case flux recovery was nearly maintained after 15 minutes. These results will also be discussed further in the section on the confocal analysis of the membranes after each treatment.

4.3.2. Fouling characterization

Permeate flux during microfiltration driven by transmembrane pressure can be described by Darcy's law:

$$J = \frac{\Delta P}{\mu R_{total}} \tag{4.4}$$

where J is the permeate flux, ΔP is the transmembrane pressure, μ is the viscosity and R_{total} is the total resistance. According to Field et al. [24] the equation can be rewritten as:

$$J = \frac{\Delta P}{\mu\left(R_m + R_{fouling}\right)} \tag{4.5}$$

where R_m is the clean membrane hydraulic resistance and $R_{fouling}$ accounts for both polarization and fouling effects on the flux. Equation (4.5) was used to calculate the total resistance and thereby the fouling for each treatment.

Figure 4.2. Resistance comparison for 0.5 g/l BSA-FITC after filtration and after 5 and 15 min cleaning steps with 0.1 % US53

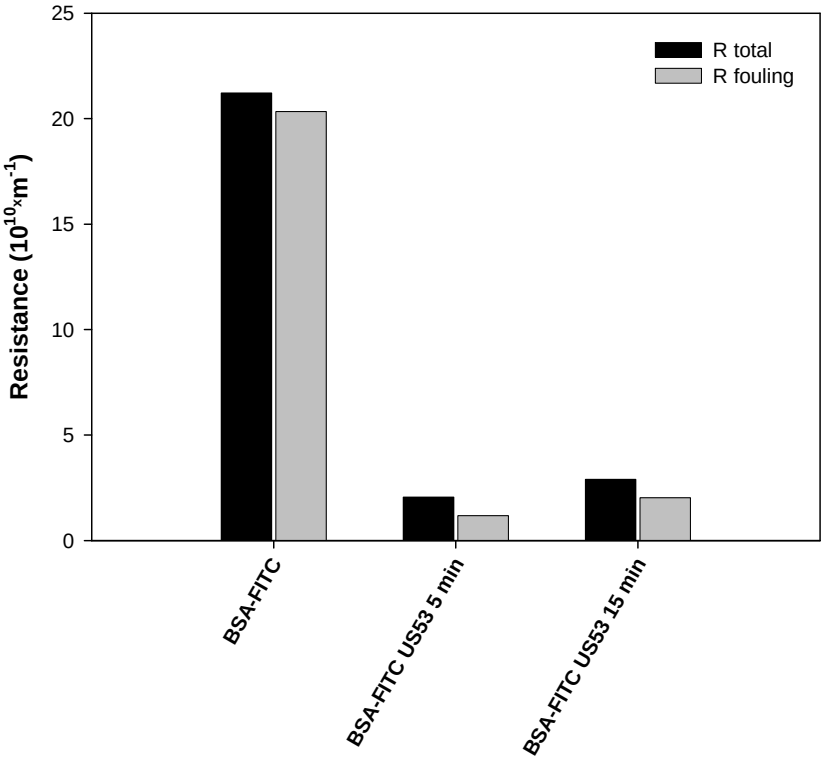

Figure 4.2 shows total (R_{total}) and fouling ($R_{fouling}$) resistances for polycarbonate membranes fouled by 0.5 g/L BSA-FITC solutions after filtration and cleaning cycles of 5 and 15 minutes with the commercial cleaning agent US53. As can be seen from the values in Figure 4.2, it is clear that resistance related to reversible and irreversible fouling is responsible for the decrease in permeate flux. It is also clear that the five minute cleaning cycle with US53 further reduces fouling resistance, while when increasing the cleaning cycle to 15 minutes, a slight increase can be observed compared to the five minute cycle. It is thought that as a result of chemical cleaning most of the protein and protein aggregates were broken down into small pieces. As the cleaning agent crosses through the membrane, some of the debris formed is driven inside the membrane and some small blockages can occur. This is thought to be the main reason that a 15-minute chemical cleaning treatment is less effective than one lasting five minutes. The results therefore indicate that determining the most favorable cleaning time is extremely important in optimizing the cleaning conditions of a membrane process.

UNIVERSITAT ROVIRA I VIRGILI
MEMBRANE FOULING CHARACTERIZATION BY CONFOCAL SCANNING LASER MICROSCOPY
Maria Malgorzata Zator
ISBN:978-84-693-0712-0/DL:T-422-2010

Figure 4.3. Resistance comparison for 0.5 g/l BSA-FITC/dextran-RITC after filtration and after 5, 15 and 30 min cleaning steps with 0.1 and 0.5 % US53

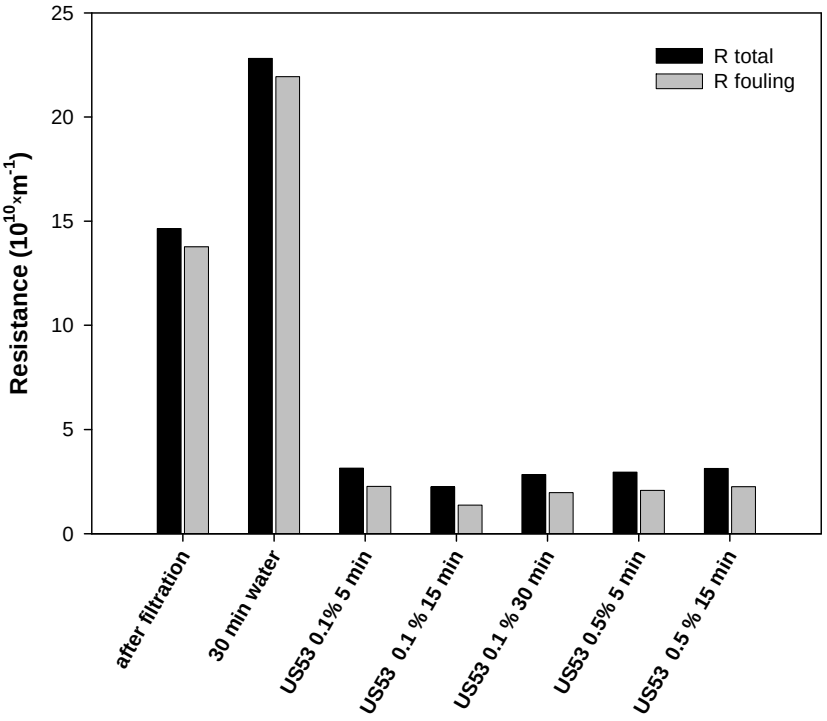

Figure 4.3 shows the resistance values for 0.5 g/L binary solutions of BSA-FITC/dextran-RITC 70 kDa, after filtration, water rinsing and 5, 15 and 30 min cleaning cycles for two different concentrations of the cleaning agent (0.1 and 0.5%). The results clearly show, as mentioned in the previous section on pure water flux recovery, that the fouling resistance increases after rinsing with water for 30 minutes, compared with the $R_{fouling}$ obtained after filtration. The increase in the fouling resistance is directly related to the extent of pore blocking and constriction, since during the rinsing step the foulant material is driven inside the membrane. The efficiency of the chemical cleaning is similar to that obtained with the protein solution alone, but 100% recovery of the pure water flux was never achieved (Table 4.4) and a slight but still significant $R_{fouling}$ was obtained after all the cleaning treatments, meaning that some fractions of foulants could be found blocking the pores [23]. Results show that an increase in US53 concentration from 0.1 to 0.5% does not significantly change the $R_{fouling}$ values obtained (Figure 4.3). From the results in Table 4.4 and Figures 4.2 and 4.3 it is clearly shown, for both studied concentrations of the chemical cleaning agent, that the length of the cleaning for a maximum recovery of the water flux depends on the concentration of the cleaning agent. After the maximum water flux recovery is attained, and increase in the cleaning time is no longer effective since foulants are driven inside the membrane, probably resulting in some irreversible plugging of the largest pores [25].

4.3.3. Fouling characterization by confocal microscopy

The macroscopic results on pure water flux recovery and fouling resistances allowed to examine the effect of water rinsing and chemical cleaning under certain experimental conditions. The data gathered up to this point does not provide any information on how the rinsing or the different cleaning cycles affect each component present in the solutions. The use of CSLM to visualize membrane samples at the end of the filtration, rinsing and cleaning periods, and the image analysis of the results obtained using CSLM made it possible to quantitatively correlate the fluorescent signal with the presence of protein or dextran adsorbed/deposited on top and inside of the membrane, thereby allowing to obtain information on how each treatment affected each compound individually. The correlation was made using the fraction of the pore surface in which the protein/dextran was detected (P_s). The P_s values were calculated using a co-localization algorithm described in Chapter 2, section 2.2. Qualitative information was also obtained from CSLM images. Even though they offer information of a single membrane field, in most of the cases they are representative enough to allow some discussion about the effect of the treatment on each foulant. All the images presented below correspond to orthogonal 3D reconstructions of reflection and fluorescent CSLM images.

Figure 4.4 shows the P_s profiles for BSA-FITC after filtration and after water rinsing for the 0.5 g/L fluorescent protein/dextran (70 and 150 kDa) solutions. As can be seen in Figure 4.4, water rinsing seems to slightly increase the P_s values for BSA-FITC, regardless of the molecular size of the fluorescent dextran present in the solution. Although some P_s values obtained after filtration and after rinsing are comparable with the standard deviations plotted in the curves, they follow the same trend, which is more noticeable for BSA/dextran-TRITC 150 kDa, where a P_s value of about 80% was found up to 1 µm inside the membrane after water rinsing. When the P_s profiles for the dextran-RITC 70 kDa are plotted versus membrane depth (z) (Figure 4.5) it can be seen that water rinsing seems to slightly reduce the dextran content inside the membrane, resulting in comparable or smaller P_s values, regardless of the dextran molecular size. Therefore, water rinsing has a different effect depending on the nature of the foulant. A slight transport of the protein can be seen inside the membrane due to the rinsing process. This results in a higher presence of the protein inside the membrane, whereas the dextrans are partially removed during the water rinsing period. Therefore, membrane fouling in this study is clearly related to protein fouling, since the rinsing period reduced the water permeate flux (Table 4.2) and increased the fouling resistance (Figure 4.3).

UNIVERSITAT ROVIRA I VIRGILI
MEMBRANE FOULING CHARACTERIZATION BY CONFOCAL SCANNING LASER MICROSCOPY
Maria Malgorzata Zator
ISBN:978-84-693-0712-0/DL:T-422-2010

Figure 4.4. Fraction of pore surface on which BSA-FITC is detected (P_s) after filtration and 30 min water rinsing of binary protein/dextran 0.5 g/L solutions; Negative ***z*** values show the position inside the membrane. Solid curve: fitting to equation (4.6).

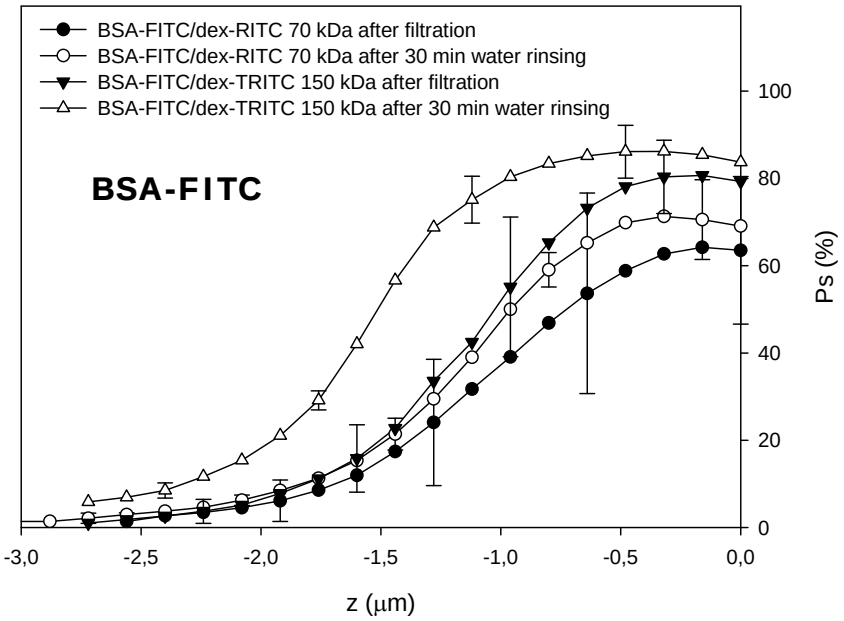

Figure 4.5. Fraction of pore surface on which dextran-RITC (70 and 150 kDa) is detected (P_s) after filtration and 30 min water rinsing of binary protein/dextran 0.5 g/L solutions; negative ***z*** values show the position inside the membrane. Solid curve: fitting to equation (4.6).

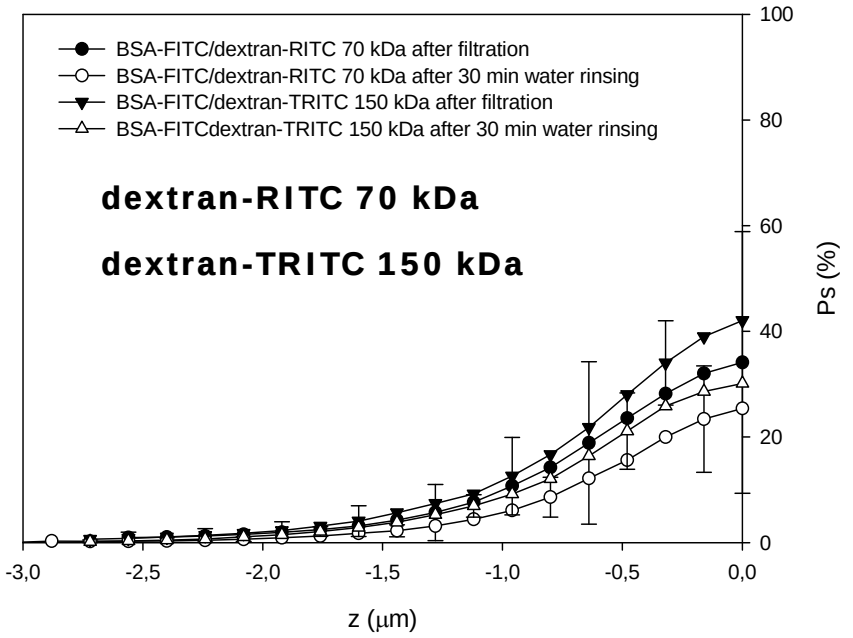

CSLM images in Figure 4.6 illustrate the extent of membrane fouling caused by deposition/adsorption of BSA-FITC on the membrane surface and pore blockage at various membrane depths after filtration of a BSA-FITC/dextran-TRITC 150 kDa solution and after rinsing the fouled membrane for 30 minutes with water. As can be seen in the images (and it was also found plotting P_s values versus membrane depth) the protein (green signal) appears blocking most of the pores up to a depth of 1.5 µm inside the membrane after rinsing, while less protein was detected on the surface and inside the membrane after the filtration for the same depth. The CSLM images in Figure 4.6 show that BSA completely blocks a high percentage of the membrane pores because the green signal is much more intense at these points than on the surface of the membrane. The areas around the pores give a much less intense green signal, therefore, it is assumed that the majority of the protein is on the interior of the pores. The same kind of information for dextran-TRITC 150 kDa can be found in Figure 4.7, which clearly shows that less foulant (red signal) is found inside the membrane after rinsing than after filtration. For both membranes in Figure 4.7, the detection of dextran-TRITC shows red signal completely covering some of the pores, while some others are only partially covered. This indicates that the fouling mechanism of dextran involves pore complete blocking and pore diameter reduction. Even though it is thought that internal fouling of BSA should also encompass those mechanisms, from the CSLM images obtained it seems that complete pore blocking is the preferred mechanisms in the present situation.

UNIVERSITAT ROVIRA I VIRGILI
MEMBRANE FOULING CHARACTERIZATION BY CONFOCAL SCANNING LASER MICROSCOPY
Maria Malgorzata Zator
ISBN:978-84-693-0712-0/DL:T-422-2010

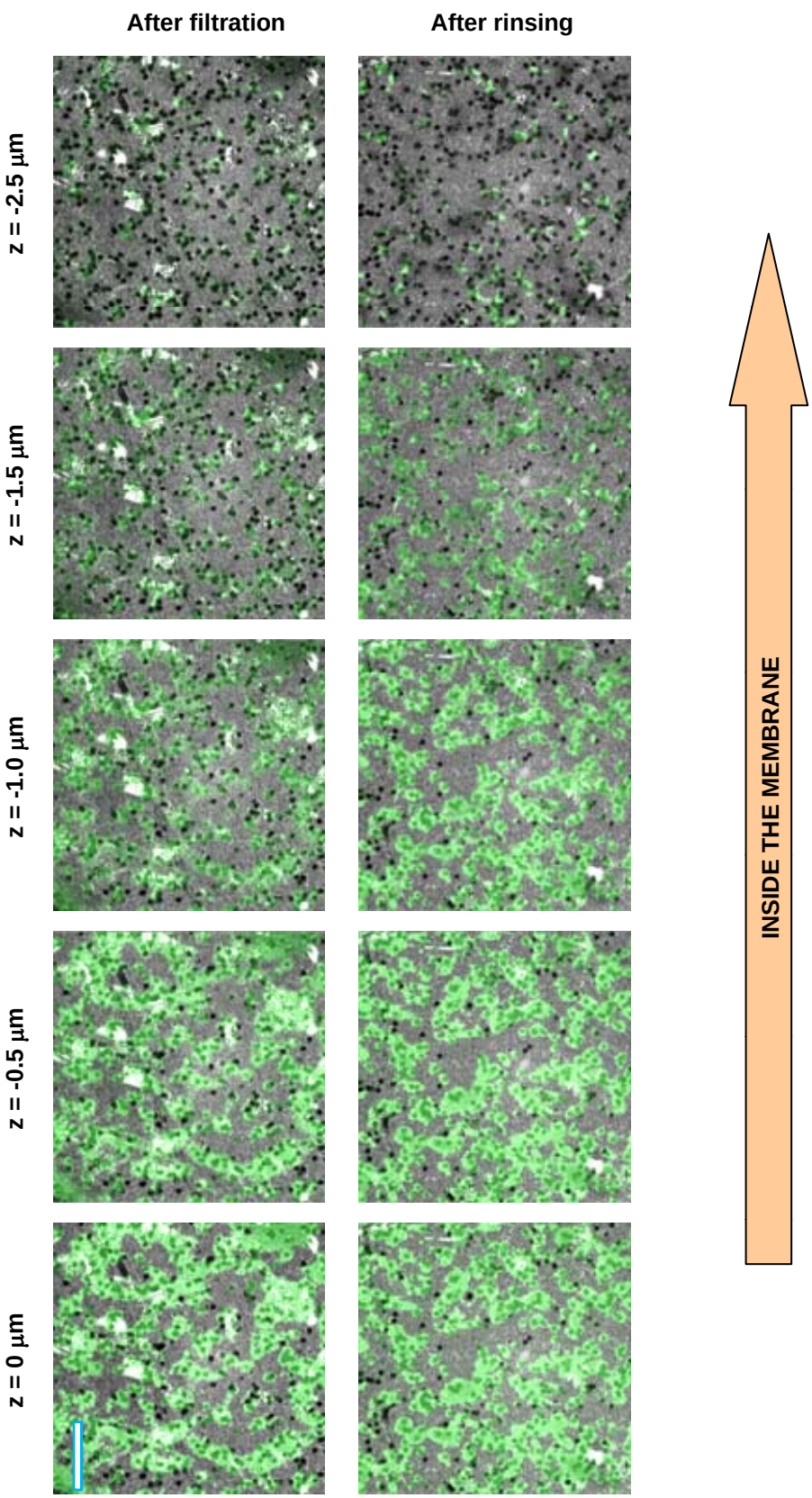

Figure 4.6. 3D orthogonal reconstruction of CSLM images: membranes after filtration of a 0.5 g/L BSA-FITC/dextran-TRITC 150 kDa solution; membrane after water rinsing. Images show the membrane (grey signal) and the protein (green signal) at different depths. Scale bar 10 µm.

UNIVERSITAT ROVIRA I VIRGILI
MEMBRANE FOULING CHARACTERIZATION BY CONFOCAL SCANNING LASER MICROSCOPY
Maria Malgorzata Zator
ISBN:978-84-693-0712-0/DL:T-422-2010

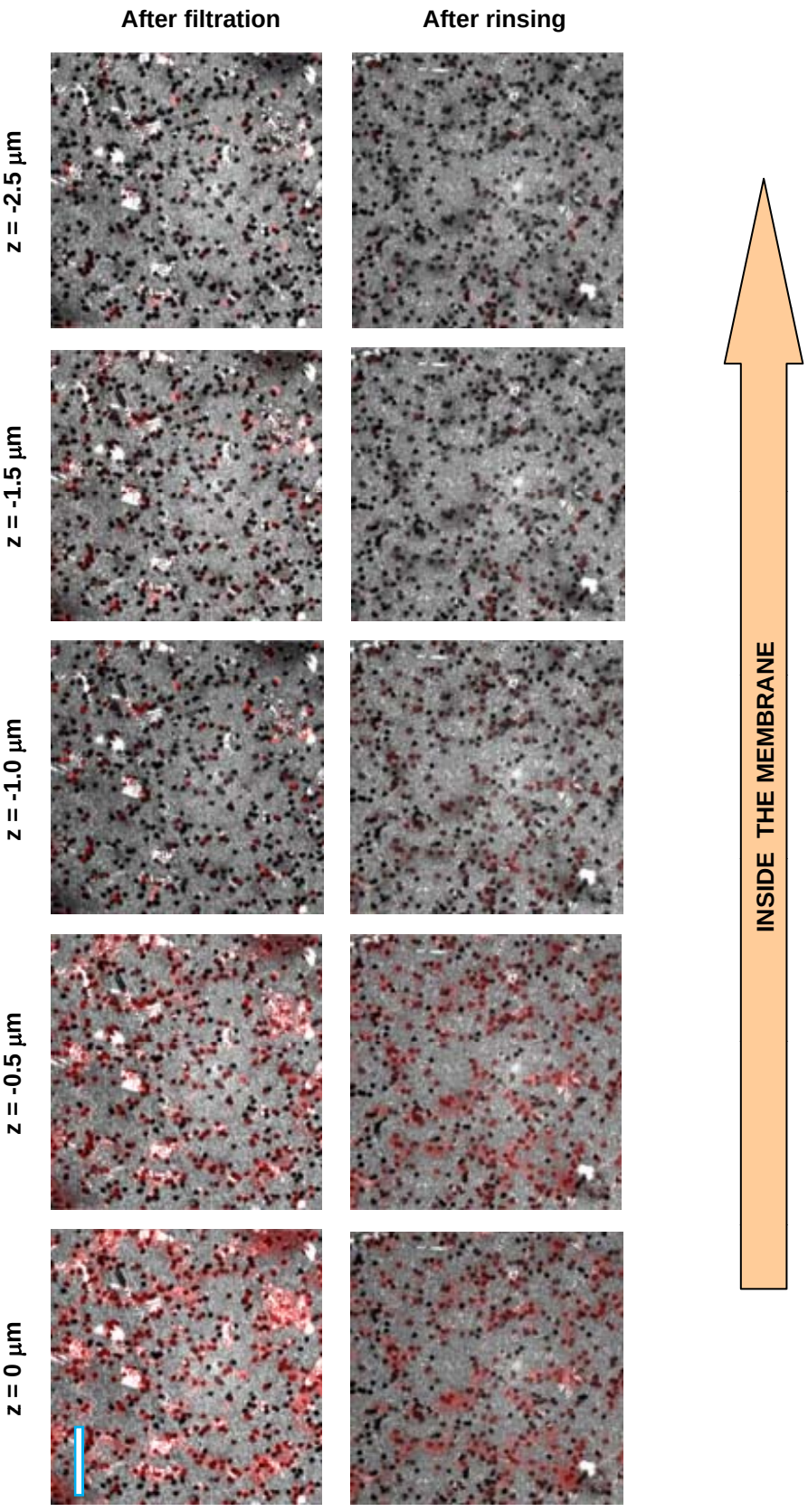

Figure 4.7. 3D orthogonal reconstruction of CSLM images: membranes after filtration of a 0.5 g/L BSA-FITC/dextran-TRITC 150 kDa solution; membrane after water rinsing. Images show the membrane (grey signal) and the dextran (red signal) at different depths. Scale bar 10 µm.

UNIVERSITAT ROVIRA I VIRGILI
MEMBRANE FOULING CHARACTERIZATION BY CONFOCAL SCANNING LASER MICROSCOPY
Maria Malgorzata Zator
ISBN:978-84-693-0712-0/DL:T-422-2010

Figure 4.8 gives an example of the P_s profile changes after 30 min rising using PBS buffer (BSA-fluorescein, polycarbonate membrane). It can be seen that buffer rising as well as water rising cause that some protein is driven inside the membrane. This observation agreed with the fact that the PBS flux after a 30 min rising period drop to the same value as obtained at the end of the BSA filtration for both membranes (Table 4.3).

Also the images obtained from CSLM are in a good agreement with macroscopic data. Figure 4.9 shows a polycarbonate membrane before and after the buffer rising step. It can be clearly seen that some proteins were removed from the membrane surface.

Figure 4.8. Fraction of pore surface in which BSA-FITC conjugate is detected (P_s) after filtration for two different fields (a,b) of the 0.8 μm polycarbonate membrane.

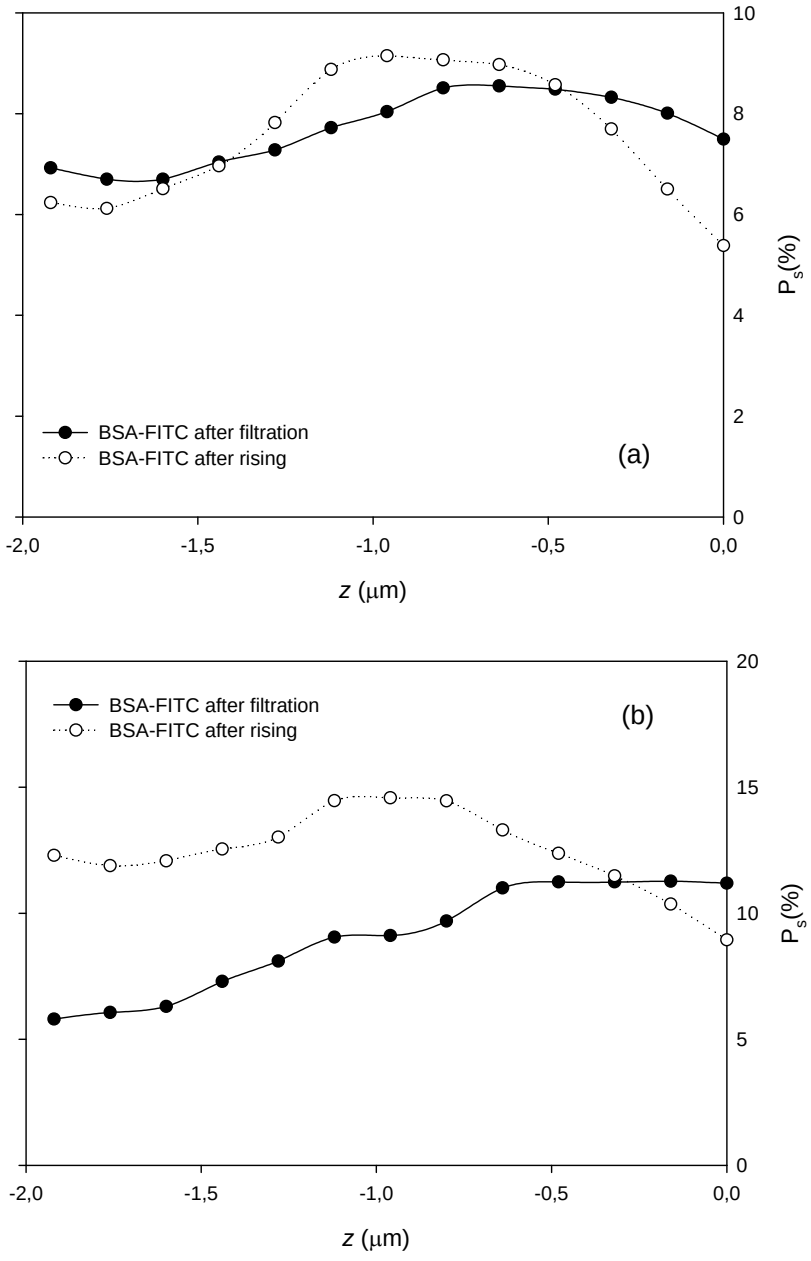

Figure 4.9. CSLM images of a 0.8 µm polycarbonate membrane fouled by a BSA-FITC conjugate. Green signal indicates the presence of the protein; (a) after filtration , (b) after rinsing with buffer.

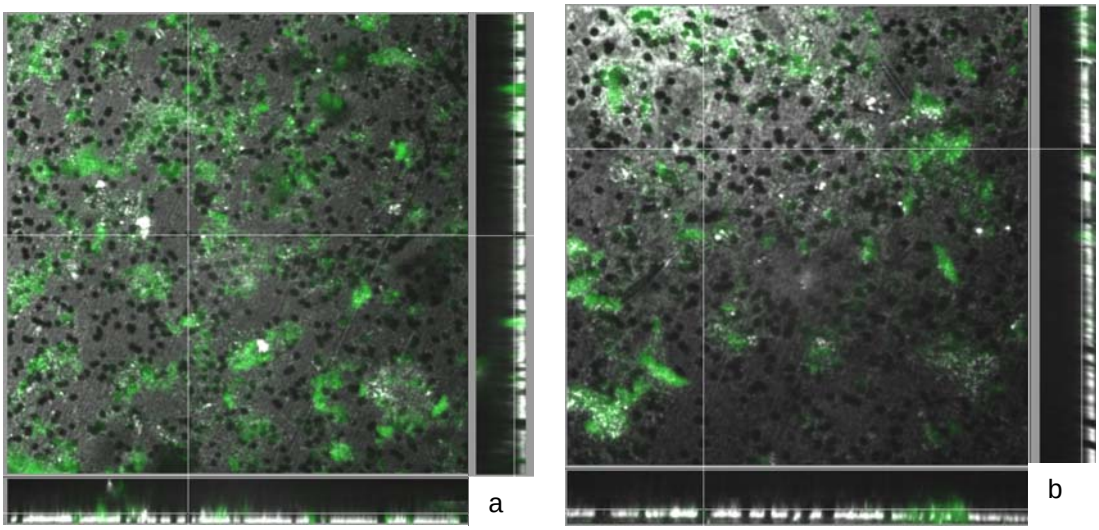

Figures 4.10 and 4.11 show the effect of chemical cleaning on the membrane fouled by 0.5 g/L BSA-FITC/dextran-RITC 70 kDa. It can clearly be seen that P_s values for BSA-FITC (figure 4.10) and dextran-RITC 70 kDa (figure 4.11) decrease significantly as a result of US53 cleaning. After a 15-minute cleaning with 0.1% US53 most of the foulants are removed from the surface and inside of the membrane. Further increase of cleaning time and cleaning agent concentration has no significant influence, since the P_s profiles show values very close to 0. However, this decrease in the P_s values was not directly found in the flux recovery data given in Table 4.4, where it is possible to observe a decrease in the *FREC* after cleaning for 30 min with US53 0.1%, compared to that obtained after 15 minutes. It is assumed that because the fragments of protein and dextran are being driven inside the membrane, pores are being blocked at depths below 3 µm, which is the maximum depth inside the membrane at which a fluorescent signal could be detected.

Figures 4.12 and 4.13 present CSLM images of the membranes, at different depths, after filtration and after chemical cleaning runs with BSA-FITC (green signal) and dextran-RITC (red signal), respectively. As already mentioned when comparing P_s values after filtration and after chemical cleaning, the green signal corresponding to BSA-FITC (Figure 4.12) is found to cover an important extent of the pores after filtration, a small portion of the pores remain blocked after 5 minutes cleaning, and the signal is almost unnoticeable after 15 and 30 minutes chemical cleaning independently of the membrane depth. The trend exhibited by dextran-RITC is the same and it is shown in figure 4.13.

UNIVERSITAT ROVIRA I VIRGILI
MEMBRANE FOULING CHARACTERIZATION BY CONFOCAL SCANNING LASER MICROSCOPY
Maria Malgorzata Zator
ISBN:978-84-693-0712-0/DL:T-422-2010

Figure 4.10. Fraction of pore surface on which BSA-FITC is detected (P_s) after filtration and cleaning steps of different lengths of binary BSA-FITC/dextran-RITC 70 kDa 0.5 g/L solutions with two concentrations of US53; Negative *z* values show the position inside the membrane. Solid curve: fitting to equation (4.6).

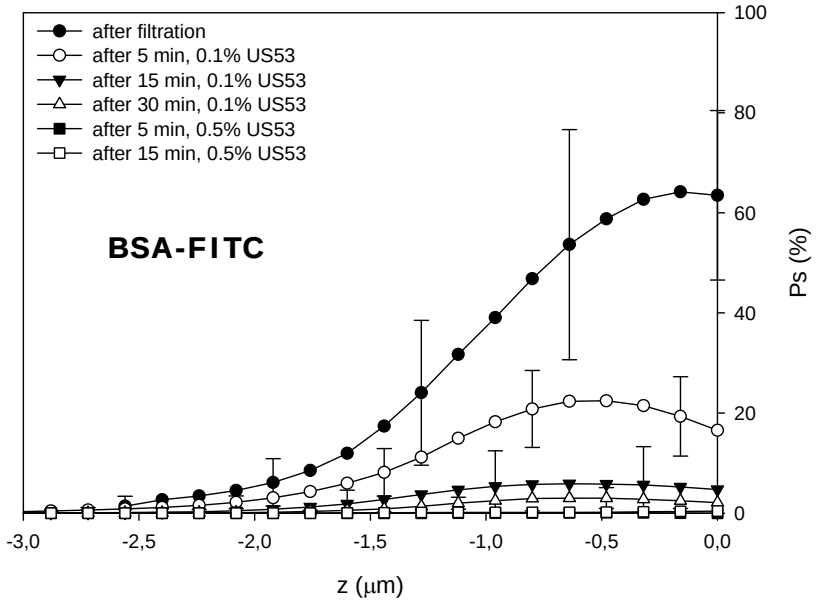

Figure 4.11. Fraction of pore surface on which dextran-RITC is detected (P_s) after filtration and cleaning steps of different lengths of binary BSA-FITC/dextran-RITC 70 kDa 0.5 g/L solutions with two concentrations of US53; negative *z* values show the position inside the membrane. Solid curve: fitting to equation (4.6).

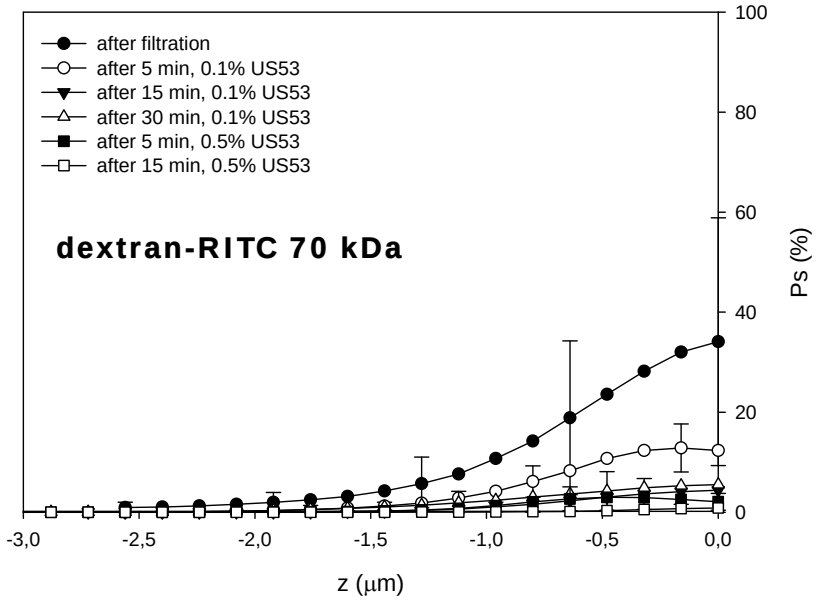

UNIVERSITAT ROVIRA I VIRGILI
MEMBRANE FOULING CHARACTERIZATION BY CONFOCAL SCANNING LASER MICROSCOPY
Maria Malgorzata Zator
ISBN:978-84-693-0712-0/DL:T-422-2010

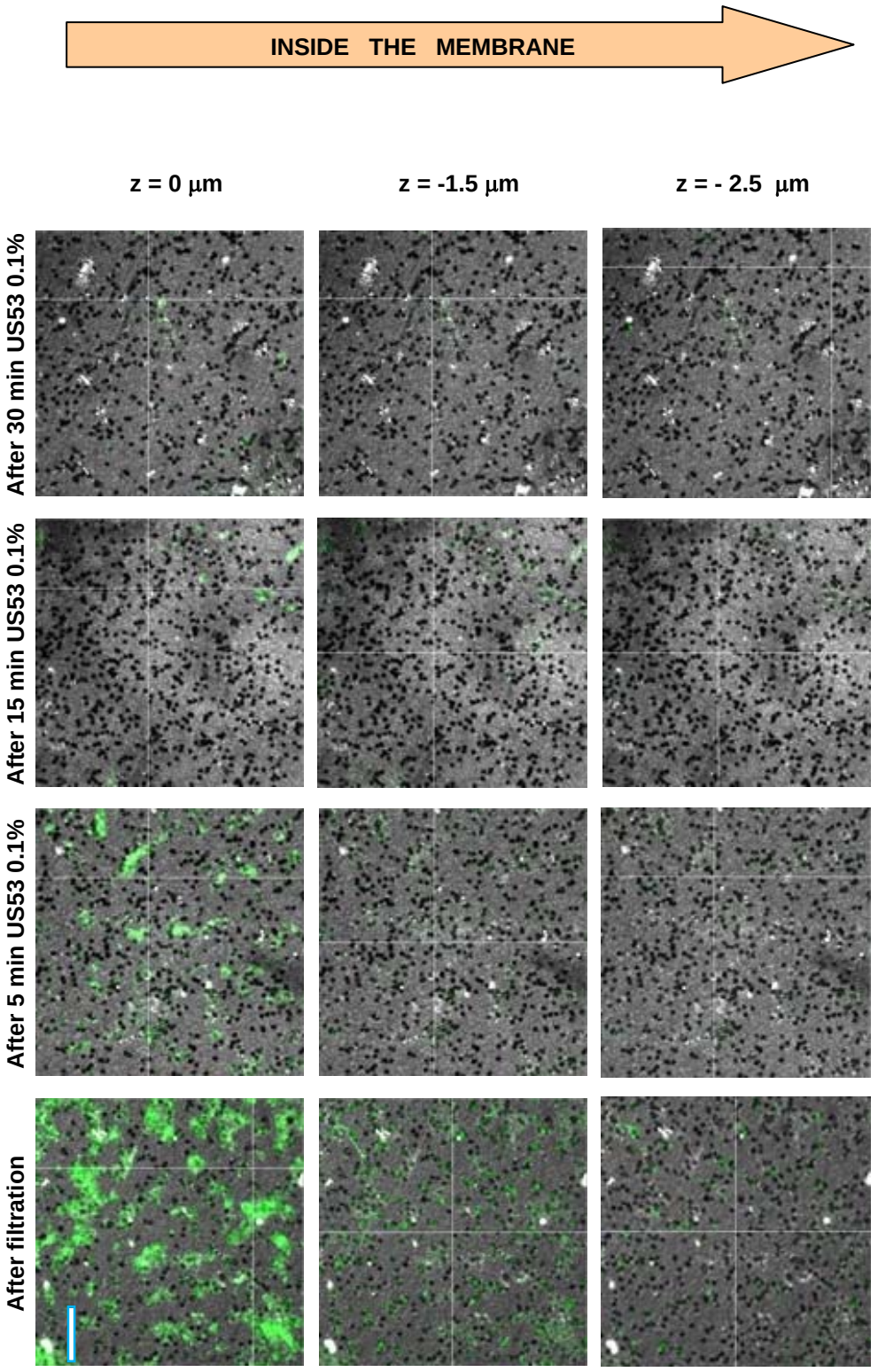

Figure 4.12. 3D orthogonal reconstruction of CSLM images: membranes after filtration of a 0.5 g/L BSA-FITC/dextran-RITC 70 kDa solution; membrane after chemical cleaning with US53 0.1%. Images show the membrane (grey signal) and the protein (green signal) at different depths. Scale bar 10 μm.

UNIVERSITAT ROVIRA I VIRGILI
MEMBRANE FOULING CHARACTERIZATION BY CONFOCAL SCANNING LASER MICROSCOPY
Maria Malgorzata Zator
ISBN:978-84-693-0712-0/DL:T-422-2010

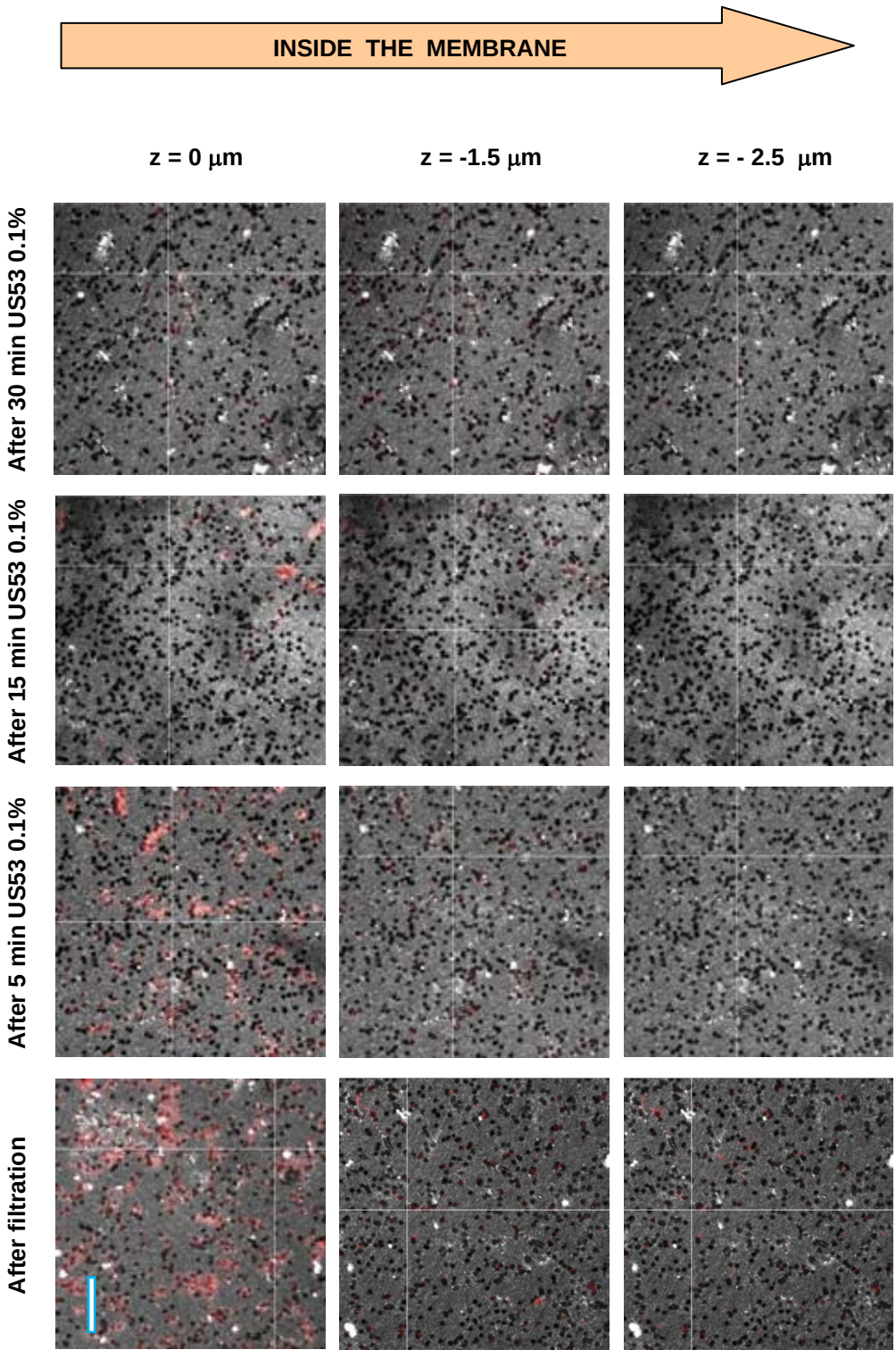

Figure 4.13. 3D orthogonal reconstruction of CSLM images membranes after filtration of a 0.5 g/L BSA-FITC/dextran-RITC 70 kDa solution; membrane after chemical cleaning with US53 0.1%. Images show the membrane (grey signal) and the dextran (red signal) at different depths. Scale bar 10 μm.

In order to obtain more quantitative data from CSLM analysis, average P_s values were fitted versus z values using an empirical equation (equation 4.6) assuming protein adsorption inside the pores. The fitting curves corresponding to equation (4.6) are plotted in Figures 4.4, 4.5, 4.10 and 4.11 as a solid line.

$$P_s = \frac{P_{s0}}{1 + e^{-\left[\frac{z - z_{1/2}}{k}\right]}} \tag{4.6}$$

where:

P_{s0}: P_s value at the membrane surface

$z_{1/2}$: z value (depth from the surface) where $P_s = P_{s0}/2$

The fitting parameters resulting from equation (4.6) will allow us to compare the effects of the rinsing or chemical cleaning processes. Table 4.5 presents the fitting parameters for the curves in Figures 4.4 and 4.5. As shown in Table 4, water rinsing increases P_{s0} and $z_{1/2}$ values for BSA-FITC. This increase indicates a greater presence of the protein on the membrane surface and inside the pores as a result of the water flow pushing the protein aggregates inside the membrane and increasing pore blockage. However, when the P_{s0} and $z_{1/2}$ values for dextran-RITC 70 kDa are compared before and after water rinsing, it is clear that regardless of the molecular size of the dextran, this compound is partially removed by the water flow through the membrane (Figure 4.7). The partial removal of dextrans from inside the membrane during the rinsing step does not improve the water flux (Table 4.3) since the fouling exhibited by BSA is much more significant.

UNIVERSITAT ROVIRA I VIRGILI
MEMBRANE FOULING CHARACTERIZATION BY CONFOCAL SCANNING LASER MICROSCOPY
Maria Malgorzata Zator
ISBN:978-84-693-0712-0/DL:T-422-2010

Table 4.5. Parameters in equation (4.6) for BSA-FITC and fluorescent dextran after filtration or water rinsing of fluorescent solutions of BSA /dextran 70 or 150 kDa, 0.5 g/L.

	P_{s0} [%]	$z_{1/2}$ [μm]	k [μm]	R^2
BSA-FITC/dextran-RITC 70 kDa				
BSA-FITC after filtration	69	1.07	0.35	0.999
BSA-FITC after rinsing	82	1.67	0.50	0.994
Dextran-RITC after filtration	45	0.51	0.41	0.998
Dextran-RITC after rinsing	34	-0.42	0.37	0.998
BSA-FITC/dextran-TRITC 150 kDa				
BSA-FITC after filtration	84	-1.16	0.30	0.998
BSA-FITC after rinsing	87	-1.61	0.29	0.997
Dextran-TRITC after filtration	60	-0.41	0.44	0.998
Dextran-TRITC after rinsing	39	-0.53	0.39	0.997

Table 4.6 shows the fitting parameters for BSA-FITC and dextran-RITC P_s values obtained after filtration and after five different cleaning cycles (Figures 4.10 and 4.11). It can be seen that chemical cleaning significantly decreases the P_{s0} values for both the protein and the dextran. There is just one case where the correlation coefficient obtained falls to 0.61 , which is the fitting for BSA-FITC after cleaning for 5 min with US53 0.5%. In this case, the P_s values obtained are almost constant throughout the membrane depth analyzed and close to zero In this situation the cleaning can be considered almost complete Regarding the $z_{1/2}$ values, for BSA-FITC and US53 0.1% a slight increase was observed when cleaning time was increased, at least after 5 and 15 minutes. This increase might be attributed to the transport of protein fragments, produced during the chemical cleaning, inside the membrane where they partially block some of the pores. For the dextran-RITC 70 kDa, the $z_{1/2}$ values obtained after cleaning with US53 0.1% were almost the same regardless of cleaning time. For US53 0.5%, the $z_{1/2}$ value after five minutes of cleaning increased compared to that obtained after filtration, but it decreased after 15 minutes cleaning. It can be assumed that after five minutes there may still be some fragments of dextran driven inside the membrane, but after 15 minutes of cleaning almost all the dextran has been removed.

UNIVERSITAT ROVIRA I VIRGILI
MEMBRANE FOULING CHARACTERIZATION BY CONFOCAL SCANNING LASER MICROSCOPY
Maria Malgorzata Zator
ISBN:978-84-693-0712-0/DL:T-422-2010

Table 4.6. Parameters in equation (4.6) for BSA-FITC and dextran-RITC after filtration or chemical cleaning with US53 (P3 Ultrasil 53) of solutions BSA-FITC/dextran-RITC 70, 0.5 g/L.

	P_{s0} [%]	$z_{1/2}$ [µm]	k [µm]	R^2
BSA-FITC/dextran-RITC 70 kDa				
BSA-FITC after filtration	69	-1.07	0.35	0.999
BSA-FITC after 5 min US53 0.1%	21	-1.37	0.25	0.970
BSA-FITC after 15 min US53 0.1%	6	-1.46	0.24	0.987
BSA-FITC after 30 min US53 0.1%	3	-1.32	0.17	0.966
BSA-FITC after 5 min US53 0.5%	0	-0.97	0.07	0.610
BSA-FITC after 15 min US53 0.5%	2	-0.63	0.66	0.960
dextran-RITC after filtration	45	-0.51	0.41	0.998
dextran-RITC after 5 min US53 0.1%	14	-0.77	0.25	0.995
dextran -RITC after 15 min US53 0.1%	4	-0.62	0.27	0.999
dextran -RITC after 30 min US53 0.1%	6	-0.75	0.40	0.999
dextran -RITC after 5 min US53 0.5%	3	-0.99	0.14	0.973
dextran -RITC after 15 min US53 0.5%	1	-0.36	0.17	0.997

UNIVERSITAT ROVIRA I VIRGILI
MEMBRANE FOULING CHARACTERIZATION BY CONFOCAL SCANNING LASER MICROSCOPY
Maria Malgorzata Zator
ISBN:978-84-693-0712-0/DL:T-422-2010

4.4. Conclusions

The use of CSLM to analyze membranes after different chemical cleaning cycles has allowed to quantify the amount of protein and dextran remaining on the surface and inside the membranes. The use of microscopic data obtained by CSLM and macroscopic results corresponding to permeate flux has allowed identifying BSA-FITC as the major contributor of membrane fouling during filtration of fluorescent BSA/dextran 70 and 150 kDa solutions on polycarbonate membranes. It has been shown that water or buffer rinsing after filtration does not improve membrane permeability, since water permeate is not recovered and it even decreases throughout rinsing. This reduction has been related to protein driven inside the membrane during rinsing, which was found quantitatively with P_s values and qualitatively by CSLM images. The use of an enzymatic cleaning agent allowed the partial recovery of water permeate flux, and depending on the concentration of the cleaning agent, the cleaning time that resulted in the highest membrane permeability recovery was determined. When this cleaning time was exceeded, water permeate flux recovery was reduced and this is thought to be related to aggregate fragments driven inside the membrane during the cleaning process.

Three-D image reconstruction of CSLM images provided a remarkable tool for visualizing the membrane and the foulants, however, it should be made clear that the 3-D reconstructions are often obtained from a single field of the membrane. It is thought that P_s profiles calculated using data from replicates and different fields of the membrane may provide a more accurate description of the foulants presence on the surface and inside the membrane.

4.5. References

1. A.L. Lim and R. Bai, Membrane fouling and cleaning in microfiltration of activated sludge wastewater, Journal of Membrane Science 216 (2003) 279-290.
2. J.P.Chen, S.L.Kim, Y.P.Ting. Optimization of membrane physical and chemical cleaning by a statistically designed approach, Journal of Membrane Science 219 (2003) 27-45.
3. P. Väisänen, M.R. Bird, M. Nyström, Treatment of UF membranes with simple and formulated cleaning agents, Trans IChemE, 80 (2002) 98-108.
4. K. Kimura, Y. Hane, Y. Watanabe, G. Amy, N. Ohkuma, Irreversible membrane fouling during ultrafiltration of surface water, Water Research, 28 (2004) 3431-3441.
5. Y. Wang, T. Wang, Y. Su, F. Peng, H. Wu, Z. Jiang, Remarkable reduction of irreversible fouling and improvement of the permeation properties of poly(ether sulfone) ultrafiltration membranes by blending with pluronic F127, Langmuir 21 (2005) 11856-11962.
6. T. Mohammadi, S.S. Madaeni, M.K. Moghadam, Investigation of membrane fouling, Desalination 153 (2002) 155-160.
7. M.J. Muñoz-Aguado, D.E. Wiley, A.G. Fane, Enzymatic and detergent cleaning of polysulfone ultrafiltration membrane fouled with BSA and whey.
8. S.J. Choi, H.J. Kim, K.H. Park, T.W. Moon, Molecular characteristic ovalbumin-dextran conjugates formed through the Millard reaction, Food Chemistry 92 (2005) 93-99.
9. D. Kuzmenko, E. Arkhangelsky, S. Belfer, V. Freger, V. Gitis, Chemical Cleaning of UF membranes fouled by BSA, Desalination 179 (2005) 323-333.
10. E. Zondervan, B. Roffel, Dynamic optimization of chemical cleaning in dead-end ultra filtration, Journal of Membrane Science 307 (2008) 309-313.
11. A. Weis, M.R. Bird, M. Nyström, The chemical cleaning of polymeric UF membranes fouled with spent sulphite liquor over multiple operational cycles, Journal of Membrane Science 216 (2003) 67-79.
12. A. Weis, M.R. Bird, M. Nyström, Ch. Wright, The influence of morphology, hydrophobicity and charge upon the long-term performance of ultrafiltration membranes fouled with spent sulphite liquor, Desalination 175 (2005) 73-85.
13. M.R. Bird, M. Bartlett, Measuring and modeling flux recovery during the chemical cleaning of MF membranes for the processing of whey protein concentration, Journal of Food Engineering 53 (2002) 143-152.
14. S. Platt, M. Nyström, Cleaning of membranes fouled by proteins to evaluate the importance of fully developed flow, Desalination 2008 (2007) 19-33.

UNIVERSITAT ROVIRA I VIRGILI
MEMBRANE FOULING CHARACTERIZATION BY CONFOCAL SCANNING LASER MICROSCOPY
Maria Malgorzata Zator
ISBN:978-84-693-0712-0/DL:T-422-2010

15. V. Chen, H. Li, D. Li, S. Tan, H.B. Petrus, Cleaning strategies for membrane fouled with protein mixtures, Desalination 200 (2006) 198-200.
16. M. Rabiller-Baudry, L. Begoin, D. Delaunay, L. Paugam, B. Chaufer, A dual approach of membrane cleaning based on physico-chemistry and hydrodynamics. Application to PES membrane of dairy industry, Chemical Engineering and Processing 47 (2008) 267-275.
17. M. Ferrando. A. Rŏzek, M. Zator, F. López, C. Güell, An approach to membrane fouling characterization by confocal microscopy, Journal of Membrane Science 250 (2005) 283-293.
18. M. Zator, M. Ferrando, F. López, C. Güell, Membrane fouling characterization by confocal scanning microscopy during filtration of BSA/dextran mixtures, Journal of Membrane Science 301 (2007) 57-66.
19. D. Spettmann, S. Eppmann, H.C. Flemming, J. Wingender, Visualization of membrane cleaning using confocal laser scanning microscopy, Desalination 224 (2008) 195-200.
20. M. Nyström, H. Zhu, Characterization of cleaning results using combined flux and streaming potential and flux recovery, Journal of Membrane Science 131 (1997) 195-205.
21. H. Zhu, M. Nyström, Cleaning results characterized by flux, streaming potential and FTIR measurements, Colloids and Surfaces, A: Physicochemical and Engineering aspects 138 (1998)309 -321.
22. Ch. Zhang, Y. Ding, L. Yuan, Y. Zhang, D. Xi, , Characteristics of Membrane Fouling in an Anaerobic-(Anoxic/Oxic)^{n}-MBR Process, Journal of China University of Mining & Technology 2007, 17(3):0387-0392.
23. J. Zhang, S.I. Padmasiri, M.Fitch, B. Norddahl, L. Raskin, E. Morgenroth, Influence of cleaning frequency and membrane history on fouling in an anaerobic membrane bioreactor, Desalination 207 (2007) 153-166.
24. R.W. Field, D. Wu, J.A. Howell, B.B. Gupta, Critical flux concept for microfiltration fouling, Journal of Membrane Science 100 (1995) 259-272.
25. M. Manttari, M. Nyström; Critical flux in NF of high molar mass polysaccharides and effluents from the paper industry,Jurnal of Membrane Science, 170 (2000) pp.257-273
26. D. Hughes, R.W. Field, Crossflow filtration of washed and unwashed yeast suspensions at constant shear under nominally sub-critical conditions, Journal of Membrane Science 280 (2006) 89-98.

UNIVERSITAT ROVIRA I VIRGILI
MEMBRANE FOULING CHARACTERIZATION BY CONFOCAL SCANNING LASER MICROSCOPY
Maria Malgorzata Zator
ISBN:978-84-693-0712-0/DL:T-422-2010

UNIVERSITAT ROVIRA I VIRGILI
MEMBRANE FOULING CHARACTERIZATION BY CONFOCAL SCANNING LASER MICROSCOPY
Maria Malgorzata Zator
ISBN:978-84-693-0712-0/DL:T-422-2010

5

MICROFILTRATION OF PROTEIN/DEXTRAN/POLYPHENOL SOLUTIONS: CHARACTERIZATION OF FOULING AND CHEMICAL CLEANING EFFICIENCY USING CONFOCAL MICROSCOPY

UNIVERSITAT ROVIRA I VIRGILI
MEMBRANE FOULING CHARACTERIZATION BY CONFOCAL SCANNING LASER MICROSCOPY
Maria Malgorzata Zator
ISBN:978-84-693-0712-0/DL:T-422-2010

UNIVERSITAT ROVIRA I VIRGILI
MEMBRANE FOULING CHARACTERIZATION BY CONFOCAL SCANNING LASER MICROSCOPY
Maria Malgorzata Zator
ISBN:978-84-693-0712-0/DL:T-422-2010

5.1. Introduction

One of the most important processes used in beverage clarification is cross-flow microfiltration. This promising alternative to traditional dead-end filtration can combine clarification, stabilization and sterile filtration in a single continuous operation. However, the process is limited by permeate flux decline due to severe membrane fouling. To avoid membrane fouling it is extremely important to identify the foulants and mechanisms that govern the process. Wine, beer and juice are complex media that include both organic and inorganic materials, so the fouling of the constituents of these beverages is largely irreversible. Analytical studies reveal the presence of irreversibly deposited polysaccharides, polyphenols and proteins on membranes and show that these molecules are likely to be involved in deposit formation. Experimental data from microfiltration experiments with model solutions confirm the fouling nature of beverage compounds, while washing procedures highlight the role of polyphenols in the build up and cohesion of irreversible fouling [1-6].

One group of polyphenols easily found in wine, beer and juice are tannins. These polyphenols are known to be very reactive towards proteins and interact with them to form insoluble associations. Tannins are thought to be involved in the cross-linking of separate protein molecules, acting as polydentate ligands on the protein surface and involving a hydrophobic effect and hydrogen bonding. However, several factors, including the type of protein and the structure of the polyphenol influence these interactions. Amino-acid residues of linear proteins and aromatic groups of polyphenols probably interact in face-to-face stacking. Globular proteins, on the other hand, involve just surface-exposed residues [7-9].

The interactions between tannins and proteins may be specific for different tannins and different proteins but they are also influenced by the presence of carbohydrates in the solution. Mateus et *al*. [7] and Carvalho et *al*. [8] recently found that some neutral and anionic polysaccharides can disturb the binding of polyphenols to proteins. This effect of carbohydrates on protein aggregation probably results from the ability of polysaccharides to form a ternary protein/polyphenol/carbohydrate complexes, thereby enhancing its solubility in aqueous medium, or from the molecular association in solution between carbohydrates and polyphenols competing with protein aggregation. Freitas et *al*. [10] reported that some polysaccharides have the ability to develop a secondary structure in solution that is able to encapsulate and complex polyphenols in hydrophobic pockets. In general, adding polysaccharides restricts the formation of protein/polyphenol insoluble aggregates. However, the carbohydrate must have a suitable structure and ionic character, as well as a sufficient size and flexibility to be able to complex polyphenols [7-10].

UNIVERSITAT ROVIRA I VIRGILI
MEMBRANE FOULING CHARACTERIZATION BY CONFOCAL SCANNING LASER MICROSCOPY
Maria Malgorzata Zator
ISBN:978-84-693-0712-0/DL:T-422-2010

To prevent membrane fouling and design washing procedures for membrane modules, it is important to know which mechanisms are involved in pore blocking/constriction and cake formation. The most common parameters influencing the interaction between protein and polyphenol are the concentration ratio of tannin to protein, the solvent composition, the ionic strength, the pH and the presence of other molecules such as polysaccharides. Carvalho et *al*. [9] and Freitas et *al*. [10] used a nephelometric method to study how the concentration of bovine serum albumin (BSA) affected the reaction with different tannin solutions. They found that with a high concentration of BSA the number of aggregates increased until a maximum was reached and that a further addition of protein reduced the formation of the insoluble aggregates. They assumed that when the protein concentration is high, polyphenols can bind to the surface of proteins, acting like polydentate ligands to form a network of protein-tannin complexes and resulting in a higher number of aggregates. They believe that when proteins exceed a maximum concentration in solution, they surround polyphenol molecules and reduce the probability of aggregate formation. They also believe that the colloidal state of tannins in wines, involving other compounds such as polysaccharides, could determine their ability to bind proteins. Vernhet et *al*. [2] observed the irreversible nature of fouling caused by model solutions containing polyphenols and polysaccharides. Using SEM imaging they observed that aggregates formed which, though much smaller than the average pore size of the membrane, were deposited within the most external pores close to the surface, partially blocking them and leading to more or less regular surface deposits. They suggested that, during microfiltration, irreversibly adsorbed polyphenols and polysaccharides are preferentially accumulated at the pore entrance to finally bridge some of the pores and form thin organic deposits on the membrane feed side. This irreversible nature of fouling is related to membrane/foulant and foulant/foulant physicochemical interactions promoted by local hydrodynamic conditions. They also concluded that membrane surface properties such as polarity and pore size distribution strongly affect polyphenol deposition. As well as the relative concentration of tannins and proteins, other parameters that influence the level of precipitates, such as pH, ionic strength and solvent composition, have also been evaluated [7-8,10].

As a preventive measure against severe and irreversible membrane fouling, periodic membrane cleaning is required. In the microfiltration of biological streams and other fields of membrane technology, feasible and cost-effective cleaning and restoration procedures are needed. Efficient membrane cleaning is a function of many parameters including hydrodynamic conditions, the concentration of the cleaning solution, and the sequence of the cleaning [11]. Membrane cleaning is usually understood as a physical, chemical or biological method but, as reported by Mohammadi et *al*. [12], chemical methods are the most popular.

Also important is a suitable technique for evaluating membrane cleaning. In the last few years, CSLM has been found to be a suitable technique for characterising membrane and membrane processes. Among other applications, CSLM has been used to study the fouling of binary mixtures of proteins [13] or binary mixtures of protein and polysaccharide [14]. The information

UNIVERSITAT ROVIRA I VIRGILI
MEMBRANE FOULING CHARACTERIZATION BY CONFOCAL SCANNING LASER MICROSCOPY
Maria Malgorzata Zator
ISBN:978-84-693-0712-0/DL:T-422-2010

obtained by using CSLM in the membrane process enables us, for example, to locate and identify the various foulants. Suitable image analysis enables us to also obtain quantitative information on the presence of the foulants on the membrane surface and inside the pores. Ferrando et *al*. [20] and Zator at *al*. [16] recently presented extensive state-of-the-art information on the use of CSLM in the characterisation of membrane and membrane processes.

In Chapter 4 has been presented the use of CSLM and macroscopic results to evaluate the effectiveness of water rinsing and chemical cleaning protocols on membranes fouled with model solutions of BSA and a polysaccharide (dextran). CSLM provides information in 3D on foulant location and quantification on the membrane and inside the pores. In accordance with the fact that most biological streams contain complex mixtures of proteins, polysaccharides and polyphenols, the main aims of this chapter are to characterize the membrane fouling of ternary mixtures comprising a protein (BSA), a polysaccharide (dextran) and a polyphenol (tannic acid) and to determine the cleaning efficiency of a commercial cleaning agent using CSLM analysis and macroscopic data.

5.2. Materials and methods

5.2.1. Membrane and fouling solutions

Polycarbonate 0.47 mm membrane discs with a nominal pore size of 0.80 μm with a clean water flux of 20565 L/(h m^2) at 51 kPa, provided by Sterlitech (PCTB0847100), were applied for each experiment. BSA-fluorescein conjugate (BSA-FITC) (A-9771), Dextran 70 kDa – rhodamine B conjugate (dextran-RITC) (R9379) and tannic acid (TA) (T-0125) were purchased from Sigma. Black membranes were selected in order to avoid disturbances in the detection of fluorescein and rhodamine signals under conditions of CSLM analysis. P3 Ultrasil 53 (US53), a neutral enzymatic detergent used for membrane cleaning (described in detailed in section 4.2 of Chapter 4) was provided by ECOLAB -Henkel.

5.2.2. Filtration plant and operation conditions

All membrane fouling experiments were carried out using a laboratory size microfiltration plant (described in detail in Chapter 3 (Figure 3.1)) consisting of a cross-flow filtration module for flat membranes with an effective filtration area of 0.0016 m2. System pressure was kept constant at 51kPa during all the experiments and the temperature was kept at 23±2°C. At the beginning of each experiment, a new polycarbonate membrane was placed in the filtration module and fresh protein/dextran/polyphenol solution was loaded and filtered until the flux reached a constant value (3 to 5 hours). Permeate and retentate were returned to the feed vessel in order to maintain a constant feed concentration. In situ chemical cleaning in the forward direction with US53 was then applied. Before each experiment, the whole filtration setup was thoroughly cleaned with 20% sodium hydroxide solution and rinsed with prefiltered deionized water until neutral pH was reached. To minimize photo-bleaching of the fluorescent reagents during the filtration runs, the set up was completely covered with aluminium foil.

From samples of permeate collected over 10 seconds at 0, 10, and 30 minutes and then every 30 minutes until the end of the filtration run, we determined permeate fluxes. Phosphate buffer (PBS) was used to adjust the pH of all the protein/dextran/polyphenol solutions to 7.4. As shown in table 5.1, the initial concentrations of BSA-FITC and dextran-RITC were always the same, while for tannic acid three concentrations were tested (0.25 g/L, 0.5 g/L and 1g/L). Two concentrations of the chemical cleaning agent (US53) were used (0.1 and 0.5%) and the cleaning cycles lasted for 5 or 15 minutes. Water flux permeate was determined at the end of the cleaning cycles in order to study the extent of water flux recovery, which indicates the efficiency of the membrane cleaning.

UNIVERSITAT ROVIRA I VIRGILI
MEMBRANE FOULING CHARACTERIZATION BY CONFOCAL SCANNING LASER MICROSCOPY
Maria Malgorzata Zator
ISBN:978-84-693-0712-0/DL:T-422-2010

Table 5.1. Initial concentrations of protein, dextran and tannic acid for all solutions tested.

Solution	BSA-FITC (g/L)	Dextran-RITC 70 kDa (g/L)	Tannic acid (g/L)
BSA	0.25	0	0
BSA/dex	0.25	0.25	0
BSA/dex/TA025	0.25	0.25	0.25
BSA/dex/TA05	0.25	0.25	0.5
BSA/dex/TA1	0.25	0.25	1

5.2.3. CSLM and image analysis

A detailed description of the protocols used to conduct CSLM analysis can be found in section 3.2 of Chapter 3. A Nikon D-Eclipse C1 confocal microscope was used to analyse the samples. The working conditions were the same for all cases: specimen magnification was 100 × objective (numerical aperture 1.3) and zoom magnification was 2.8. The detection conditions were kept constant for samples obtained under the same filtration conditions. Images were taken from the surface of the membrane to the inside and to the outside each 0.15µm, producing a series of 40 to 100 images depending on the presence or absence and thickness of a cake layer. This optical sectioning provided data on foulant penetration inside the membrane down to 3.5 µm and through the cake layer up to around 20 µm.

The software used for image analysis was ImageJ 1.30v (National Institutes of Health, USA) and Imaris (Bitplane). ImageJ 1.30v measured the surface occupied by pores (Ap) and the fraction of the pore surface in which protein/polysaccharide was detected (P_s) [13-14,16]. The size of the digital images obtained during CSLM analysis was 512 × 512 pixels, with an integral value ranging from 0 to 255. Processing of the images included identifying the features to be analyzed and segmenting and extracting the measurements of interest (see section 2.2 of Chapter 2.

To extract more quantitative information from CSLM imagining data, image structure analyzer (ISA3D) was used [21-24]. Using ISA3D is possible to calculate two kinds of parameters: textural, which show the microscale heterogeneity of analyzed structures, and volumetric which describe morphology of the cake. Detailed description of this software developed to analyze biofilms can be found elsewhere [23].

5.2.4. Protein and polyphenol analysis

The concentrations of protein and polyphenol in the permeate and retentate decreased slightly over the filtration experiment. The concentration of polyphenol was determined using Folin-Ciocalteu's method described in detail by Singleton et *al*. [17]. The total concentration of protein was measured by Bradford´s method using Coomassie Brilliant Blue reagent [18]. Absorbance was measured on the spectrophotometer (Cecil CE 2021, England) at 750 nm after 30 minutes of incubation for tannic acid and at 595 nm after 5 minutes of incubation for BSA. The amount of protein or polyphenol in the sample was calculated with BSA and tannic acid standardization curves as referenced. Protein/polyphenol rejection is defined by:

$$R = \left(1 - \frac{C_p}{C_b}\right) 100\% \tag{5.1}$$

where C_p and C_b are the protein or polyphenol concentration in the permeate and bulk, respectively.

UNIVERSITAT ROVIRA I VIRGILI
MEMBRANE FOULING CHARACTERIZATION BY CONFOCAL SCANNING LASER MICROSCOPY
Maria Malgorzata Zator
ISBN:978-84-693-0712-0/DL:T-422-2010

5.3. Results and discussions

5.3.1. Fouling of ternary mixtures: effect of increasing polyphenol concentration

Applying the experimental conditions outlined in Section 5.2.2., we carried out microfiltration experiments with ternary protein/dextran/polyphenol solutions with an increasing amount of tannic acid (Table 5.1). The permeate fluxes obtained are plotted in Figure 5.1 and contrasted with the permeate flux obtained during microfiltration of BSA and BSA/dextran solutions (Table 5.1). The results clearly show that adding a polyphenol to the protein/dextran solution considerably reduces permeate flux, regardless of the polyphenol concentration added. As reported in a previous study [4], the fouling caused by a separate protein solution or a polyphenol solution was considerably lower than the fouling caused by a combined solution of both these substances at the same degree of concentration. In the present case, this is probably due to the formation of insoluble protein/polyphenol and/or protein/dextran/polyphenol aggregates. Even though polysaccharides are considered to be effective inhibitors of protein precipitation by polyphenols, dextran is known to have the weakest ability both to inhibit BSA-tannin interactions and to increase aggregation [8, 10]. As reported by Freitas et *al*. [10], the observed increase in the percentage of aggregates could be explained by an increase in the tannin/BSA aggregate size, which would result from the adsorption of some dextran molecules. This would not, however, be to a sufficient extent to dissolve the complex.

Table 5.2 gives permeate flux values throughout the filtration of the solutions listed in Table 5.1. It shows that the value of the steady state permeate flux attained for all five solutions studied is approximately the same. However, very different permeate flux plots were obtained depending on whether tannic acid was or not present in the solution (Figure 5.1). It is clear that with tannic acid in the solution, regardless of its concentration, fouling was very severe, since after half an hour of filtration the permeate flux was between one and two orders of magnitude lower than the ones for the protein or the protein/dextran solutions (Table 5.2). The permeate flux decline for BSA-FITC took around two hours to reach the steady-state value and for BSA-FITC/dextran-RITC solution almost four hours, while the flux decline for solutions containing tannic acid decreased dramatically from the start of the filtration.

Table 5.2. Permeate flux values during microfiltration of five solutions composed of BSA-FITC, dextran RITC and different concentrations of tannic acid on 0.8 µm polycarbonate membranes.

t [h]	Flux [L/h m^2]				
	BSA	**BSA/dex**	**BSA/dex/TA025**	**BSA/dex/TA05**	**BSA/dex/TA1**
0.0	-----	21181	3034	2474	411
0.2	18474	20850	459	393	190
0.5	10312	20231	215	162	138
1.0	3474	15812	152	126	110
1.5	405	10190	116	113	97
2.0	150	6277	102	101	88
2.5	106	3129	97	89	81
2.8	98	1230	93	89	75
3.0	89	503	91	88	77
3.5	-----	222	-----	-----	-----
4.0	-----	98	-----	-----	-----
4.5	-----	114	-----	-----	-----
5.0	-----	111	-----	-----	-----

UNIVERSITAT ROVIRA I VIRGILI
MEMBRANE FOULING CHARACTERIZATION BY CONFOCAL SCANNING LASER MICROSCOPY
Maria Malgorzata Zator
ISBN:978-84-693-0712-0/DL:T-422-2010

Figure 5.1. Permeate flux evolution during microfiltration of solutions listed in Table 5.1 on 0.8 µm polycarbonate membranes.

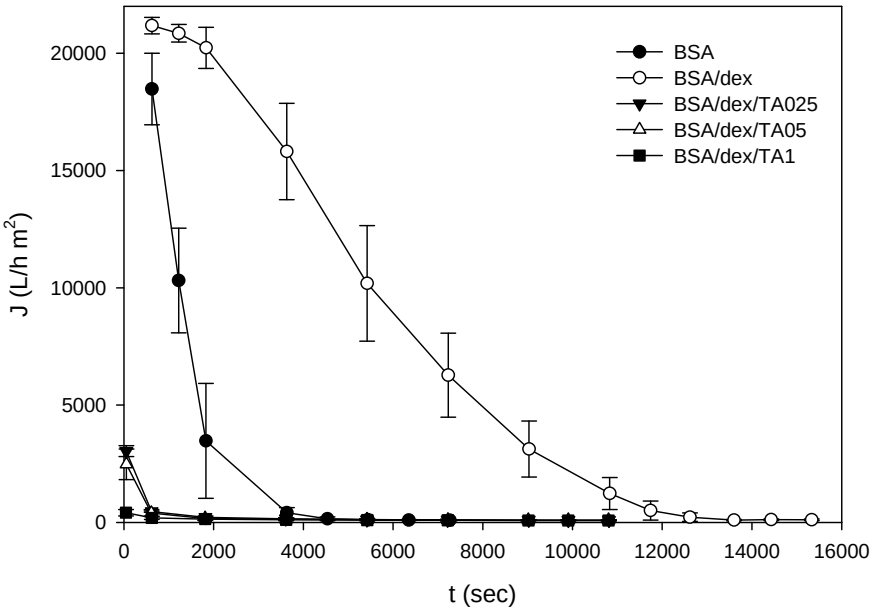

Table 5.3 shows the evolution of protein and polyphenol content in the permeate and in the retentate during microfiltration of BSA-FITC/dextran-RITC/tannic acid solutions on PC membranes. For all the solutions studied, regardless of the initial concentration of tannic acid, we observed a reduction in the content of protein and polyphenol which we attributed to internal and external fouling. We hypothesized that this reduction occurs during the early stages of the filtration process; some protein, dextran or polyphenol molecules as well as aggregates combining two or three of these may be adsorbed into and/or deposited within the membrane pores, resulting in pore constriction. Further decrease in BSA-FITC and tannic acid concentration is thought to be due to the deposition of particles and aggregates on the membrane surface, which results in formation of a cake layer. These results will be discussed further in the sections on the confocal analysis of the fouled membranes and cake layer.

Figure 5.2 shows BSA and tannic acid rejection profiles versus time, calculated using equation 5.1, for the model solutions containing protein/polysaccharide and three different concentrations of tannic acid filtered with polycarbonate membranes. We observed that during the first half hour of the filtration, rejection of tannic acid increases significantly compared with rejection values obtained for BSA. Maximum rejection values for tannic acid were obtained after two hours of filtration, regardless of the concentration of TA present in the solution. The rejection profile obtained for BSA differs from the one obtained for TA. During the first half hour of filtration there is a slight increase in the observed rejection. After this point, the observed rejection for BSA in solutions containing 0.25 g/L of tannic shows a rapid increase, reaching its maximum after 2 hours of filtration. In solutions with higher TA concentration (0.5 and 1 g/L) the

increase in the observed rejection is lower, reaching its maximum value by the end of the filtration time. It is clear from Figure 5.2 that the highest rejections for both tannic acid and for BSA are obtained for those solutions with the lowest content. These results are also confirmed by the CSLM observation of fouled membranes at the end of filtration runs, and will be further discussed in section 5.2.

Table 5.3. Reduction in protein and polyphenol content during microfiltration of three solutions composed of BSA-FITC/dextran RITC and different concentrations of tannic acid on 0.8 µm polycarbonate membranes.

Permeate						
Time [h]	Protein [g/L]			Polyphenol [g/L]		
	BSA/dex/TA025	BSA/dex/TA05	BSA/dex/TA1	BSA/dex/TA025	BSA/dex/TA05	BSA/dex/TA1
0	0,250±0,005	0,250±0.008	0,250±0,006	0,250±0,003	0,500±0,001	1,000±0,007
0.5	0,243±0,004	0,236±0,004	0,248±0,004	0,222±0,004	0,420±0,031	0,954±0,005
1	0,220±0,010	0,243±0,013	0,244±0,007	0,221±0,004	0,470±0,005	0,943±0,006
2	0,201±0,006	0,228±0,004	0,245±0,007	0,210±0,005	0,461±0,004	0,911±0,003
3	0,219±0,008	0,209±0,011	0,227±0,016	0,212±0,004	0,412±0,002	0,982±0,050
Retentate						
Time [h]	Protein [g/L]			Polyphenol [g/L]		
	BSA/dex/TA025	BSA/dex/TA05	BSA/dex/TA1	BSA/dex/TA025	BSA/dex/TA05	BSA/dex/TA1
0	0,250±0,005	0,250±0.008	0,250±0,006	0,250±0,003	0,500±0,001	1,000±0,007
0.5	0,223±0,004	0,239±0,004	0,244±0,006	0,225±0,004	0,458±0,031	0,912±0,006
1	0,236±0,003	0,234±0,013	0,244±0,004	0,212±0,005	0,472±0,005	0,976±0,006
2	0,231±0,007	0,241±0,004	0,243±0,007	0,214±0,005	0,451±0,014	0,894±0,003
3	0,225±0,008	0,230±0,011	0,237±0,016	0,201±0,004	0,470±0,006	0,957±0,050

Figure 5.2. Observed rejection for BSA (a) and tannic acid (b) during microfiltration of ternary solutions with 0.8 μm polycarbonate membrane.

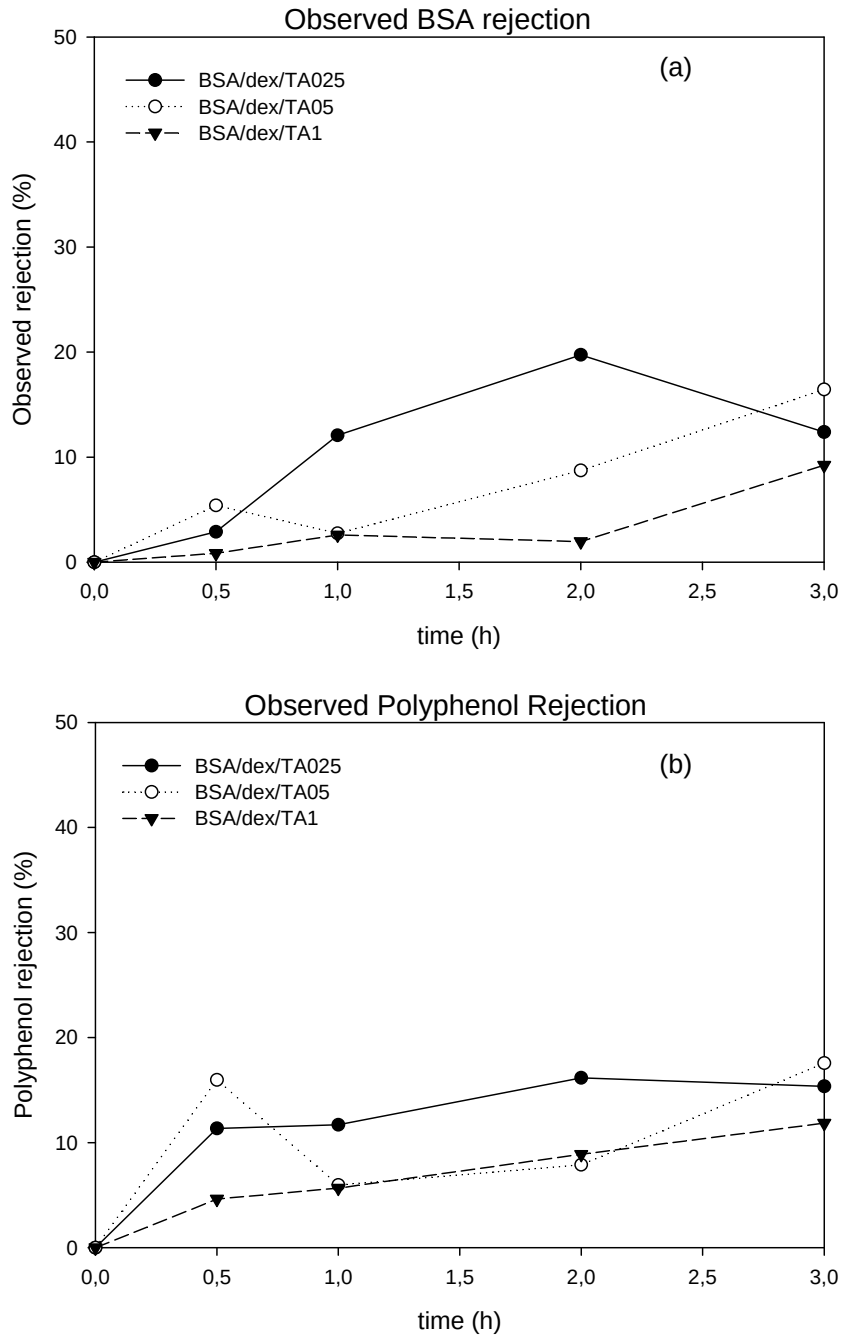

Nephelometry is a simple, sensitive and reliable technique for monitoring the gradual formation of insoluble protein-tannin aggregates. Table 5.4 shows initial and final turbidity values for solutions with different tannic acid concentrations. The increase in turbidity is directly related to a higher content of insoluble aggregates. Tannins that bind onto the protein surface can act as polydenate ligands forming large networks of protein-tannin complexes, resulting in large aggregates and more scattered light. When the polyphenol-protein molar ratio is high, only few polyphenol molecules can bind to the small number of protein molecules present in the solution.

UNIVERSITAT ROVIRA I VIRGILI
MEMBRANE FOULING CHARACTERIZATION BY CONFOCAL SCANNING LASER MICROSCOPY
Maria Malgorzata Zator
ISBN:978-84-693-0712-0/DL:T-422-2010

This results in small aggregates and less light scattered [9]. As can be seen, most of these aggregates are formed during the first few minutes after preparing the filtration solution, and the number of aggregates formed during the filtration process is not significant. The results in Table 5.4 show that the initial turbidity values increase proportionally to the increase in tannic acid concentration in the solution. As reported by [4], membrane fouling is mainly caused by the light-scattering polyphenol/protein complexes formed, and is highly dependent on the initial turbidity of the solution. Lower initial turbidity results in lower final resistance (Figure 5.3). These authors also reported that filtration of model solutions containing tannic acid is initially dominated by internal fouling followed by a period during which external fouling dominates. The increase in the initial turbidity of the model solution led to an increase in final resistance and reduce the initial period in which internal fouling dominated.

Table 5.4. Turbidity of BSA-FITC/dextran-RITC 70 kDa/tannic acid solutions before and after microfiltration on 0.8 μm polycarbonate membrane.

	Turbidity [NTU]	
	Initial	**Final**
BSA/dex/TA025	6,08 ± 1,08	8,47 ± 1,64
BSA/dex/TA05	15,60 ± 0,82	17,58 ± 0,93
BSA/dex/TA1	56,83 ± 6,68	67,35 ±6,06

Figure 5.3. Resistance comparison for ternary solutions containing BSA-FITC/dextran RITC 70 kDa/ and three concentrations of tannic acid (0.25 g/L; 0.5 g/L; 1 g/L).

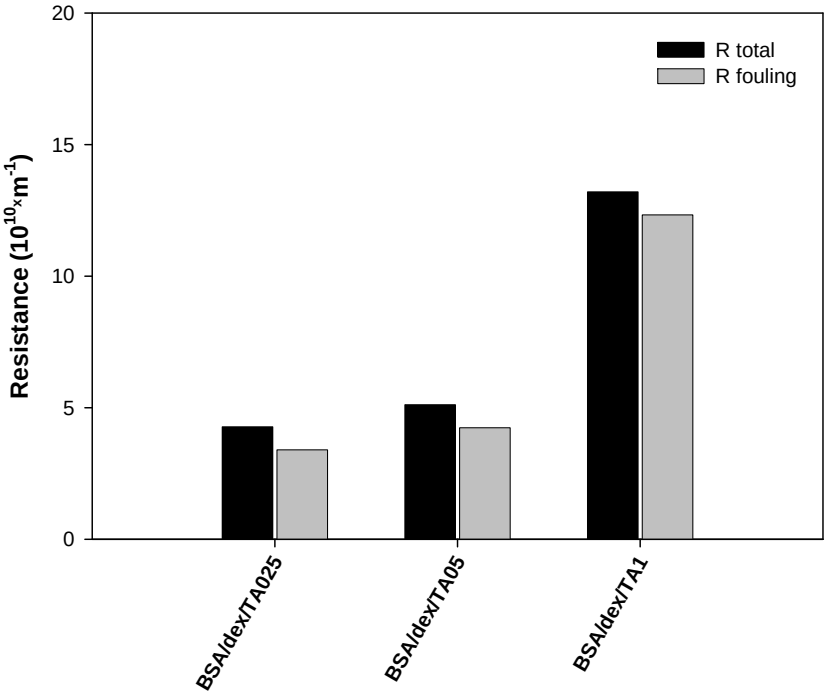

5.3.2. CSLM analysis of fouled membranes

Extensive internal and external membrane fouling resulted from the addition of tannic acid, regardless of its concentration, to the solution containing protein (BSA) and polyphenol (dextran 70 kDa). CSLM was applied to characterize the extent of pore blockage, cake layer thickness and composition. In accordance with the protocols described in Chapter 2, we obtained quantitative information about internal fouling inside the membrane pores using P_s profiles. Moreover, through an analysis of image stacks obtained by CSLM, we obtained qualitative information about cake layer structural morphology and quantitative information about deposit thickness

5.3.2.1. CSLM analysis of internal fouling

As both the protein and the polysaccharide used for the model solutions were fluorescently labeled, we were able to use CSLM to obtain three-dimensional views of the fouled membranes. The use of fluorescently stained species made it possible to locate and visualize BSA and dextran separately. The resulting information can be used to understand how each component of the solution contributes to the membrane fouling. Although tannic acid could not be visualized under the imaging conditions used in CSLM analysis, it obviously contributes greatly to the membrane fouling, since it was possible to compare images of fouled PC membranes after filtration of solutions with and without tannic acid (see results on Chapters 3 and 4).

At the end of each filtration run, we analyzed membrane samples using CSLM, In accordance with the protocols described in previous chapters, and calculated the P_s profiles (see Chapter 2). Figure 5.4a shows the P_s profiles for BSA-FITC inside the membrane obtained for the five solutions studied. As Figure 5.4a shows, the P_s profile for BSA is very similar whether filtered alone or with the 70 kDa dextran. The presence of a polyphenol in the solution clearly only increases the presence of the protein inside the pores when the solution contains the highest amount of tannic acid, reaching a P_s value of 100%, which is maintained from the membrane surface up to 1 μm inside the membrane. For the other two tannic acid concentrations, the P_s values obtained are not significantly different from the ones corresponding to BSA-FITC, either alone or with dextran-RITC. The P_s profiles obtained for the dextran are shown in Figure 5.4b, which reveals that the presence of the polyphenol does not affect dextran deposition/adsorption in the pores, regardless of the tannic acid concentration. The higher content (1g/L) of tannic acid in the solution seems to lead to the formation of aggregates of a size sufficient to enter the pores and block them completely, to a depth of 1μm depth.

Figure 5.5 shows the results obtained from 3D reconstruction of the stacks obtained by CSLM and using Imaris software. These results reveal the extent of membrane fouling caused by the deposition/adsorption of BSA-FITC on the membrane surface and at various membrane depths after microfiltration of single, binary and ternary solutions containing BSA, dextran and different

UNIVERSITAT ROVIRA I VIRGILI
MEMBRANE FOULING CHARACTERIZATION BY CONFOCAL SCANNING LASER MICROSCOPY
Maria Malgorzata Zator
ISBN:978-84-693-0712-0/DL:T-422-2010

concentrations of tannic acid. The images illustrate well the information found by plotting P_s profiles versus membrane depth. As can be clearly seen, blockage of pores by BSA is very similar in the cases of BSA, BSA/dex, BSA/dex/TA025 and BSA/dex/TA05 solutions, while in the case of the solution with the highest concentration of tannic acid (BSA/dex/TA1), the green signal indicating protein presence is much stronger, and practically all pores can be considered blocked. Figure 5.6 shows the same kind of information about the presence of dextran-RITC on the membrane surface and within the pores. In all the cases studied, many pores are found to be completely blocked while others are only partially blocked or free of dextran. In the case of dextrans, the addition of polyphenol, regardless of concentration, has not such a visible effect as in the case of proteins.

Figure 5.4. Fraction of pore surface on which (a) BSA-FITC and (b) dextran-RITC are detected (P_s) at the end of the microfiltration process for five solutions composed of BSA-FITC, dextran RITC and different concentrations of tannic acid on 0.8 μm polycarbonate membranes.

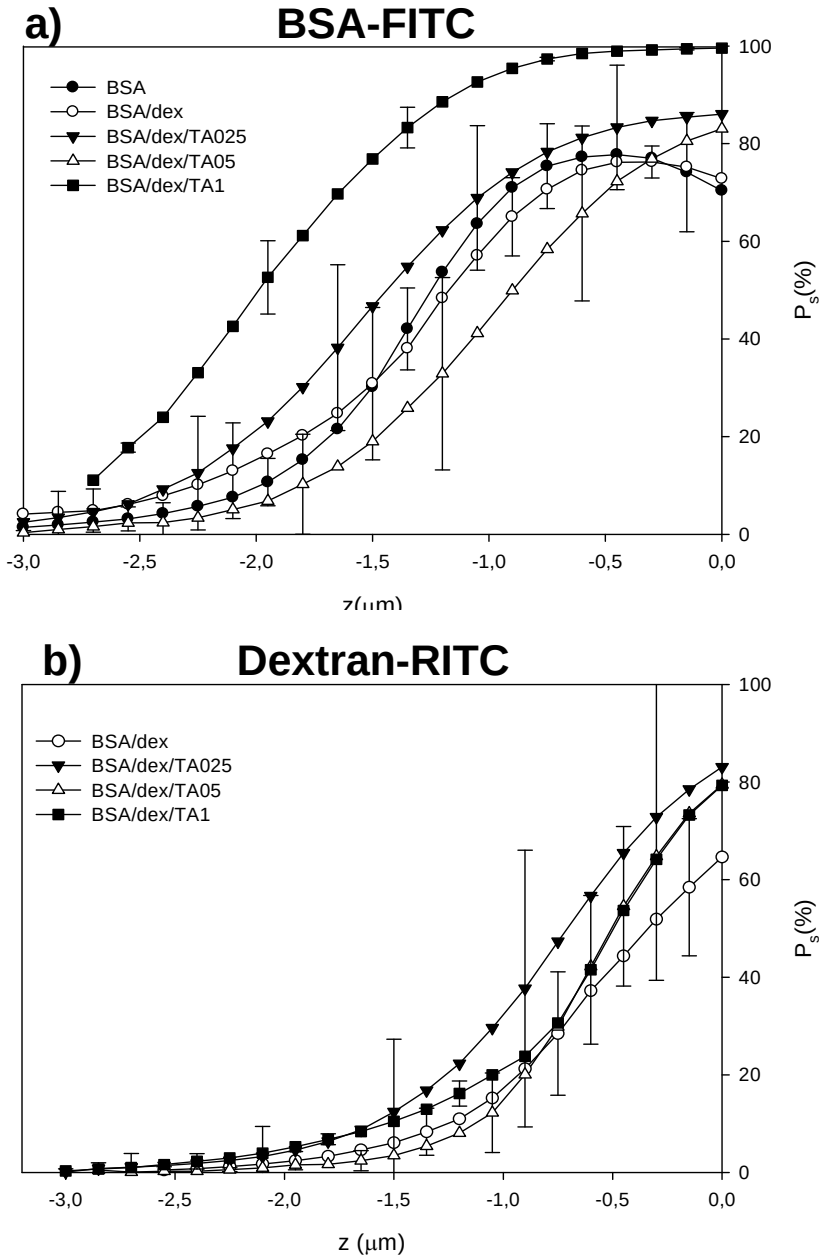

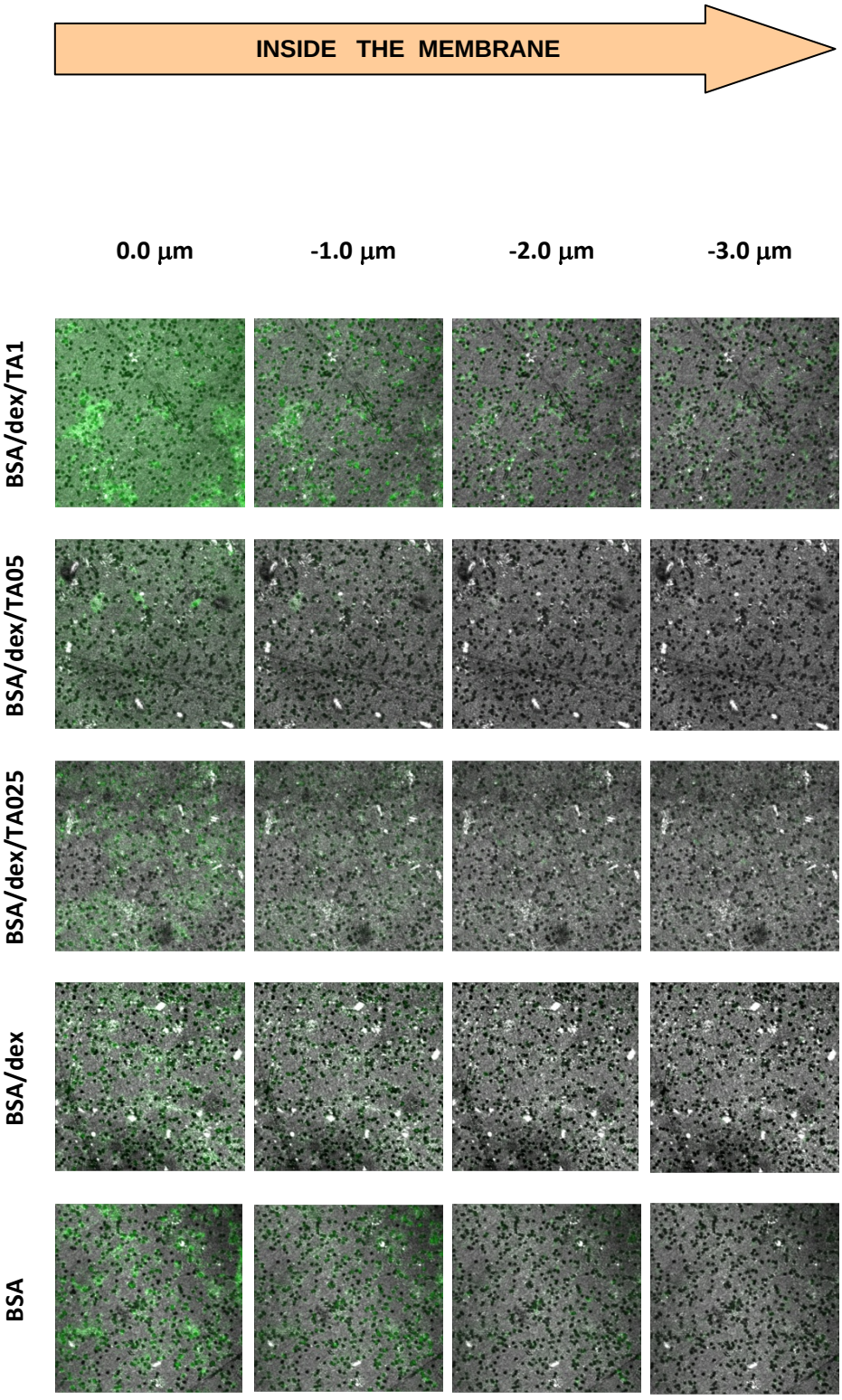

Figure 5.5. 3D orthogonal reconstruction of CSLM images: membranes after filtration of single BSA solution, binary BSA/dex solution and ternary solutions of BSA/dex/TA with three different concentrations of tannic acid (TA). Images show the membrane (grey signal) and the protein (green signal) at different depths. Scale bar 10μm.

UNIVERSITAT ROVIRA I VIRGILI
MEMBRANE FOULING CHARACTERIZATION BY CONFOCAL SCANNING LASER MICROSCOPY
Maria Malgorzata Zator
ISBN:978-84-693-0712-0/DL:T-422-2010

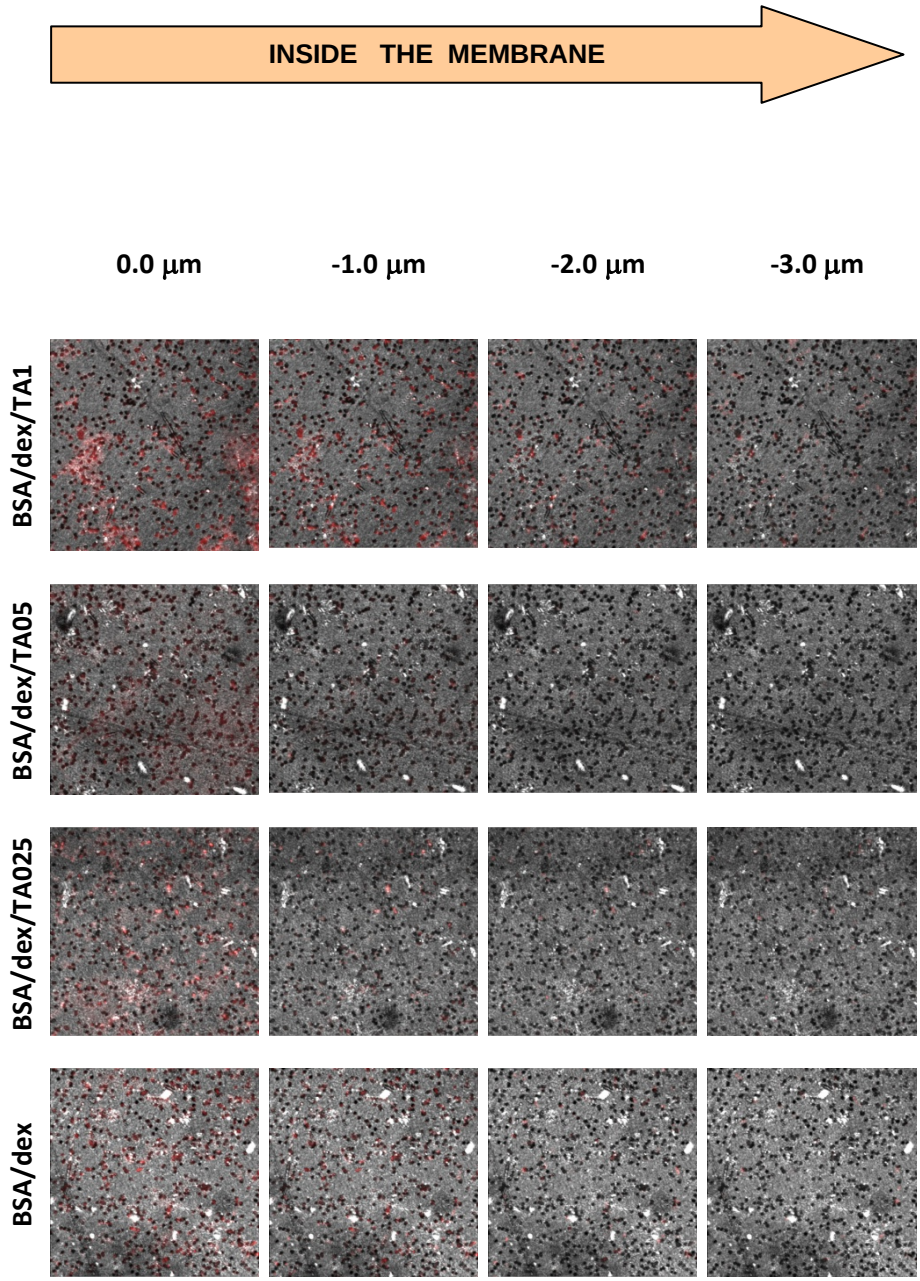

Figure 5.6. 3D orthogonal reconstruction of CSLM images: membranes after filtration of single BSA solution, binary BSA/dex solution and ternary solutions of BSA/dex/TA with three different concentrations of tannic acid (TA) Images show the membrane (grey signal) and the dextran (red signal) at different depths. Scale bar 10 µm.

5.3.2.2. CSLM analysis of cake layer

When the solutions with BSA/dextran/tannic acid were filtered, we always observed the formation of a cake layer on the surface of the membrane, regardless of the concentration of tannic acid in the solution. CSLM helped us to study this cake to gain qualitative information regarding its composition and quantitative information regarding its thickness.

The use of CSLM protocols enabled us to visualize the three-dimensional structure of the fouling layer composed of BSA-FITC, dextran-RITC and tannic acid. Application of image analysis software made it possible to determine cake layer thickness of approximately 8.50 µm for the higher concentrations of tannic acid (0.5 g/L and 1 g/L) and up to 17.17 µm for the lowest concentration (0.25 g/L) (Table 5.5). Thicknesses of the cake layer were calculated from the images obtained at two different wavelengths of microscope laser: 488 nm specific for BSA-FITC, and 520 nm specific for dextran-RITC. The thickness values in Table 5.5 are presented as average values obtained from three images and six different regions for each image (18 values). The information gathered by CSLM showed that both protein and polysaccharide aggregates were present in the cake layer and determined their distribution profiles within the cake structure.

Table 5.5. Cake layer thickness after microfiltration of five solutions composed of BSA-FITC, dextran-RITC and different concentrations of tannic acid on 0.8 µm polycarbonate membrane.

Filtration solution	Cake layer thickness [µm]	
	FITC	RITC
BSA	0	0
BSA/dex	0	0
BSA/dex/TA025	16.33 ± 4.86	17.17 ± 4.84
BSA/dex/TA05	8.84 ± 0.98	9.88 ± 0.59
BSA/dex/TA1	8.82 ± 1.89	8.44 ± 1.47

UNIVERSITAT ROVIRA I VIRGILI
MEMBRANE FOULING CHARACTERIZATION BY CONFOCAL SCANNING LASER MICROSCOPY
Maria Malgorzata Zator
ISBN:978-84-693-0712-0/DL:T-422-2010

Image analysis employing ISA3D software was used to gain more information about the structural features of the cake layer thicknesses obtained after microfiltration of BSA-FITC, dextran-RITC and using different concentrations of tannic acid solutions on 0.8 µm polycarbonate membranes (Table 5.5), it was thought that image analysis of the cake using ISA3D software would give more information about structural features of these deposits. Initially, ISA3D was developed for image structure analysis of biofilms and used to extract information from three dimensional image sets, calculating textural and volumetric parameters of the biofilm deposit. Textural parameters quantify the gray scale intensity position, and/or pixel orientation. For the purpose of our study, the following parameters were selected and calculated using ISA3D software: (1) *Textural entropy,* which is a measure of randomness in the gray scale of the image. The higher the textural entropy, the more heterogeneous is the image due to increased gray level variability; (2) *Energy,* which is a measure of regularity in patterns of pixels and is sensitive to the orientation of the pixel cluster and similarity of the their shapes. Low values of energy mean frequent and repeated patterns of pixel clusters, while high energy values indicate a more homogenous character of the structure; (3) *Homogeneity,* which measures the similarity of the spatially close image structures: a more homogenous image structure gives higher values of homogeneity. The amount of homogeneity decreases as the number of pixel clusters increases; (4) *Porosity,* which is defined as the ratio of the void pixels area to the total area of pixels.

To explain why the cake deposit obtained after the filtration of BSA-FITC/dextran-RITC/tannic acid solutions containing 0.25 g/L was the thickest, we hypothesized that it must have the highest porosity as a result of less compacted aggregates. However, the porosity values obtained with ISA3D software (Table 5.6) do not concur with this hypothesis. Porosity calculated using ISA3D for the solution containing 0.25 g/L is the lowest (12% or 13%), regardless of the image stacks used, whereas the porosity obtained for solutions of 0.5 and 1g/L tannic acid is about 40%, whatever the tannic acid concentration and the image stacks employed in the calculation. The lower porosity of the cake obtained after filtration of solutions containing 0.25 g/L of tannic acid indicates a lower void area in the cake, which could be related to the higher rejection observed for the protein and the polyphenol (Figure 5.2). Regarding the rest of the parameters calculated using ISA3D software, these do not differ significantly with an increase of polyphenol concentration in the filtered solution, and they provide no extra information about the cake layer structures. Even though the use of an image structure analyzer seems to be an easy way to compare structural parameters of various specimens, it is still a new tool, developed to characterize cell clusters, and which requires further research and standardization of procedures when applied to fouling characterization.

Table 5.6. Three dimensional structural parameters obtained by ISA-3D software analysis of the cake layer deposited on the surface of 0.8 µm polycarbonate membranes after microfiltration of solutions containing BSA-FITC/dextran RITC and different concentrations of tannic acid.

	BSA/dex/TA025	**BSA/dex/TA05**	**BSA/dex/TA1**
	FITC		
Porosity (P)	0,12±0.06	0,42±0.04	0,37±0.1
Textural entropy (TE)	4,95±0.27	5,15±1.15	4,34±0.33
Energy (E)	0,01±0.00	0,01±0.01	0,03±0.01
Homogeneity (H)	0,66±0.03	0,65±0.12	0,76±0.03
	RITC		
Porosity (P)	0,13±0.08	0,40±0.05	0,41±0.07
Textural entropy (TE)	5,50±0.32	5,94±0.98	4,51±0.44
Energy (E)	0,01±0.00	0,01±0.00	0,03±0.01
Homogeneity (H)	0,63±0.04	0,56±0.12	0,78±0.07

As stated earlier in this study, adding tannic acid to the solution of BSA/dextran resulted in deposition of cake layer on the top of the membrane surface. Therefore, detection of BSA and dextran within the deposit should be directly related to BSA/dex/TA aggregation induced by the presence of tannic acid. Figure 5.7 shows qualitative information obtained by CSLM analysis on the cake layer composition: the normalized intensity profiles for protein and dextran fluorescent signal within the cake layer which formed on the top of the polycarbonate membranes fouled after filtration of BSA/dextran/TA solutions. In all the cases studied, regardless of the tannic acid concentration, the fluorescence signal coming from dextran molecules in the cake was stronger close to the membrane surface, while the signal coming from the protein molecules was more intense in the upper part of the cake layer. These results are clearly reflected in the volumetric 3D reconstructions in Figure 5.8, which were obtained using Imaris software. The cake layer formed on the membrane surface after filtration of the solution with the lowest concentration of tannic acid (0.25 g/L) is much thicker than for the solutions with higher tannic acid concentrations (0.5 g/L and 1g/L) (Table 5.5). Cake layer obtained after filtration of BSA/dex/TA025 and BSA/dex/TA05 is composed of many different sized aggregates of proteins and polysaccharides (probably together with polyphenols) which can be observed as points of greater intensity within the whole deposit (green signal coming from BSA-FITC molecules, red signal coming from dex-RITC molecules). This feature of the cake layer would lead to a less compact deposit and would also explain the higher values of protein rejections for solutions with

UNIVERSITAT ROVIRA I VIRGILI
MEMBRANE FOULING CHARACTERIZATION BY CONFOCAL SCANNING LASER MICROSCOPY
Maria Malgorzata Zator
ISBN:978-84-693-0712-0/DL:T-422-2010

lower concentration of tannic acid (Figure 5.2). For the membrane fouled with BSA/dex/TA1 a more uniform deposit is observed, probably due to the higher density of the cake layer.

Figure 5.7. Normalized intensity profiles for BSA-FITC and dextran-RITC for three different concentrations of Tannic acid.

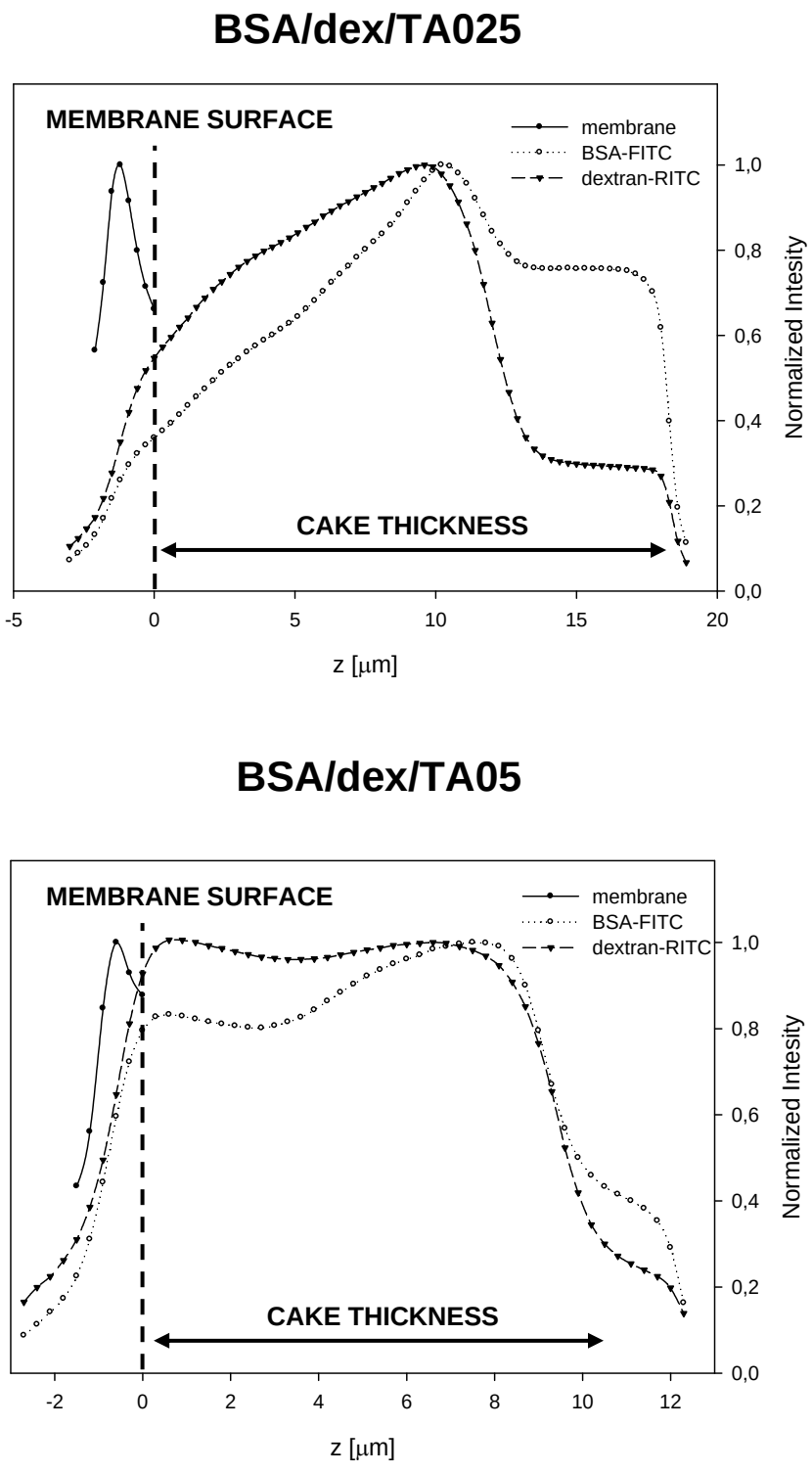

UNIVERSITAT ROVIRA I VIRGILI
MEMBRANE FOULING CHARACTERIZATION BY CONFOCAL SCANNING LASER MICROSCOPY
Maria Malgorzata Zator
ISBN:978-84-693-0712-0/DL:T-422-2010

BSA/dex/TA1

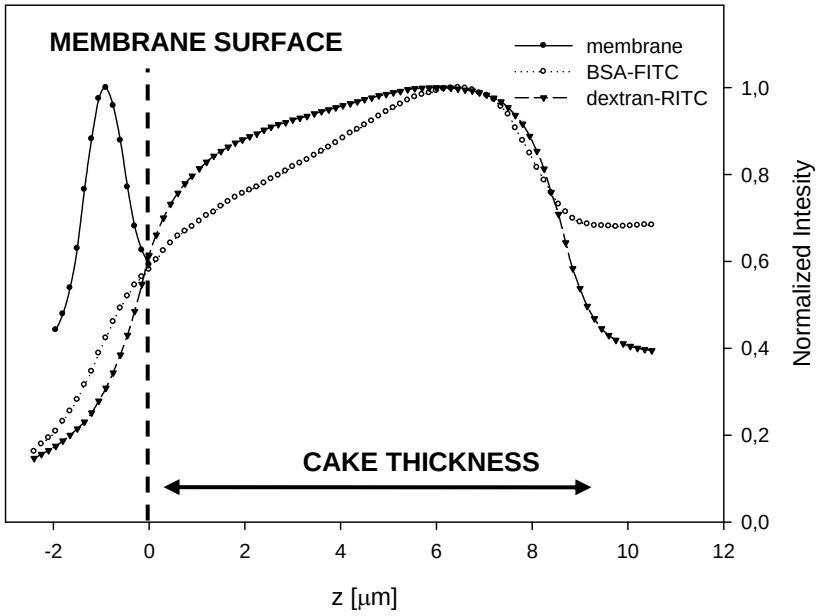

UNIVERSITAT ROVIRA I VIRGILI
MEMBRANE FOULING CHARACTERIZATION BY CONFOCAL SCANNING LASER MICROSCOPY
Maria Malgorzata Zator
ISBN:978-84-693-0712-0/DL:T-422-2010

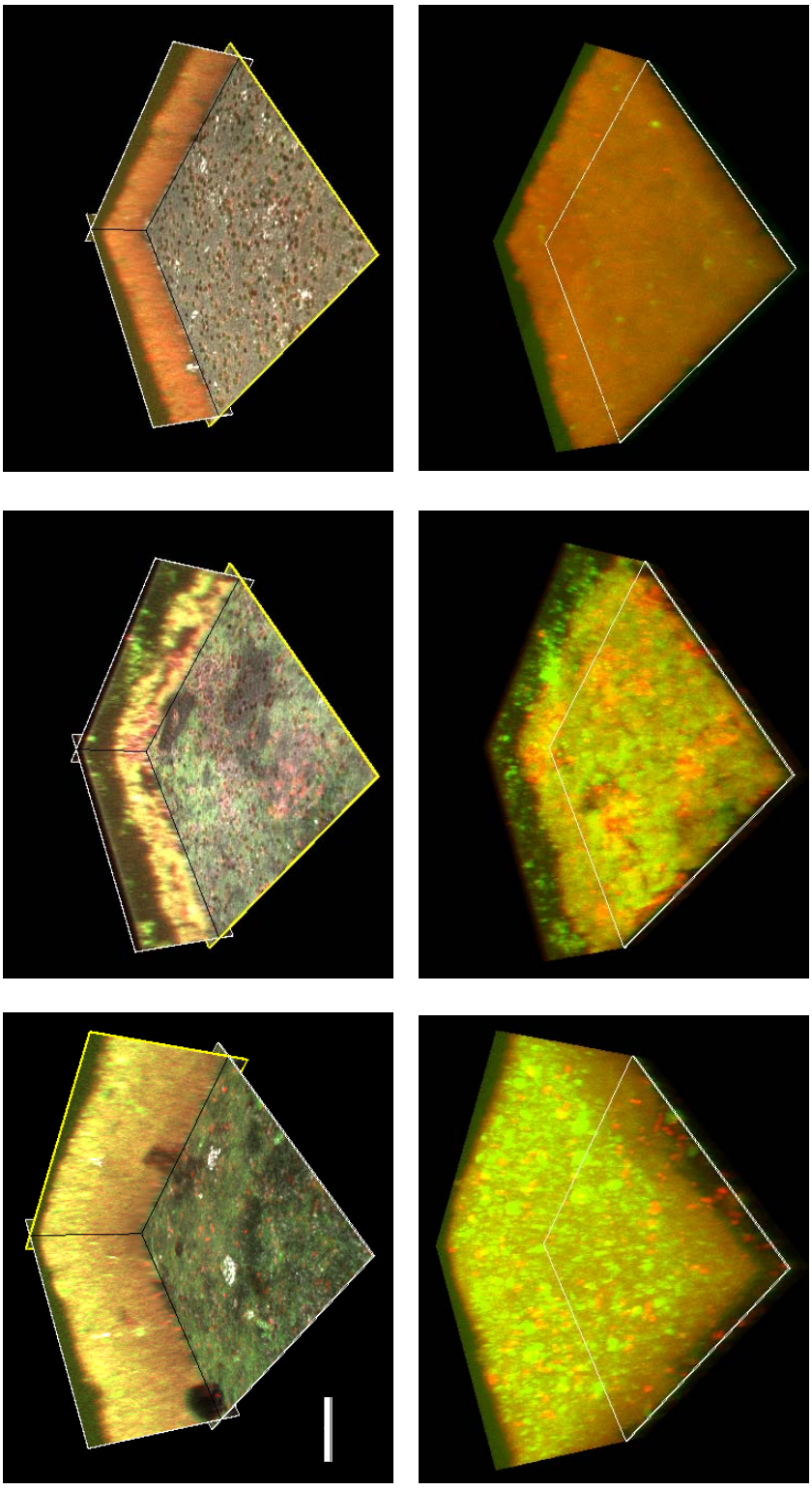

Figure 5.8. A volumetric 3D reconstruction of a 0.8 µm polycarbonate membrane fouled by ternary solutions of BSA-FITC/dextran-RITC/tannic acid. Gray and black colors represents membrane and membrane pores, respectively. Green color represents signal coming from BSA-FITC, red color represents signal coming from Dextran-RITC. The white/yellow square shows the membrane surface. (Scale bar = 10 µm).

5.3.3. Chemical cleaning

The efficiency of the chemical cleaning protocols applied to polycarbonate membranes after filtration of ternary solutions was evaluated using macroscopic and microscopic results. Regarding macroscopic data, the reduction of pure water flux is used in order to assess irreversible fouling [6]. For this purpose pure water fluxes before and after filtration were determined and pure water flux reduction (FRED) calculated according to equation 5.2.

$$FRED = \frac{J_{original} - J}{J_{original}} \times 100\% \quad (5.2)$$

Where J is the pure water flux after filtration and $J_{original}$ is the pure water flux for the clean membrane.

Table 5.7 shows FRED values for all the model solutions studied in this chapter Comparing the FRED values obtained for protein or protein/dextran solutions with the ones for protein/dextran/polyphenol solutions, it is clear that in all the cases the fouling was extremely severe after the filtration. It is noteworthy, however, that the length of the filtration varied depending on the composition of the solution (see Table 5.2).

To remove the compounds responsible for irreversible fouling from the membrane, thus recovering the membrane permeability, we applied chemical cleaning using US53 for 5 or 15 minutes and at two concentrations, 0.1% and 0.5%. The cleaning efficiency in terms of pure water flux recovery (FREC) was defined as the ratio of pure water flux after cleaning ($J_{cleaning}$) to the pure water flux of the clean membrane ($J_{original}$) measured under the same conditions and calculated according to equation 5.3.

$$FREC = \frac{J_{cleaning}}{J_{original}} \times 100\% \quad (5.3)$$

Table 5.7 shows the FREC values. As the table indicates, the higher water flux recoveries were obtained after 5 minutes of cleaning for all solutions with the exception of BSA/dextran solution, where the best flux recovery was reached after 15 minutes of cleaning with 0.1 % US53. The decrease in FREC after 15 minutes of cleaning is thought to be due to the broken aggregates and small pieces caused by the action of the cleaning agent; these are driven deeper into the membrane by the cleaning flux. It is also clear that none of the cleaning treatments allowed FREC values of over 60% to be attained. Moreover, the FREC values in Table 5.7 show that the increase in the cleaning agent concentration does not improve the recovery of the pure water

UNIVERSITAT ROVIRA I VIRGILI
MEMBRANE FOULING CHARACTERIZATION BY CONFOCAL SCANNING LASER MICROSCOPY
Maria Malgorzata Zator
ISBN:978-84-693-0712-0/DL:T-422-2010

flux, except from membranes fouled with BSA/dextran/tannic acid with 1g/L of polyphenol. For that specific situation, the increase in the concentration of the cleaning agent resulted in a higher value of FREC after 5 minutes of cleaning. These results will receive further mention below when analyzing the data obtained from CSLM analysis of the cleaned membranes.

Table 5.7. Pure water fluxes after filtration of BSA/dextran/tannic acid solutions and after chemical cleaning with two different times and concentrations of US 53.

Filtration solution	J after filtration [L/h m^2]	FRED [%]	$J_{cleaning}$ after 5 min US53 [L/h m^2]	FREC [%]	$J_{cleaning}$ after 15 min US53 [L/h m^2]	FREC [%]
US 53 0.1 %						
BSA	848 ±375	96±4	8757±384	43±5	6205±145	30±3
BSA/dex	1148±158	94±3	5726±157	28±3	8019±88	39±3
BSA/dex/TA025	2888±1248	86±13	7085±848	34±6	4261±407	21±3
BSA/dex/TA05	3016±1051	85±11	8784±2044	43±13	6118±261	30±3
BSA/dex/TA1	2036±1721	90±17	8486±1528	41±10	5374±780	26±6
US 53 0.5 %						
BSA/dex	1148±158	94±3	6099±277	31±3	5746±225	28±3
BSA/dex/TA025	2888±1248	86±13	7375±480	36±5	NA	NA
BSA/dex/TA05	3016±1051	85±11	8831±227	39±4	NA	NA
BSA/dex/TA1	2036±1721	90±17	12637±1885	61±13	5337±407	26±4

UNIVERSITAT ROVIRA I VIRGILI
MEMBRANE FOULING CHARACTERIZATION BY CONFOCAL SCANNING LASER MICROSCOPY
Maria Malgorzata Zator
ISBN:978-84-693-0712-0/DL:T-422-2010

CSLM analysis provided microscopic data on how chemical cleaning processes affect membranes that have been used to filter solutions containing BSA-FITC and dextran-RITC,. Figures 5.9 and 5.10 show the P_s profiles of BSA-FITC and dextran-RITC, respectively, after the cleaning protocols. These figures show clearly that applying US53 cleaning cycles significantly reduced P_s values for all cleaning times and concentrations tested. Chapter 4 discussed the partial recovery of water flux permeate flux for single and binary solutions containing BSA-FITC and dextran-RITC 70 kDa as a result of US53 chemical cleaning, and similar results were obtained for ternary mixtures containing TA. We found that cleaning time and concentration of the cleaning agent influenced the effectiveness of the cleaning process. We noted that, for binary mixtures, an increase in the duration of the cleaning did not always increase the water flux recovery.

Moreover, when a certain length of the cleaning time was exceeded and/or the concentration of the cleaning agent was increased, lower flux recoveries were obtained. In the case of ternary solutions, figures 5.9 and 5.10 show that the maximum foulant removal (minimum P_s values) is obtained after cleaning cycles of five minutes, regardless of the polyphenol concentration present in the initial solution. Both a very small shift in the P_s values and a slight increase in the water flux recovery (Table 5.6) were observed when the concentration of cleaning agent increased from 0.1 to 0.5 % for a 5 minute cleaning cycle. Extending the cleaning time of the membranes with US53 up to 15 minutes did not improve the removal of BSA or dextran. In fact, in some cases, higher P_s values were found (Fig 5.9a) for the protein. As described in Chapter 4, this is probably due to the aggregate breakage which occurs during the cleaning process and which results in small pieces of foulant aggregates being driven inside the membrane, thus blocking the pores below the membrane depth that can be visualized by CSLM.

Figures 5.11 and 5.12 show reconstructions of image stacks of polycarbonate membranes at different depths, after filtration of BSA/dex/TA1 solution, and after cleaning with US53 under different conditions. The reconstructions were obtained after processing CSLM images with ImageJ [BSA FITC: green signal and dextran-RITC: red signal]. As stated earlier, almost all of the membrane pores after filtration seem to be completely blocked by the green signal, which corresponds to the presence of BSA-FITC, and also many pores remain totally or partially blocked by the red signal coming from dextran-RITC. After 5 minutes of cleaning, the signal coming from both fluorescent compounds is almost unnoticeable.

UNIVERSITAT ROVIRA I VIRGILI
MEMBRANE FOULING CHARACTERIZATION BY CONFOCAL SCANNING LASER MICROSCOPY
Maria Malgorzata Zator
ISBN:978-84-693-0712-0/DL:T-422-2010

Figure 5.9. Fraction of pore surface on which BSA-FITC is detected (P_s) at the end of microfiltration process for ternary mixture of BSA-FITC/dextran-RITC and different concentrations of tannic acid on 0.8 μm polycarbonate membranes.

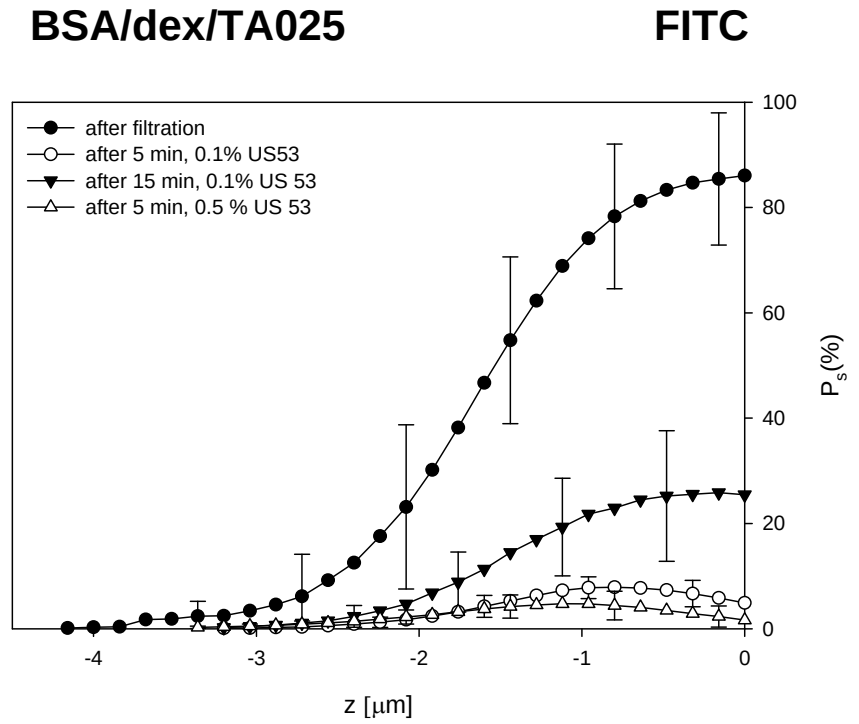

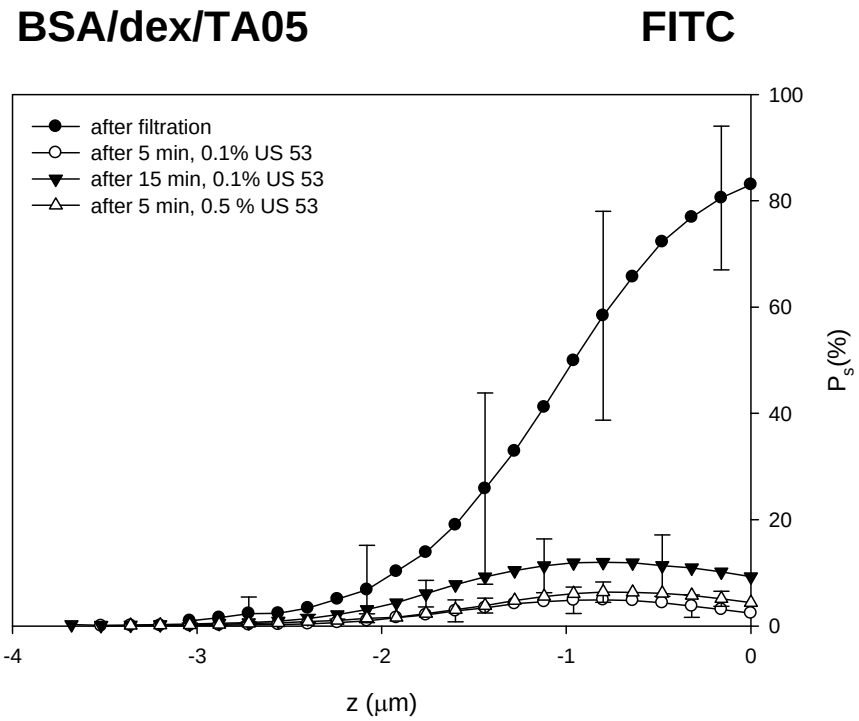

UNIVERSITAT ROVIRA I VIRGILI
MEMBRANE FOULING CHARACTERIZATION BY CONFOCAL SCANNING LASER MICROSCOPY
Maria Malgorzata Zator
ISBN:978-84-693-0712-0/DL:T-422-2010

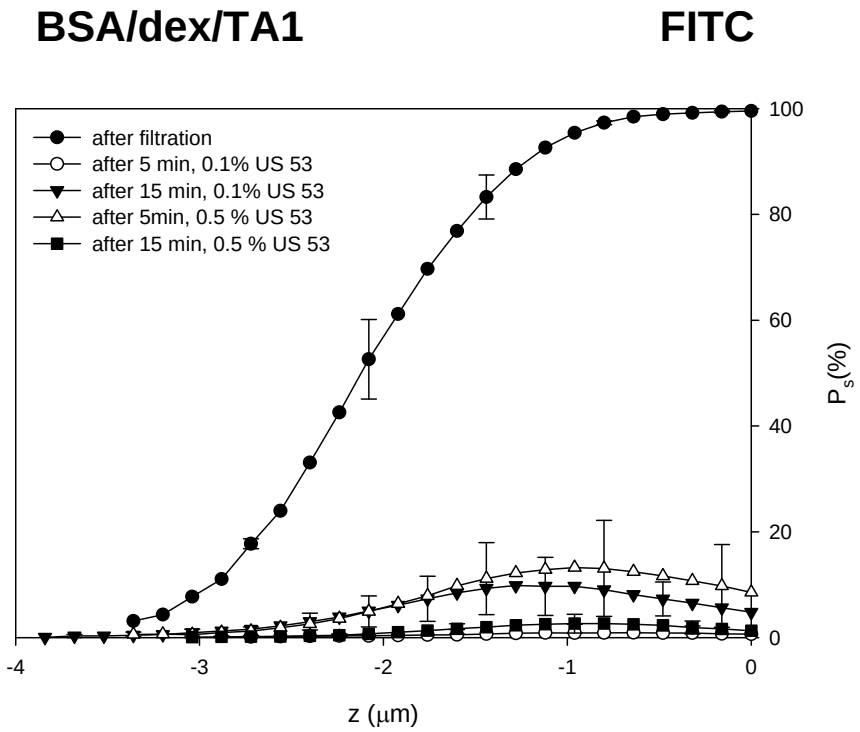

Figure 5.10. Fraction of pore surface on which dextran-RITC is detected (P_s) at the end of microfiltration process for ternary mixture of BSA-FITC/dextran-RITC and different concentrations of tannic acid on 0.8 μm polycarbonate membranes.

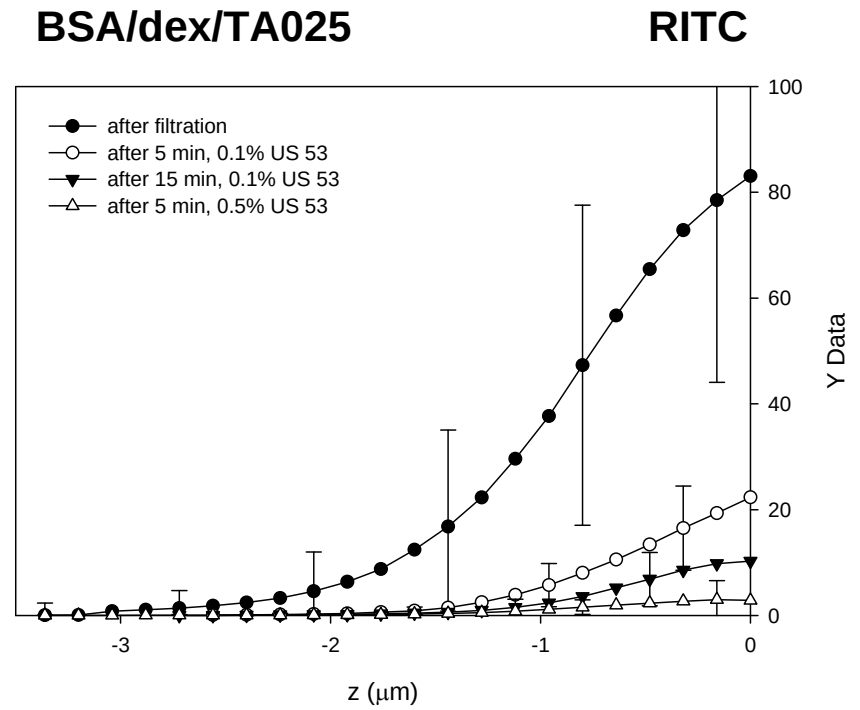

UNIVERSITAT ROVIRA I VIRGILI
MEMBRANE FOULING CHARACTERIZATION BY CONFOCAL SCANNING LASER MICROSCOPY
Maria Malgorzata Zator
ISBN:978-84-693-0712-0/DL:T-422-2010

BSA/dex/TA05 **RITC**

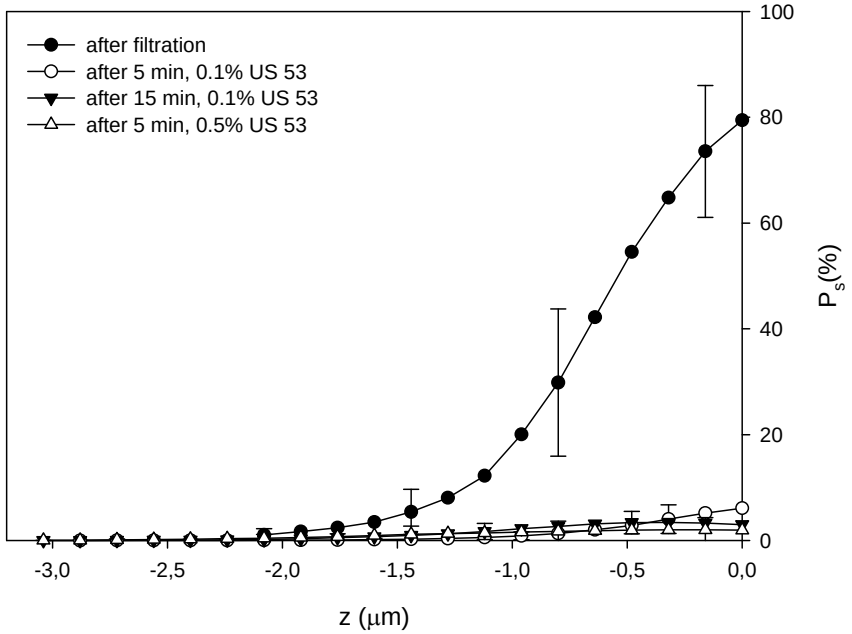

BSA/dex/TA1 **RITC**

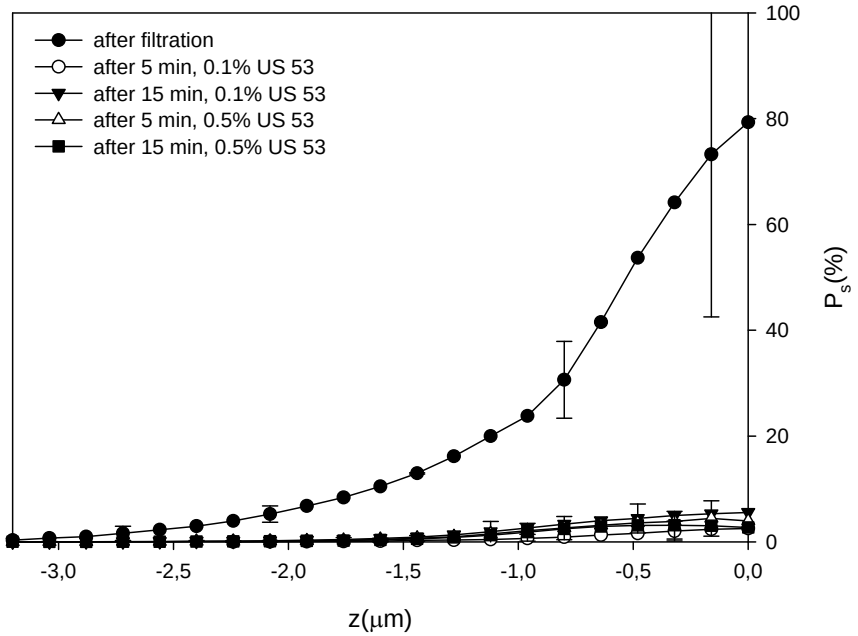

UNIVERSITAT ROVIRA I VIRGILI
MEMBRANE FOULING CHARACTERIZATION BY CONFOCAL SCANNING LASER MICROSCOPY
Maria Malgorzata Zator
ISBN:978-84-693-0712-0/DL:T-422-2010

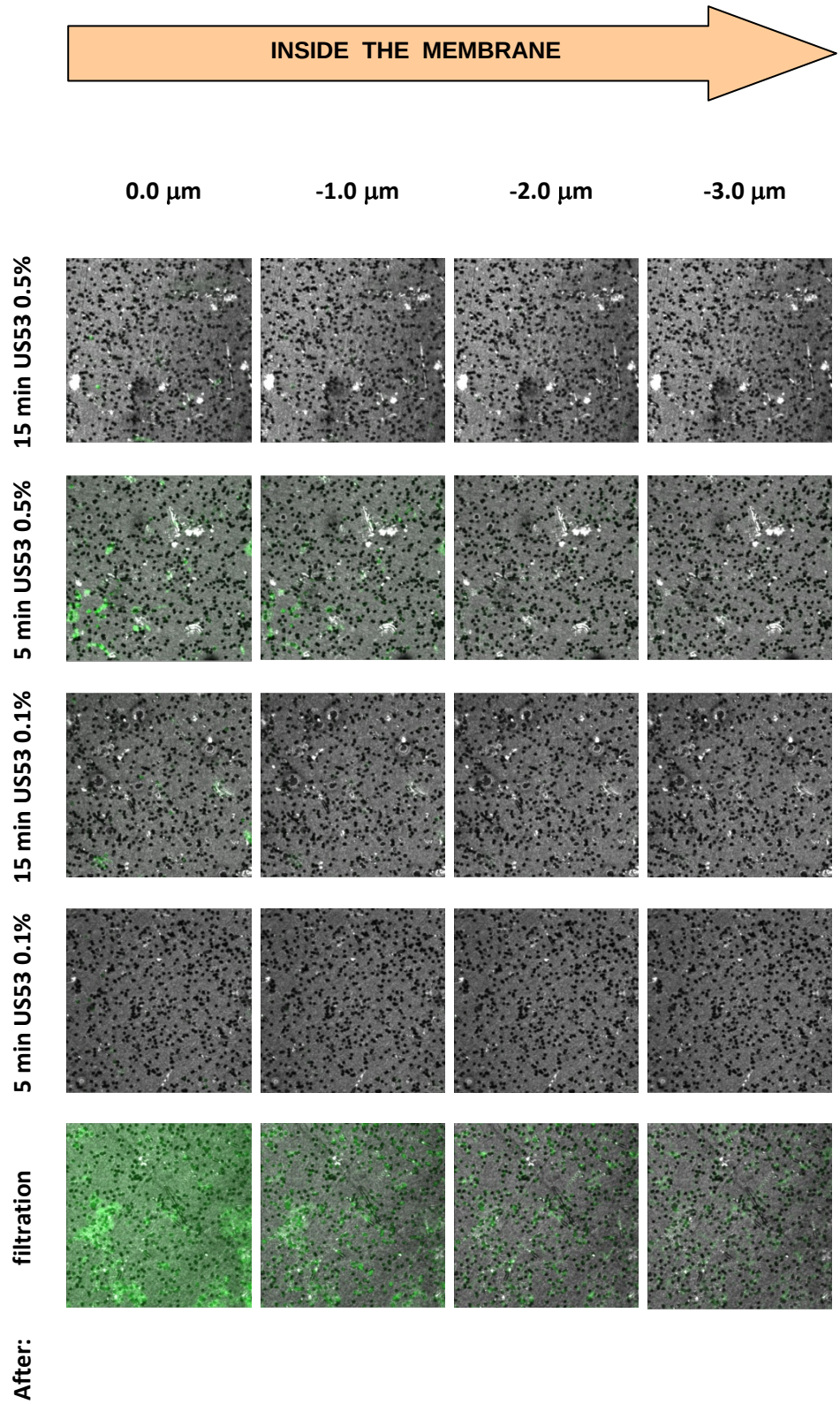

Figure 5.11. 3D orthogonal reconstruction of CSLM images: membranes after filtration of BSA/dex/TA1 solution and cleaning with US53. Images show the membrane (grey signal) and the dextran (red signal) at different depths. Scale bar 10 µm.

UNIVERSITAT ROVIRA I VIRGILI
MEMBRANE FOULING CHARACTERIZATION BY CONFOCAL SCANNING LASER MICROSCOPY
Maria Malgorzata Zator
ISBN:978-84-693-0712-0/DL:T-422-2010

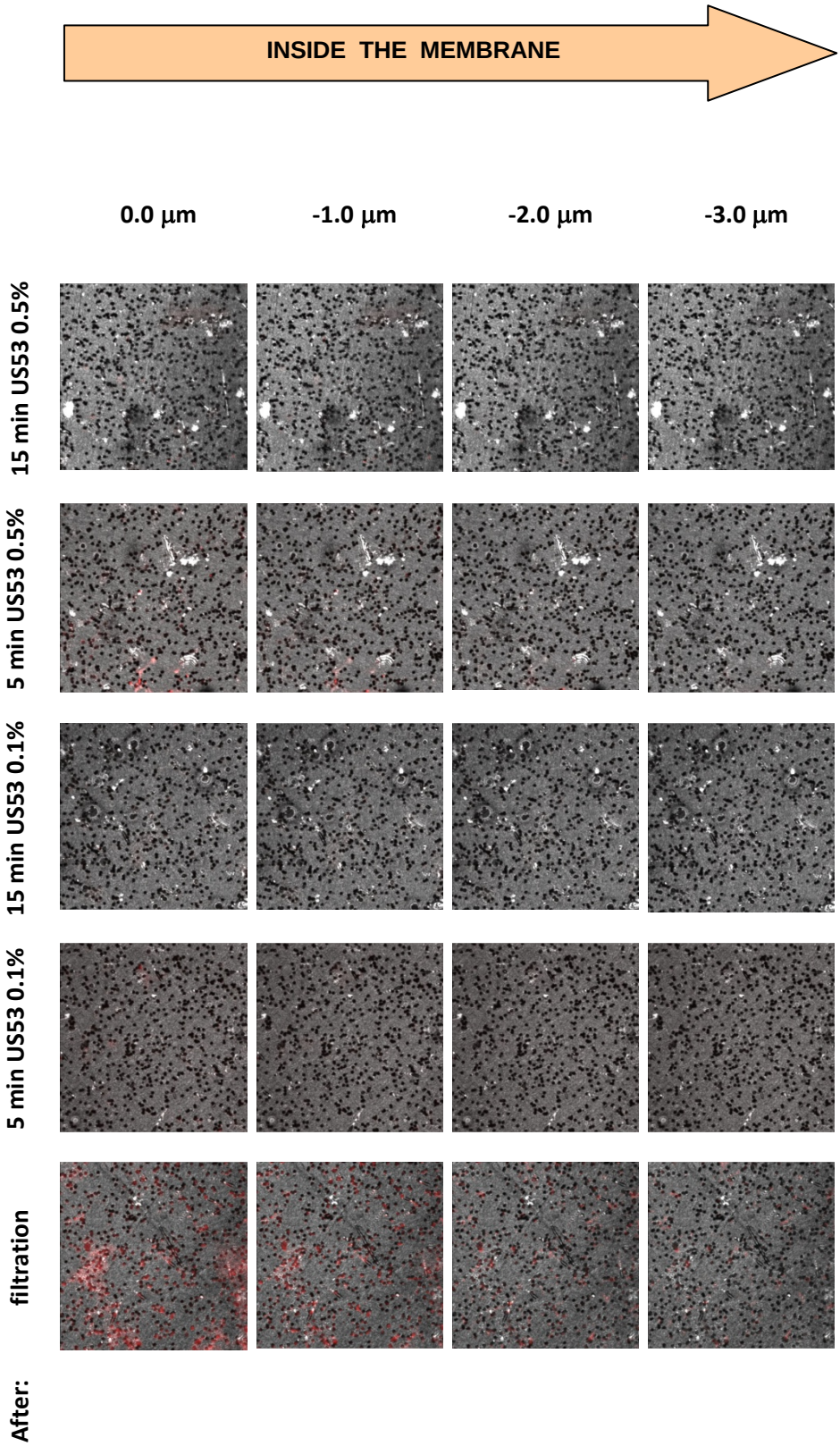

Figure 5.12. 3D orthogonal reconstruction of CSLM images: membranes after filtration of BSA/dex/TA1 solution and cleaning with US53. Images show the membrane (grey signal) and the dextran (red signal) at different depths. Scale bar 10 µm.

UNIVERSITAT ROVIRA I VIRGILI
MEMBRANE FOULING CHARACTERIZATION BY CONFOCAL SCANNING LASER MICROSCOPY
Maria Malgorzata Zator
ISBN:978-84-693-0712-0/DL:T-422-2010

5.4. Conclusions

From the results reported in this chapter it can be concluded that CSLM was successfully applied to obtain qualitative and quantitative data with which to characterize membrane fouling during microfiltration of ternary solutions of BSA/dextran/tannic acid. The addition of a polyphenol in protein/polysaccharide solutions appears to result in a much more severe fouling than is observed for binary BSA/dextran solutions. CSLM images enabled us to quantify the protein/dextran presence inside the pores and to measure the cake thickness formed on top of the membrane.

Regarding the nature of the fouling, the BSA/dextran/tannic acid solutions studied in this work cause extensive internal and external membrane fouling, while for the single protein and binary BSA/dextran solutions studied only internal fouling was observed. The extent of internal fouling related to P_s values calculated from CSLM images for BSA-FITC and dextran-RITC showed that solutions with the highest weight ratio of protein/polyphenol (1:4) made the greatest contribution to the internal membrane fouling, resulting in 100 % P_s values for BSA-FITC.

The thickness of the cake layer formed on top of the membrane was quantitatively and qualitatively analyzed using CSLM image analysis. The three dimensional reconstruction of the CSLM images allowed us to calculate the thickness of the cake layer present on the top of the membrane surface. The normalized intensity profiles of BSA-FITC and dextran-RITC obtained by image analysis software from CSLM images made it possible to differentiate between each fluorescently marked foulant present in the cake layer, thus obtaining information on the presence of BSA-FITC and dextran-RITC at different depths of the cake layer. We found that the most severe external fouling and the highest rejection values were for the solution containing the lowest tannic acid concentration (0.25 g/L). Our hypothesis that, in this case, the cake layer was less compact than the ones obtained with higher polyphenol concentration could not be confirmed.

The application of cleaning procedures with an enzymatic cleaning agent US 53 did not restore the original water fluxes of the polycarbonates membranes in any of the cases studied. However, according to CSLM image analysis, for all the cleaning conditions studied the complete removal of the cake layer was obtained, and most of the particles deposited/adsorbed inside the membrane pores were removed, as shown by the P_s values close to 0 for both the protein and the dextran. As stated in Chapter 3, prolonging the cleaning time after a certain optimum value did not result in an increase of water flux recovery for the membrane. An increase in the concentration of the cleaning agent resulted in a shorter cleaning time being necessary to attain this maximum water flux recovery. The results obtained in this chapter show that cleaning times of 5 minutes with 0.1 % US53 permitted the recovery of about forty percent

of the original water flux of the polycarbonate membranes. We believe that even though the P_s values obtained from CSLM images are almost zero at 3 μm inside the membrane, small aggregate fractions are driven inside the membrane during the cleaning process, blocking them at certain depths not reachable using CSLM analysis.

UNIVERSITAT ROVIRA I VIRGILI
MEMBRANE FOULING CHARACTERIZATION BY CONFOCAL SCANNING LASER MICROSCOPY
Maria Malgorzata Zator
ISBN:978-84-693-0712-0/DL:T-422-2010

5.5. References

1. L. Fillaudeau, H. Carrere, Yeast cells, beer composition and mean pore diameter impacts on fouling and retention during cross-flow filtration of beer with ceramic membranes, Journal of Membrane Science 196 (2002) 39-57.
2. A. Vernhet, M. Moutounet, Fouling of organic microfiltration membranes by wine constituents: importance, relative impact of wine polysaccharides and polyphenols and incidence of membrane properties, Journal of Membrane Science 201 (2002) 103-122.
3. P. Czekaj, F. López, C. Güell, Membrane fouling during microfiltration of fermented beverages, Journal of Membrane Science 166 (2000) 199-212.
4. P. Czekaj, F. López, C. Güell, Membrane fouling by turbidity constituents of beer and wine: characterization and prevention by means of infrasonic pulsing, Journal of Food Engineering 49 (2001) 25-36.
5. P. Blanpain, M. Lalande, Investigation of fouling mechanisms governing permeate flux in the crossflow microfiltration of beer, Filtration&Separation (1997) 1065-1069.
6. M. Mänttäri, L. Puro, J. Nuortila-Jolinen, M. Nyström, Fouling effects of polysaccharides and humic acid in nanofiltration, Journal of Membrane Science 165 (2000) 1-17.
7. N. Mateus, E. Carvalho, C. Luis, V. Freitas, Influence of the tannin structure on the disruption effect of carbohydrates on protein-tannin aggregates, Analytica Chimica Acta 513 (2004) 135-140.
8. E. Carvalho, M.J. Póvoas, N. Mateus, V. Freitas, Application of flow nephelometry to the analysis of the influence of carbohydrates on protein-tannin interactions, Journal of the Science of Food and Agriculture 86: 891-896 (2006).
9. E. Carvalho, N. Mateus, V. Freitas, Flow nephelometric analysis of protein-tannin interactions, Analytica Chimica Acta 513 (2004) 97-101.
10. V. Freitas, E. Carvalho, N. Mateus, Study of carbohydrate influence on protein-tannin aggregation by nephelometry, Food Chemistry 81 (2003) 503-509.
11. J.P. Chen, S.L. Kim, Y.P. Ting, Optimization of membrane physical and chemical cleaning by statistically designed approach, Journal of Membrane Science 219 (2003) 27-45.
12. T. Mohammadi, S.S. Madaeni, M.K. Moghadam, Investigation of membrane fouling, Desalination 153 (2002) 155-160.
13. M. Ferrando, A. Rózek, M. Zator, F. López, C. Güell, An approach to membrane fouling characterization by confocal scanning laser microscopy, Journal of Membrnae Science 250 (2005) 283-293.
14. M. Zator, M. Ferrando, F. López, C. Güell, Membrane fouling characterization by confocal microscopy during filtration of BSA/dextran mixtures, Journal of Membrane Science 301 (2007) 57-66.

15. D. Spettmann, S. Eppman, H-C. Flemmng, J. Wingender, Visualization of membrane cleaning using confocal laser scanning microscopy, Desalination 224 (2008) 195-200.
16. M. Zator, J. Warczok, M. Ferrando, F. López, C. Güell, Chemical cleaning of polycarbonate membranes fouled by BSA/dextran mixtures, Journal of Membrane Science (2008), doi:10.1016/j.memsci.2008.11.006
17. V. L. Singleton, J. A. Rossi, Colorimetry of total phenolics with phosphomdybdic-phosphotungstic acid agents. American Journal of Enology and Viticulture 16 (1965) 144-158.
18. M. Bradford, A rapid and sensitive method for quantification of microgram quantities of proteins utilizing the principle of protein-dye binding. Analitical Biochemistry 72 (1976) 248-254.
19. D. Wu, M.R. Bird, The fouling and cleaning of ultrafiltration membranes during the filtration of model tea component solutions, Journal of Food Process Engineering 30 (2007) 293-323.
20. M. Ferrando, **M. Zator**, F. López, C. Güell, (2009), Confocal Scanning Laser Microscopy: Fundamentals and uses on membrane fouling characterization and opportunities for on-line monitoring in “Monitoring and Visualizing Membrane –based Processes, Whiley-VCH Verlag GmbH & Co.KGcA Wanheim, Germany, pp. 57-77.
21. X.Yang, H. Beyenal, G. Harkin, Z. Lewandowski, Quantifying biofilm structure using image analysis, Journal of Microbiological Methods 39 (2000) 109-119.
22. X.Yang, H. Beyenal, G. Harkin, Z. Lewandowski, Evaluation of biofilm images tresholding methods, Water Research 35 (2001) 1149-1158.
23. H. Beyenal, Z. Lewandowski, G. Harkin, Quantifying biofilm structure: facts and fiction, Biofouling 20 (2004) 1-23.
24. H. Beyenal, C. Donovan, Z. Lewandowski, G. Harkin, Three-dimentional biofilm structure quantification, Journal of Microbiological Methods 59 (2004) 395-413.

UNIVERSITAT ROVIRA I VIRGILI
MEMBRANE FOULING CHARACTERIZATION BY CONFOCAL SCANNING LASER MICROSCOPY
Maria Malgorzata Zator
ISBN:978-84-693-0712-0/DL:T-422-2010

UNIVERSITAT ROVIRA I VIRGILI
MEMBRANE FOULING CHARACTERIZATION BY CONFOCAL SCANNING LASER MICROSCOPY
Maria Malgorzata Zator
ISBN:978-84-693-0712-0/DL:T-422-2010